

Detailed Finite Element Modeling of the Human Ligamentous Cervical Spine

by

Faisal Agah

A thesis submitted in partial fulfillment of the requirements for the degree of

Master of Science

in

Structural Engineering

Department of Civil and Environmental Engineering

University of Alberta

© Faisal Agah, 2016

Abstract:

The main purpose of this study was creating a finite element model with bio-realistic geometry of ligaments in the cervical spine region. A ligamentous finite element model was created that allows the study of the stress distribution on ligaments under six different moments: flexion, extension, biaxial moments and bilateral moments. The created model was constructed considering comprehensive geometrical representation of the soft tissues such as ligaments and intervertebral disc and material laws that would make the model respond in a similar manner to the in vitro studies.

The constructed model was tested against other numerical models as well as in vitro studies to ensure the current model can mimic the behaviour of the spine under any given static load. The in vitro study that was used was carried by Panjabi et al. (2001) and the finite element models used for validation are: Zhang et al. (2006); Palomar et al. (2007); Toosizadeh et al. (2011); Han et al. (2012); and Moglo et al. (2013).

Using the created model, the following was demonstrated: 1) the response of the created model against in vitro studies as well as some other created models under the applied moments, 2) the load sharing percentage of the ligaments comparing to the other load bearing components in each of the six moments, 3) the stress initiation area, path prediction along the ligaments, and high stress areas in the ligaments, and 4) the most critical ligament in limiting the rotation of the spine under each of the six moments.

Under the applied loads, the model had a similar response in comparison to the other finite element models mentioned earlier. It was found that stress distribution along the ligaments varied based on the ligament orientation with respect to the applied load. In addition, it was determined that high stress region changed based on the imposed load on the model. Also, the stress

propagation along the ligament was dependent on the applied moment as in flexo-extension rotation, the stress was concentrated in the middle region of the ligaments while in biaxial rotation, the stress distributed diagonally along the ligament and in bilateral rotation, the stress was high on one half of the ligament and minimal on the other half. Further explanation of the stress distribution will be discussed in the discussion chapter.

Table of Contents

1	Background and motivation.....	1
2	Introduction to Cervical Spine Anatomy.....	3
2.1	Anatomy and Function of Human Spine.....	3
2.2	Cervical Spine Anatomy.....	5
2.2.1	C1 (Atlas).....	6
2.2.2	C2 (Axis).....	8
2.2.3	C3 - C7.....	10
2.2.4	Intervertebral disc.....	14
2.2.5	Ligaments.....	16
2.3	Planes of Motion.....	23
2.4	Range of motion of the cervical spine.....	24
3	Literature Review.....	27
3.1	In vitro experiment.....	27
3.2	Finite Element models (FEA).....	30
3.3	The current study.....	35
4	Finite Element Model creation.....	36
4.1	Geometry acquisition.....	36
4.2	Modeling.....	38
4.2.1	Hypermesh.....	38
4.2.2	Finite element analysis (Abaqus).....	43
5	Validation.....	48
5.1	Experimental data (in vitro).....	48
5.2	Numerical data (Finite element models).....	51
6	Model detailed output.....	54
6.1	Ligaments.....	56
6.1.1	Flexo-extension.....	56
6.1.2	Axial rotation.....	63
6.1.3	Lateral Bending.....	69
6.2	Facet joint.....	75
6.2.1	Flexo-extension.....	75
6.2.2	Axial rotation.....	76

6.2.3	Lateral bending	78
6.3	Intervertebral disc.....	80
6.3.1	Flex-extension	80
6.3.2	Axial rotation.....	81
6.3.3	Lateral bending	83
7	Discussion and Recommendation.....	85
8	References	92
	Appendix	97

List of Figures

Figure 2.1. Axial skeleton. From “Human Axial Skeleton,” by OpenStax College, 2013, http://cnx.org/resources/40030aca8b222cf06c673422c5307f904a45fd04/Figure_38_01_04.jpg . Copyright 2013 by OpenStax College.	3
Figure 2.2. Different regions of the human spine. From “Vertebral Column,” by OpenStax College, 2013, http://cnx.org/resources/5934b9fecf14874c1ec99a57ec73b9c9648fd5ae/Figure_38_01_07.jpg . Copyright 2013 by OpenStax College.	4
Figure 2.3. Neural foramen. From “Cervical Spine Anatomy,” by Medical MultiMedia Group, 2002, http://eorthopod.com/cervical-spine-anatomy/ . Copyright 2002 by Medical MultiMedia Group.	5
Figure 2.4. Structure of the cervical spine. From “Cervical Spine Fractures,” by Parker, L., http://www.hughston.com/hha/a.cspine.htm . Copyright by Parker, L.	6
Figure 2.5. Atlas vertebra. From “Atlas,” by The Chiropractic Resource Organization, 2016, http://www.chiro.org/chimages/diagrams/ , Copyright 2016 by The Chiropractic Resource Organization.	7
Figure 2.6. Atlas-occipital joint. From “Atlanto occipital Joint,” by Dugan, L., 2011, http://www.chiropractic-help.com/Atlanto-Occipital-Joint.html . Copyright 2011 by Dugan, L.	7
Figure 2.7. Transverse process on each side of the atlas vertebra. From “ANTPHY 1 Study Guide,” by Williamson, 2011, https://www.studyblue.com/notes/n/antphy-1-study-guide-2011-12-williamson-deck/9727461?blurry=e&ads=true . Copyright 2011 by Williamson.	8
Figure 2.8. Odontoid (dens). From “Vertebral Column,” by Bridwell, K., 2016, http://www.spineuniverse.com/anatomy/vertebral-column . Copyright 2016 by Bridwell, K.	8
Figure 2.9. Odontoid held in position by transverse ligament. (Hata, T., 2005).	9
Figure 2.10. Side and plan views of C2 axis. From “The Axis Vertebra,” by Galileo Site Manager, 2016, http://www.edoctoronline.com/medical-atlas.asp?c=4&id=21631 . Copyright 2016 by Galileo Site Manager.	10
Figure 2.11. Vertebral body. From “Cervical Spine Anatomy Animation,” by Vertical health, 2014, http://www.spineuniverse.com/anatomy/cervical-spine-anatomy-animation . Copyright 2014 by Vertical health.	11
Figure 2.12. Spinous processes connected by interspinous ligament.	12
Figure 2.13. Transverse process of cervical vertebra. From “Atlas-C1 vertebra,” by The art of medicine, 2015, https://theartofmed.wordpress.com/2015/06/05/c1-vertebra-atlas-and-accompanying-structures/ . Copyright 2015 by The art of medicine.	12
Figure 2.14. Intervertebral foramen (foreman). From “Cervical Spine Anatomy,” by Medical MultiMedia Group, 2002, http://eorthopod.com/cervical-spine-anatomy/ . Copyright 2002 by Medical MultiMedia Group.	13
Figure 2.15. Facet joint. From “Spinal facet joint,” by Berovic, M. 2015, http://www.claphamsportsmassage.com/spinal-pain-what-is-it/ . Copyright 2015 by Berovic, M.	14
Figure 2.16. Intervertebral disc. From “Cervical Spine Anatomy,” by Medical MultiMedia Group, 2002, http://eorthopod.com/cervical-spine-anatomy/ . Copyright 2002 by Medical MultiMedia Group.	15
Figure 2.17. Different parts of intervertebral disc.	15
Figure 2.18. Different ligaments in the cervical spine region. From From “Cervical Spine,” by Warrior, W., 2015, http://clinicalgate.com/cervical-spine-3/ . Copyright 2015 by Warrior, W.	17
Figure 2.19. Different ligaments at skull-atlas and atlas-axis joints (viewed from behind). From “The Cervical Vertebrae; Inter-Vertebral and Cranio-Vertebral Joints,” by Pujari, S., 2015, http://www.yourarticlelibrary.com/biology/human-beings/the-cervical-vertebrae-inter-vertebral-and-cranio-vertebral-joints-human-anatomy/9514/ . Copyright 2015 by Pujari, S.	17
Figure 2.20. Frontal view of Atlanto-occipital ligament.	18
Figure 2.21. Posterior view of apical ligament.	18
Figure 2.22. Top view of Alar ligament. From “Alar Ligament Treatment for CCJ Instability,” by Centeno, C., 2015, http://www.regenexx.com/alar-ligament-treatment/ . Copyright 2015 by Centeno, C.	19
Figure 2.23. Posterior view of Transverse ligament. (Hata, T., 2005).	19
Figure 2.24. Side view of anterior longitudinal ligament. From “Supraspinous Ligament,” by Sareen, A., 2014, http://www.physio-pedia.com/File:Supraspinous_lig.jpg . Copyright 2014 by Sareen, A.	20
Figure 2.25. Posterior view of Posterior longitudinal ligament. From “Roof of neck,” by Megan L. 2014, https://www.studyblue.com/notes/n/4-root-of-neck/deck/9360518 . Copyright 2014 by Megan L.	20

Figure 2.26. Frontal view of Ligamentum flavum.....	21
Figure 2.27. Side view of Interspinous ligament.....	21
Figure 2.28. Posterior view of Nuchal ligament.....	22
Figure 2.29. Frontal view of Intertransverse.....	22
Figure 2.30. Side view of Capsular ligament.....	23
Figure 2.31. Three different planes used in the anatomy of the human body. From “Find your direction,” by Dyke, J., 2014, http://www.crossfitsouthbay.com/find-your-direction/ . Copyright 2014 by Dyke, J.....	24
Figure 2.32. The three different rotations of head.....	25
Figure 3.1. Pulley system used to translate force into moments. (Panjabi, M. 2001).	28
Figure 3.2. Parametrized vertebra (Maurel N., 1997).	31
Figure 3.3. Part “a” designed showing the intervertebral disc and “b” showing the annulus fibers (Maurel N., 1997).	32
Figure 4.1. Showing the raw state of the model, without skull (C0).	37
Figure 4.2. Showing the penetration between C6-C7.....	38
Figure 4.3. a) Ligament lines b) Ligament surface.....	39
Figure 4.4. Showing the end-plates at the inferior surface at the vertebral body.....	39
Figure 4.5. Meshed end-plate.....	41
Figure 4.6. Annulus fibrosus elements.....	41
Figure 4.7. Cortical and cancellous bones.....	42
Figure 4.8. C3-C4 motion segment with all the soft tissues a) intervertebral disc, b) motion segment.....	43
Figure 4.9. Force vs deformation of annulus fibrosus.....	45
Figure 4.10. Nodes tied to a single reference node. From “Rigid body,” by Abaqus 6.14, 2015, http://ivt-abaqusdoc.ivt.ntnu.no:2080/v6.14/books/gsa/default.htm?startat=ch03s02.html . Copyright 2015 by Abaqus 6.14. ..	46
Figure 5.1. Flexo-extension of Panjabi 2001 and the current FEA model.....	49
Figure 5.2. Axial rotation of Panjabi 2001 and the current FEA model. Values summate both right and left sides. ..	49
Figure 5.3. Lateral bending rotation of Panjabi 2001 and the current FEA model. Values summate both right and left sides.....	50
Figure 5.4. Flexo-extension of the current FEA model and other FEA models.....	51
Figure 5.5. Axial rotation of the current FEA model and other FEA models. Values summate both right and left sides.....	52
Figure 5.6. Lateral bending of the current FEA model and other FEA models. Values summate both right and left sides.....	53
Figure 6.1. Transection of the ligaments into anterior and posterior sections in flexo-extension rotation. (Panjabi, M. 1978). Used with permission.....	54
Figure 6.2. Transection of the spine into two symmetrical halves. From “Which X-Ray Views Should Be Obtained?,”2015, http://www.ebmedicine.net/topics.php?paction=showTopicSeg&topic_id=51&seg_id=936; . Copyright 2015.....	55
Figure 6.3. Stress development along the ALL for all the motion segments from C0-C1 ligament down to C2-C3 section. Negative moment is extension while positive moment is flexion.....	57
Figure 6.4. Stress distribution along ITL. Negative moment is extension while positive moment is flexion.....	57
Figure 6.5. Stress distribution along PLL. Negative moment is extension while positive moment is flexion.....	58
Figure 6.6. Stress distribution along CL. Negative moment is extension while positive moment is flexion.....	59
Figure 6.7. Stress distribution along LV. Negative moment is extension while positive moment is flexion.....	59
Figure 6.8. Stress distribution along ITL. Negative moment is extension while positive moment is flexion.....	60
Figure 6.9. Stress distribution along SSL. Negative moment is extension while positive moment is flexion.....	61
Figure 6.10. Stress distribution along Alar ligament, Transverse ligament and Apcai ligament. Negative moment is extension while positive moment is flexion.....	62
Figure 6.11. Stress distribution along ALL. Negative moment indicates rotation to the left side while positive indicates right side rotation.....	63
Figure 6.12. Stress distribution along ITL. Negative moment indicates rotation to the left side while positive indicates right side rotation.....	64

Figure 6.13. Stress distribution along PLL. Negative moment indicates rotation to the left side while positive indicates right side rotation.....	65
Figure 6.14. Stress distribution along PLL. Negative moment indicates rotation to the left side while positive indicates right side rotation.....	65
Figure 6.15. Stress distribution along PLL. Negative moment indicates rotation to the left side while positive indicates right side rotation.....	66
Figure 6.16. Stress distribution along ISL. Negative moment indicates rotation to the left side while positive indicates right side rotation.....	67
Figure 6.17. Stress distribution along SSL. Negative moment indicates rotation to the left side while positive indicates right side rotation.....	68
Figure 6.18. Stress distribution of Alar ligament, Transverse ligament and Apical ligament. Negative moment indicates rotation to the left side while positive indicates right side rotation.	68
Figure 6.19. Stress distribution along ALL. Negative moment indicates the spine rotates to the left side while positive indicates the right side rotation.	69
Figure 6.20. Stress distribution along ITL. Negative moment indicates the spine rotates to the left side while positive indicates the right side rotation.....	70
Figure 6.21. Stress distribution along PLL. Negative moment indicates the spine rotates to the left side while positive indicates the right side rotation.	71
Figure 6.22. Stress distribution along CL. Negative moment indicates the spine rotates to the left side while positive indicates the right side rotation.....	71
Figure 6.23. Stress distribution along LV. Negative moment indicates the spine rotates to the left side while positive indicates the right side rotation.....	72
Figure 6.24. Stress distribution along ISL. Negative moment indicates the spine rotates to the left side while positive indicates the right side rotation.....	73
Figure 6.25. Stress distribution along SSL. Negative moment indicates the spine rotates to the left side while positive indicates the right side rotation.	73
Figure 6.26. Stress distribution of Alar ligament, Transverse ligament and Apical ligament. Negative moment indicates the spine rotates to the left side while positive indicates the right side.	74
Figure 6.27. Contact force between facet joints at all levels of cervical spine in flexo-extension rotation.	75
Figure 6.28. Contact force between facet joints at all levels of cervical spine in axial rotation with positive indicating rotation to the right while negative indicating rotation to the left.....	77
Figure 6.29. Contact force between facet joints at all levels of cervical spine in axial rotation. Positive rotation indicates spine rotation to the right while negative indicates the spine rotating to the left. L-side and R-side are set of facet joints on the left and right side of a single vertebra respectively from anterior view.	79
Figure 6.30. Stress distribution along nucleus pulposus in extension (negative moment) and flexion (positive moment).....	80
Figure 6.31. Total force in the annulus fibrosus at each levels.	81
Figure 6.32. Stress distribution along nucleus pulposus in axial rotation, positive moment indicates spine turning to the right and negative moment indicates spine turning to the left.	82
Figure 6.33. Total force in the annulus fibrosus at each level.	82
Figure 6.34. Stress distribution along nucleus pulposus in lateral bending, positive moment indicates spine rotating to the right and negative moment indicates spine turning to the left.	83
Figure 6.35. Total force in the annulus fibrosus at each levels.	83
Figure 7.1. High stress region in ligamentum flavum in flexion rotation at 1 N·M.....	86
Figure 7.2. High stress region in supraspinous ligament in flexion rotation at 1 N·M.....	87
Figure 7.3. Front view of high stress region in ALL in positive axial rotation at 1 N·M.....	88
Figure 7.4. Front view of high stress region in ALL in positive lateral bending at 1 N·M.....	90

List of Tables

Table 2.1 Range of motion of the spine in response to different mechanical load. Flexo-extension combined the rotation of both flexion and extension movement, also, values for axial rotation and lateral flexion summate both right and left sides.....	25
Table 3.1. Number of nodes and 8-node elements for each vertebra component at each level.	31
Table 4.1. Showing the disc area and the ratio of nucleus to the total area as well as annulus and nucleus areas. All units are in mm ²	40
Table 4.2. Element type and number of elements used for each part.	42
Table 4.3. Material properties of the created model.	43
Table 4.4. Annulus and fibers area at each level.	44

1 Background and motivation

Cervical spine relies on soft tissues to establish stability as well as providing flexibility to the spine. When it comes to the soft tissues, ligaments are the main components of the soft tissues that help in bonding vertebrae together and preventing excessive movement that may lead to injuries. Ligament tear is a common injury in the spine as it occurs due to extreme straining in the ligaments. Sport activities, car accidents, and sudden movement are the main reasons for such injuries Cameron R. Bass et al., (2007). Most of the time, the injury is located in the ligaments as being the soft tissue and it would tear under excessive loading cases N. Yoganandan et al., (1989).

There had been many studies addressing the ligament injuries such as in vivo and in vitro experiments. However, these test studies resulted only in range of motion of the spine under certain types of loads. These studies failed in reporting the local stress in the ligaments due to lack of instruments that would enable to measure the stress. Some factors that would affect the obtained results are specimen age, sample preparation, number of units being tested and loading protocol. In addition, in vitro studies are difficult to carry as it is hard to find healthy samples.

With the finite elements analysis software, it was possible to create models that would imitate the spine behaviour. There had been many models that would simulate the spine for a better understanding of the load sharing among the individual spine components. One of the critical components is the ligaments. Most of the models used the same technique in constructing ligaments, and it was done by using 2 node elements. The created spring elements would help in predicting internal axial loads and strain. However, it would fail in simulating the stress initiation and failure mode in the ligaments. Therefore, ligaments have to be modeled in a different way that would enable to calculate the stress value and stress distribution.

The main objective of this study is preparing bio-realistic and fine meshed elements that would represent ligament members in cervical spine region. This model allows visualization of the initiation and path prediction of the stress in the internal members of the soft tissues such as ligaments subject to external loads. Using this model would help in predicting injury mechanism and finding methods to prevent or minimize the exposure to injuries.

The created model in this study would be using an accurate geometry of the spine for obtaining an enhanced response of the cervical spine. Material property variability was found during in-vitro experimental tests would be a useful tool in enhancing the model's ability to mimic the in vitro reported data under static loading case M. Shea et al., (1991). Furthermore, the model would take into account the proper loading protocols such as the applied moments and boundary conditions that carried during in vitro investigations.

The current model would be validated against in vitro studies as six moments would be applied on three different planes. These moments are flexion, extension, axial rotation in both directions and lateral bending in both directions as well (positive and negative moments). Under these loadings, the stress distribution would be studied among the spine components; ligaments, intervertebral disc and facet joint. It also helps in predicting the contribution of each individual component in resisting each moment.

Once the model is ready and validated, it could be used for other applications such as injuries sustained during a car accident, direct impact on the head from sport activities like football and many other applications where the spine would be the main focus.

2 Introduction to Cervical Spine Anatomy

2.1 Anatomy and Function of Human Spine

The backbone or vertebral column is a bony structure that serves as a locus for all the other body bony parts that are connected to it. For example, skull on the top end rests on the spine, rib cages are fused at the mid height part of the spine along with the collarbone that is connected to the shoulder blades at the other end. From the bottom, the spine sits on coxa (hips) which itself is jointed to the two lower limbs (legs) as shown in Figure 2.1. (Kim, 2013).

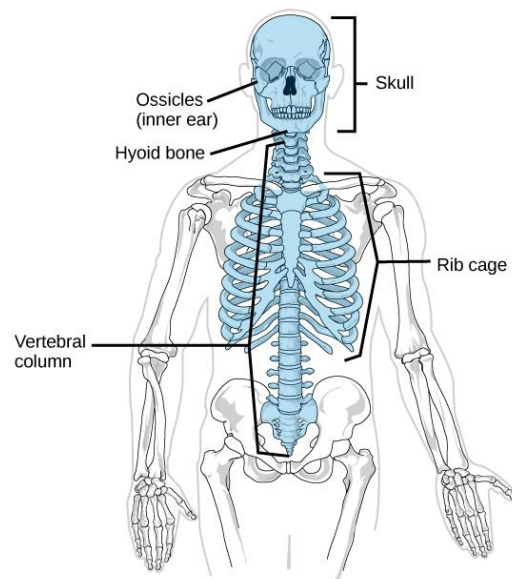


Figure 2.1. Axial skeleton. From “Human Axial Skeleton,” by OpenStax College, 2013, [http://cnx.org/resources/40030aca8b222cf06c673422c5307f904a45fd04/Figure 38 01 04.jpg](http://cnx.org/resources/40030aca8b222cf06c673422c5307f904a45fd04/Figure_38_01_04.jpg). Copyright 2013 by OpenStax College.

Besides linking all the major bony structures together, the spine has two other major functions; One of them is supporting the upper body weight as it tends to link them to the lower limbs and the second one is acting as a shield for the highly sensitive nerve cord that passes through it. (Kim, 2013).

In the study of vertebral column anatomy, the back bone is divided into five regions; the thirty-three vertebrae of the spine are separated into each region according to the functions they perform. Vertebrae in each section collaborate together achieving certain tasks. In total, human vertebral column consists of 33 vertebrae. The upper-most (closest to the skull) region is the

cervical spine and consists of seven vertebrae. Below the cervical spine lies the twelve vertebrae of the thoracic spine. The region under thoracic is called lumbar spine. It consists of five vertebrae in total. The very bottom part is the trunk and it is made of sacral and coccygeal spines. Sacral is formed by five vertebrae fused together acting as one unit and it is tailed by a single and small in size vertebra, coccygeal. Figure 2.2 shows full vertebral column and the subdivided regions. (Kim, 2013).

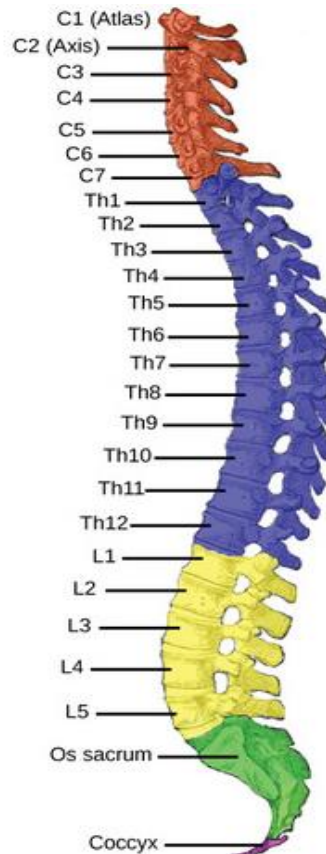


Figure 2.2. Different regions of the human spine. From “Vertebral Column,” by OpenStax College, 2013, http://cnx.org/resources/5934b9fecf14874c1ec99a57ec73b9c9648fd5ae/Figure_38_01_07.jpg. Copyright 2013 by OpenStax College.

In Figure 2.2, the red colored region is referred to as cervical spine and it consists of 7 vertebrae C1-C7. From the top, it is attached to the skull through occipital joint. From the bottom, it is attached to the thoracic spine. The safety of the cervical spine is very critical whether to the function of the spine itself or to the rest of the body. (Kim, 2013).

The function of the cervical spine is very essential as it provides stability to the head as well as load sharing with the rest of the spine. As the head is being located on the top of the cervical spine, it exerts a compressive load due to the weight of the head. The role of the cervical spine especially the very top vertebra is safely transferring the compressive load down the spine as well as securing the head on top preventing it from slipping. The skull is connected to C1 (atlas) by occipital joint, which is a synovial joint. the Atlanto-occipital joint allows skull only movement to some range, the osteokinematics of Atlanto-occipital joint are in flexion 10 degrees while 20 degrees in extension, and 8-10 degrees in lateral flexion. (Kim, 2013).

Another important function of the spine especially the cervical spine is protecting the nerve system. The nerve fibers that branch out the cervical spine through neural foramen gaps between each motion segments (two adjacent vertebrae) as shown in Figure 2.3. (KenHub, 2013)

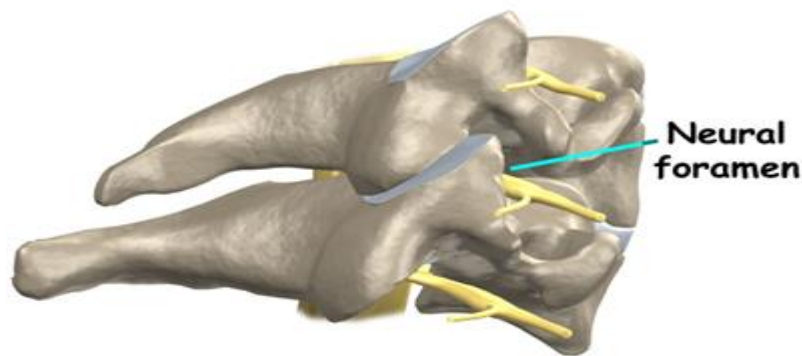


Figure 2.3. Neural foramen. From “Cervical Spine Anatomy,” by Medical MultiMedia Group, 2002, <http://eorthopod.com/cervical-spine-anatomy/>. Copyright 2002 by Medical MultiMedia Group.

2.2 Cervical Spine Anatomy

Cervical spine is the upper part of the human spine. The skull sits at top joining on the first vertebrae C1 through occipital condyle joint. At the bottom, an intervertebral disc joins last vertebrae C7 with the first thoracic vertebrae along with ligaments and muscles. Figure 2.4 shows the cervical spine. (Kopt-Maier, 2005)

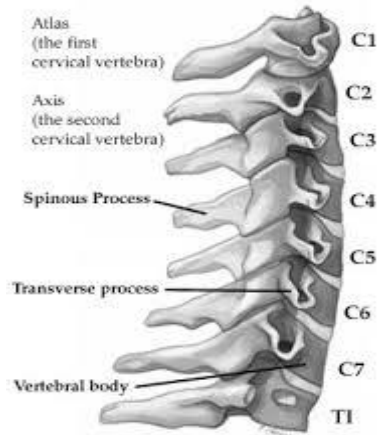


Figure 2.4. Structure of the cervical spine. From “Cervical Spine Fractures,” by Parker, L., <http://www.hughston.com/hha/a.cspine.htm>. Copyright by Parker, L.

As mentioned earlier, the cervical spine consists of seven vertebrae connected together by intervertebral discs and ligaments along with muscles. All vertebrae have the same geometry and shape except for the first two vertebrae which the geometry is completely different. The difference exists between them due to their role in the movement of the head. C3 and down the spinal column have the same structure, however they vary in size, vertebrae get bigger in size as moving down the spinal cord. (Kopt-Maier, 2005)

2.2.1 C1 (Atlas)

It is the most top vertebrae in the spinal column as it is unique in its shape and structure. Atlas, unlike the other vertebrae, does not have vertebral body. Atlas is constructed basically from two arches, anterior and posterior arches. These two arches fused together to form C1 vertebrae and they make the shape of a ring. Anterior arch is convex at its front tip. At this point, anterior tubercle presents providing area for anterior longitudinal ligament and Longus colli muscles attachment. As there is anterior tubercle, there is also posterior tubercle at the convey part of the posterior arch. This area is for the attachment of ligaments and muscles and its function is preventing interference between atlas and skull movement as shown Figure 2.5, C1 (atlas) Bogduk et al., (2000).



Figure 2.5. Atlas vertebra. From “Atlas,” by The Chiropractic Resource Organization, 2016, <http://www.chiro.org/chimages/diagrams/>, Copyright 2016 by The Chiropractic Resource Organization.

Atlas supports head from the top and rest on top of C2 (axis). Atlas has two facets on the superior surface for the occipital condyles of the skull to rest on. These facets are concave inwards while the occipital condyles are convex. As mentioned earlier, this joint provides nodding movement (flexion-extension) as well as lateral flexion and axial rotation which is associated with flexion-extension rotation. In the Figure 2.6, part “A” shows Atlanto-occipital joint Bogduk et al., (2000).

On the inferior face, there are two smooth articulating facets that mount onto another two facets on top of the C2 vertebra (axis) as shown in the Figure 2.6 part “B”. This joint articulates atlas with axis allowing the head side to side movement. Between atlas and axis, there is no intervertebral disc like the rest of the cervical spine vertebrae Bogduk et al., (2000).

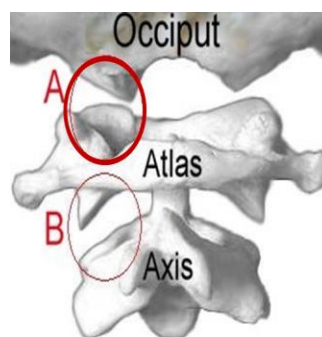


Figure 2.6. Atlas-occipital joint. From “Atlanto occipital Joint,” by Dugan, L., 2011, <http://www.chiropractic-help.com/Atlanto-Occipital-Joint.html>. Copyright 2011 by Dugan, L.

On the two side of the facets, there are lateral projection of bony structure. This projection is called transverse process. Each transverse process has a hole in it for the passage of the vertebral artery and this hole is called transverse foramen as shown in the following Figure 2.7 Bogduk et al., (2000).

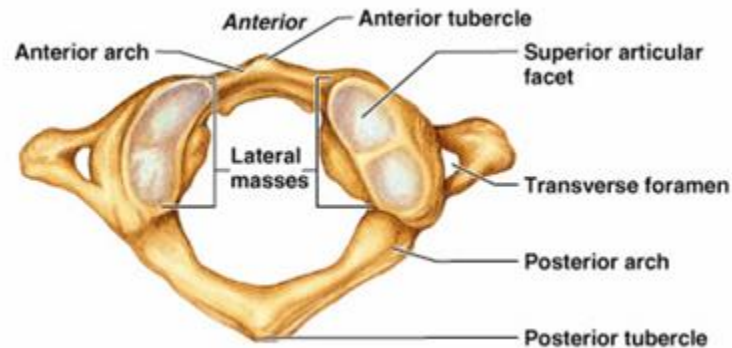


Figure 2.7. Transverse process on each side of the atlas vertebra. From “ANTPHY 1 Study Guide,” by Williamson, 2011, <https://www.studyblue.com/notes/n/antphy-1-study-guide-2011-12-williamson-/deck/9727461?blurry=e&ads=true>. Copyright 2011 by Williamson.

At the posterior aspect of the anterior arch, odontoid is held tight to it by the alar ligament. Odontoid is an upward projected part from axis that is attached to atlas. Odontoid acts as pivot point at which atlas rotates about enabling head to rotate. Another name for odontoid is dens as shown in Figure 2.8 Bogduk et al., (2000).

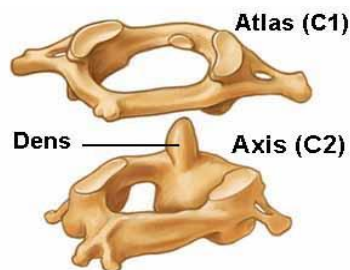


Figure 2.8. Odontoid (dens). From “Vertebral Column,” by Bridwell, K., 2016, <http://www.spineuniverse.com/anatomy/vertebral-column>. Copyright 2016 by Bridwell, K.

2.2.2 C2 (Axis)

At this level, vertebrae tend to shape more like a normal vertebrae; having a vertebral body and spinous processes. Although the vertebral body is very small in size and barely developed, but it can be clearly noticed. One additional prominent part that distinguish axis from the rest of the vertebrae is that it has a vertically upward bony projection called odontoid or dens. Dens goes

right through the atlas and is affixed to the posterior part of the anterior arch. Dens is held in place by two main ligaments; alar and transverse ligaments. From the bottom, dens is fused to the vertebral body of C2 (axis) Bogduk et al., (2000).

Vertebral body is relatively small comparing to the rest of the vertebrae, C3 and down the cervical column. It is cylindrical in shape; it is thicker in the front and is prolonged downward. This prolongation overlaps the anterior superior surface of the vertebral body in the vertebra underneath. Vertebra is a composed of two different density bone, cortical and cancellous bones. Cortical bone is the outer layer since it is denser and the rigid one Bogduk et al., (2000).

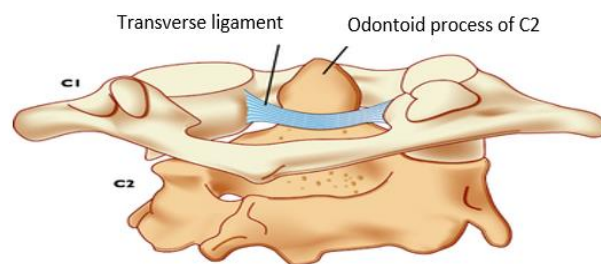


Figure 2.9. Odontoid held in position by transverse ligament. (Hata, T., 2005).

From the vertebral body, two arches extend posteriorly on each side. It starts with pedicles and then develops into lamina. At the end point or joint point between the two laminae, a small bony structure exists and it is called spinous process. Pedicles are two transversely projected processes that provide area for the attachment of ligaments and muscles. Pedicles have hole in them called transverse foramen. The objective of these holes is serving as passage for the vertebral artery Bogduk et al., (2000).

At the junction of the laminae is where spinous process is formed. At this level, the spinous process is considered very small and it develops into larger sizes as moving down the spinal column. Spinous process has two main functions. The first one is maintaining area for the muscles attachments. Since most of the back muscles are attached to the spinal column through this part of the spine. The second purpose is resisting the flexion of the head through intervertebral ligaments between spinous processes Bogduk et al., (2000)

On the superior surface, there are two smooth facets. These facets are convex surfaces articulating with convex surfaces of the inferior facets of atlas. On the inferior surfaces there are also another two facets. However, they are not smooth as the superior ones. These facets are

projections from lamina and pedicle joint point. The surfaces of these facets are covered with cartilage and each joining point is contained in a capsule called synovial joint. Figure 2.10 shows the various parts of the C2 (axis) Bogduk et al., (2000).

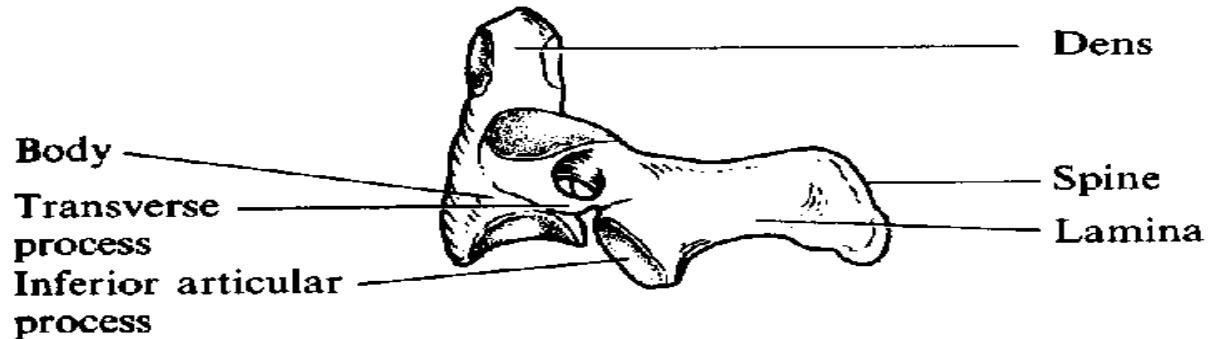


Figure 2.10. Side and plan views of C2 axis. From “The Axis Vertebra,” by Galileo Site Manager, 2016, <http://www.edoctoronline.com/medical-atlas.asp?c=4&id=21631>. Copyright 2016 by Galileo Site Manager.

2.2.3 C3 - C7

Vertebrae from C3 and down have the same geometry except the vertebra gets bigger in size. Just like the top two vertebrae, they have holes in the middle for the nerve system cord passing through them as they tend to protect them. This hole is called vertebral foramen as shown in Figure 2.11. This hole is surrounded by vertebral body in the anterior aspect. Vertebral body takes kidney shape and it gets larger moving down the spinal column. All the bony structures are made of two composite materials, the strong outside layer and inner soft material. The outside bone is made of hard rigid material and called cortical bone, providing protection to the cancellous bone which forms the inner, less dense and soft part of the bone (Kopt-Maier, 2005).

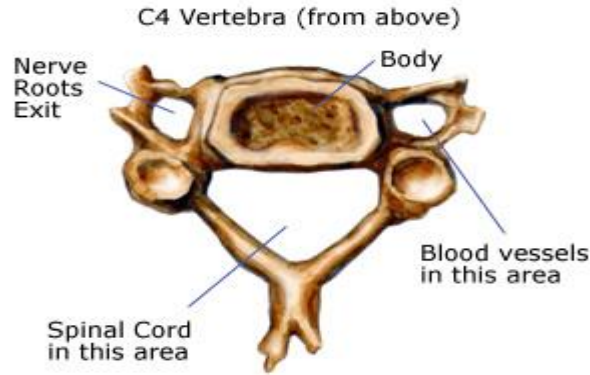


Figure 2.11. Vertebral body. From “Cervical Spine Anatomy Animation,” by Vertical health, 2014, <http://www.spineuniverse.com/anatomy/cervical-spine-anatomy-animation>. Copyright 2014 by Vertical health.

From the vertebral body, two broad plates extend posteriorly, called vertebral arches. These vertebral arches are made of strong, tubular bone named Pedicle, and broad plate bone named Lamina. Vertebral arches exist on both sides of the sagittal plate. Arches (pedicle and lamina) are made of two composed bones. Similar to those of the vertebral body, they are cortical bone on the outside, and cancellous bone on the inside (Kopt-Maier, 2005).

At the posterior aspect of laminae, a small bony ridge structure attaches the two arches. This bone is referred to as spinous process. Spinous processes at each motion segments are connected to each other with interspinous ligament, as shown in Figure 2.12 (Kopt-Maier, 2005).

All vertebral bodies have two transversely projected processes. The function of these processes is providing areas for ligament and muscles attachment. In cervical spine region, these processes have a canal in them, it is called foramen. The purpose of this hole is for vertebral artery and vein to pass through. Similar to spinous processes, there are intertransverse ligaments connecting them together. As shown in the Figure 2.13. On the outer circumference of the transverse process, there are two small bumps called the anterior and posterior tubercles (Kopt-Maier, 2005).

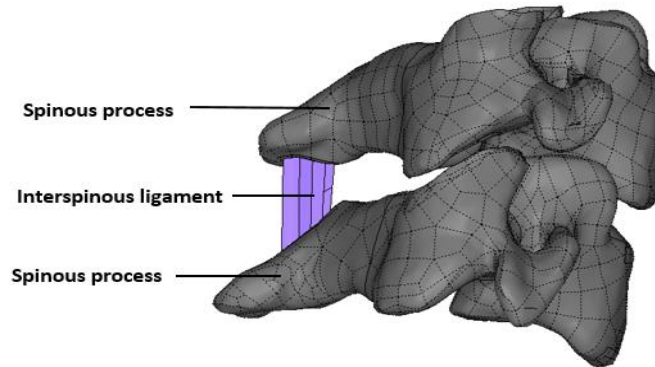


Figure 2.12. Spinous processes connected by interspinous ligament.

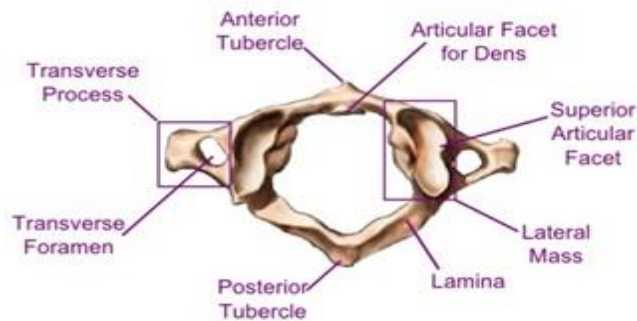


Figure 2.13. Transverse process of cervical vertebra. From “Atlas-C1 vertebra,” by The art of medicine, 2015, <https://theartofmed.wordpress.com/2015/06/05/c1-vertebra-atlas-and-accompanying-structures/>. Copyright 2015 by The art of medicine.

Pedicle from inferior vertebra form some sort of foramen with pedicles from the superior vertebra. This canal is called intervertebral or neural foramen, which through it passes the spinal nerve and it branches out and reaches to rest of the body (Kopt-Maier, 2005).

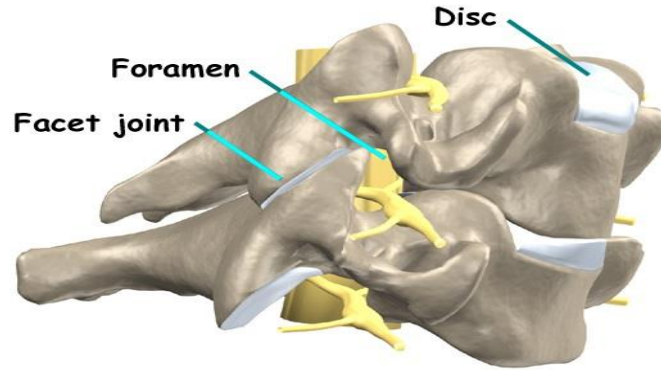


Figure 2.14. Intervertebral foramen (foreman). From “Cervical Spine Anatomy,” by Medical MultiMedia Group, 2002, <http://eorthopod.com/cervical-spine-anatomy/>. Copyright 2002 by Medical MultiMedia Group.

There are four facets processes on each vertebra, two on each side of the vertebral body. These facet processes are located at the joining point of the pedicle and lamina and they stick out superiorly and inferiorly. Basically, Two facet processes on the left side, one pointing upwards and the other one pointing downwards. Each one of those facet processes articulate with another facet process from superior or inferior vertebrae, depending on the position on the facet process. This articulation is called facet joint. Facet joint play very important role in the rotation process of the cervical spine; as they limit the rotation, as well as transferring loads. Besides, it prevents some sort of movements that are detrimental to the spinal cord. These movements are based on the orientation of the facet joint. Facet processes are bony structures and same as any bone of the vertebra, it is made up from cancellous bone from inside and it is contained by cortical bone layer from outside. Facet processes grinding onto one another will cause damage and will be painful, thus the surfaces of the facet joints are covered by cartilage that provides smooth gliding. Also, capsule joints are covered by connective tissues (synovial membrane) (Berovic, 2015).

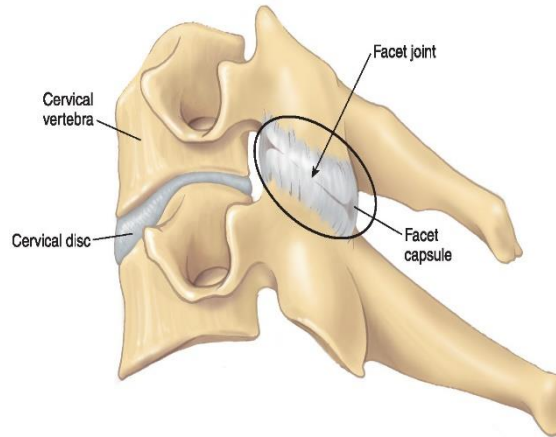


Figure 2.15. Facet joint. From “Spinal facet joint,” by Berovic, M. 2015, <http://www.claphamsportsmassage.com/spinal-pain-what-is-it/>. Copyright 2015 by Berovic, M.

2.2.4 Intervertebral Disc

The intervertebral disc is a soft tissue that lies between each two adjacent vertebrae. All vertebrae have a disc in-between them except atlas and axis as mentioned earlier. The disc looks differently viewing it from different planes. In the transverse plane, it looks like a kidney, while in frontal plane, it looks like a rectangular, and viewing it from median plane, it looks thicker anteriorly than posteriorly. Intervertebral disc gets thicker as size of vertebra gets larger, mainly the size of the vertebral body. For example, in the cervical region, the average thickness of disc is 3 mm, in thoracic region is 5 mm and, in lumbar region 9 mm in fully grown spinal column, the disc makes about 20% of the total length of the spine (Shapiro, 2014).

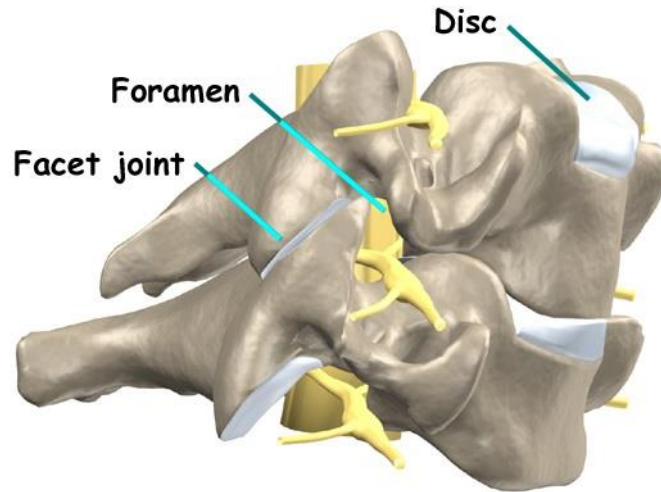


Figure 2.16. Intervertebral disc. From “Cervical Spine Anatomy,” by Medical MultiMedia Group, 2002, <http://eorthopod.com/cervical-spine-anatomy/>. Copyright 2002 by Medical MultiMedia Group.

Intervertebral disc is made up of two materials in two layers. The outer layer is called annulus and it is made of fibrous tissues. Another name for it is fibrous ring. The core of intervertebral disc is called nucleus pulposus. Annulus fibrosus consists of many layers, the most outer layer is a thin ring of fibrous tissue, while inner ring is a fibrocartilage board layer. Fibrocartilage portion, the inner layers, is made up of a number of concentric layers. Annulus fibrosus layers are made up of collagen fibers and these fibers run in the same direction in one layer but in a different direction in the next layer. Annulus fibers make about 25 degrees with the horizontal axis (Palomar et al., 2007).

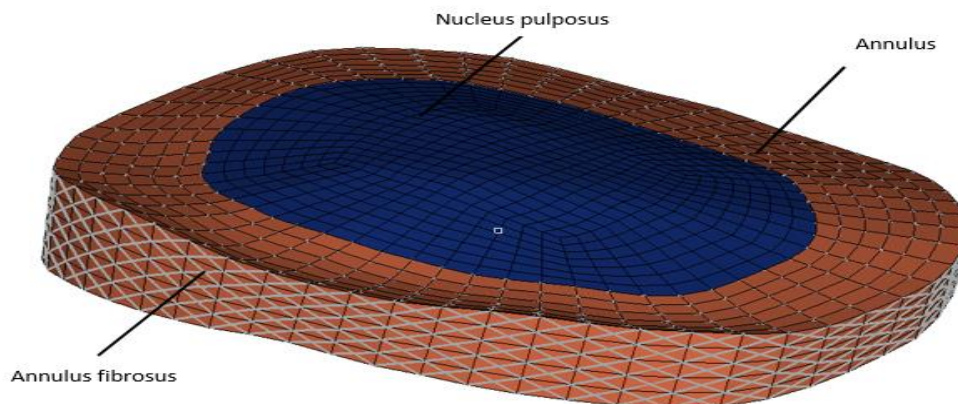


Figure 2.17. Different parts of intervertebral disc.

Nucleus pulposus is the core of the intervertebral disc. It consists of an outer layer surrounding a gel like material; mainly made of water and it is called proteoglycan gel. This material enables the nucleus pulposus to absorb a large amount of liquids especially water (Shapiro, 2014)..

Intervertebral disc absorbs water in all its layers, but nucleus pulposus has a tendency to absorb more than annulus. It uses a special technique called osmotic swelling pressure (OSP). Usually, 80-90 % of the nucleus is filled with water that has been absorbed from adjacent vertebral bodies. As water being absorbed by nucleus pulposus, it expands in size and exerts pressure in the annulus and vertebral bodies. However, this expansion is limited. This absorption happens when the pressure on the disc is limited or the person is in relaxing position (Shapiro, 2014).

2.2.5 Ligaments

Ligaments are made up from connective tissues that tend to connect two or more bones together. The connective tissues are bunch of small parallel running collagenous fibers. Those fibers tend to be very elastic and flexible. As they are made of fibers, ligaments are active in tension only. The main function of ligaments is providing stability to the spine as they hold bones in place. Also, they play a major role in defining the range of motion at each level. In the spinal movement, there is at least one single ligament involved in the motion limitation (Clark, 2005).

In cervical spine there are various ligaments that help stabilizing the vertebrae in place as well as resisting tension forces and limiting the range of motion. Most of the ligaments in the cervical spine are a continuous bundle running down the spine, starting at the bottom surface of the skull and continue down the spine. Ligaments like anterior longitudinal ligament, posterior longitudinal ligament, ligamentum flavum, interspinous ligaments, supraspinous and many other ligaments run all the way from skull down to the rest of the spine (Clark, 2005).

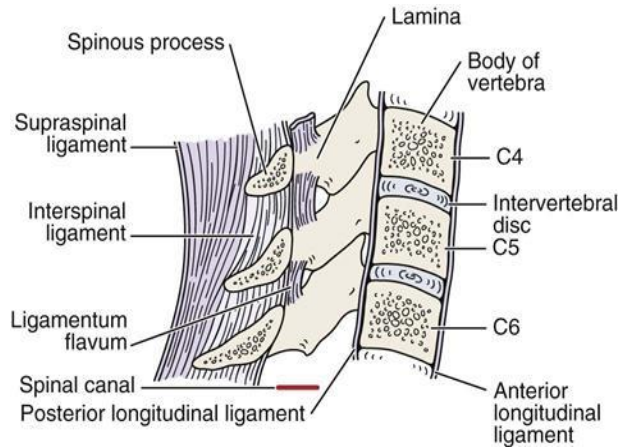


Figure 2.18. Different ligaments in the cervical spine region. From From “Cervical Spine,” by Warrior, W., 2015, <http://clinicalgate.com/cervical-spine-3/>. Copyright 2015 by Warrior, W.

Cervical spine has some ligaments that do not exist in the other regions of the spine and that is due to the unique geometry of the top two vertebrae. Ligaments like transverse ligament, alar ligament, tectorial membrane, apical ligament, Atlanto-occipital ligaments and many others that help holding the top vertebrae in place. Figure 2.19 shows the unique ligaments in skull-atlas and atlas-axis joints (Clark, 2005).

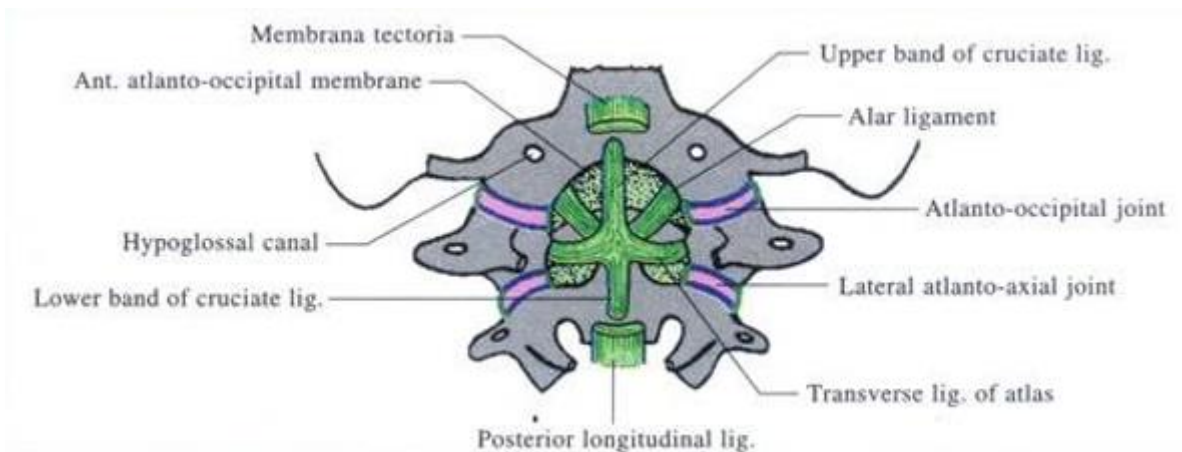


Figure 2.19. Different ligaments at skull-atlas and atlas-axis joints (viewed from behind). From “The Cervical Vertebrae; Inter-Vertebral and Cranio-Vertebral Joints,” by Pujari, S., 2015, <http://www.yourarticlelibrary.com/biology/human-beings/the-cervical-vertebrae-inter-vertebral-and-cranio-vertebral-joints-human-anatomy/9514/>. Copyright 2015 by Pujari, S.

Atlanto-occipital ligament: connects atlas to the occipital bone. It joins the anterior arch of the atlas with the anterior superior part of occipital bone. It helps in limiting extension movement

along with the anterior longitudinal ligament. Figure 2.20 showing the location of the Atlanto-occipital ligament (Clark, 2005).

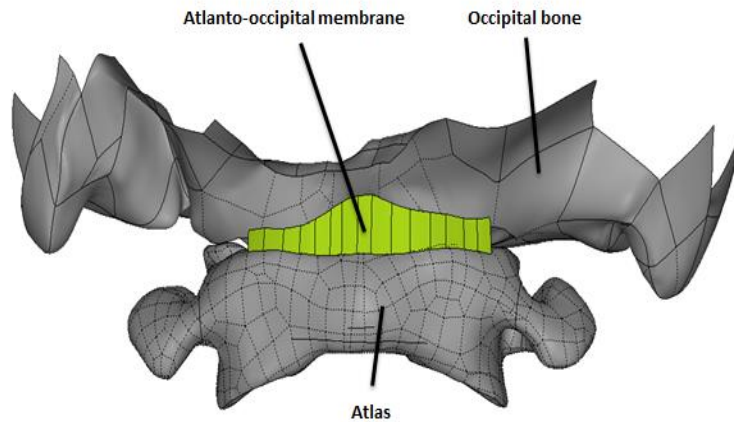


Figure 2.20. Frontal view of Atlanto-occipital ligament.

Apical ligament: it is a small band that spans from inferior part of the occipital bone down the tip of the odontoid (dens). It helps holding the odontoid in place as it helps in stabilizing craniocervical junction (Clark, 2005).

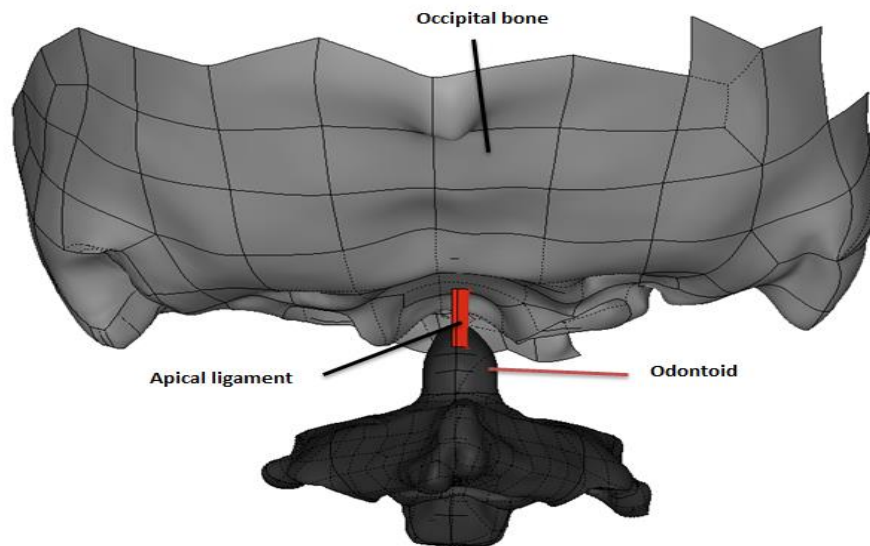


Figure 2.21. Posterior view of apical ligament.

Alar ligament: made of two parts extending from both sides of the odontoid. They link odontoid to the medial aspect of the occipital condyles. They play a role in limiting the rotation of the upper cervical spine and lateral flexion movement as well as, stabilizing the atlas and axis motion segment (Clark, 2005).

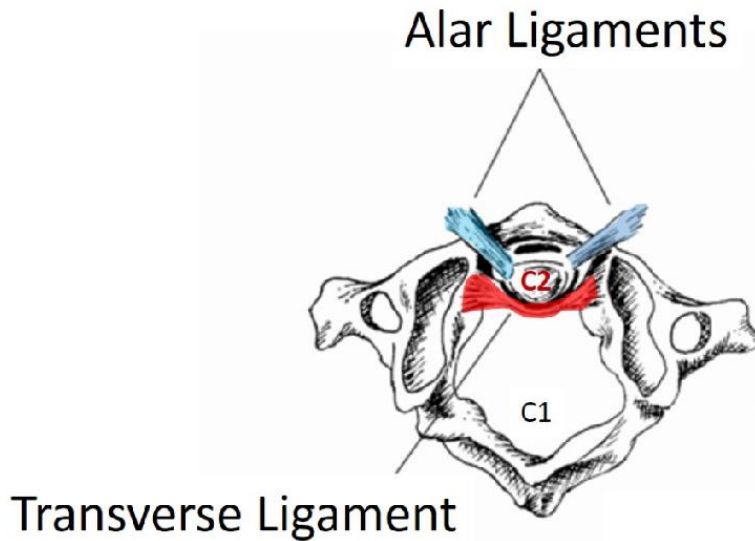


Figure 2.22. Top view of Alar ligament. From “Alar Ligament Treatment for CCJ Instability,” by Centeno, C., 2015, <http://www.regenexx.com/alar-ligament-treatment/>. Copyright 2015 by Centeno, C.

Transverse ligament: a long thick band that runs on the inside wall of the anterior arch of atlas from one side to another passing on the posterior face of odontoid. The function of transverse ligament is pushing on odontoid against the inside wall of the anterior part of atlas providing stability to the joint. Figure 2.23 showing the transverse ligament (Clark, 2005).

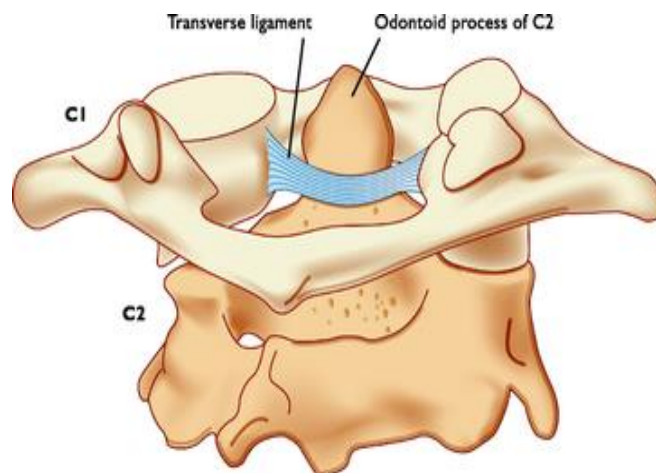


Figure 2.23. Posterior view of Transverse ligament. (Hata, T., 2005).

Anterior longitudinal ligament: a broad band running from C1 down to lower part of the spine. It is a continuous band of fibers that is attached to the vertebral bodies of the vertebrae as well as the intervertebral disc. Anterior longitudinal ligament plays a role in limiting the extension of the spine (Clark, 2005).

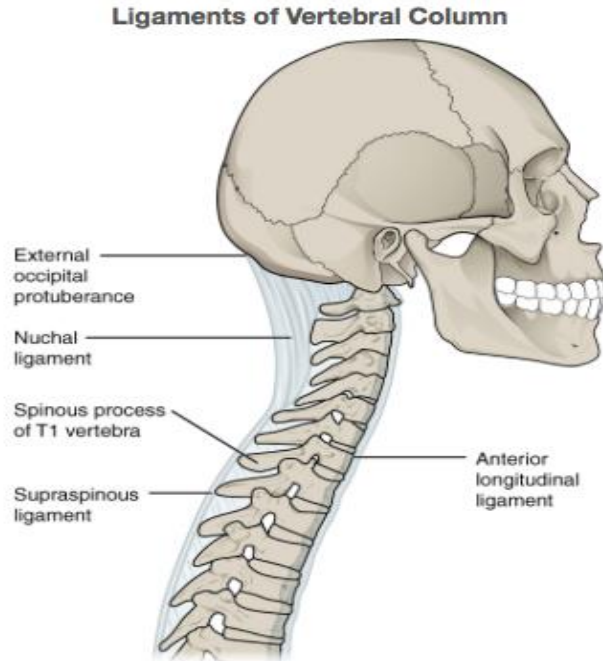


Figure 2.24. Side view of anterior longitudinal ligament. From “Supraspinous Ligament,” by Sareen, A., 2014, http://www.physio-pedia.com/File:Supraspinous_lig.jpg. Copyright 2014 by Sareen, A.

Posterior longitudinal ligament: similar to the anterior longitudinal ligament, it is a broad thick ligament running on the posterior surface of the vertebral body starting at Atlas and extending down the spinal column. The function of the posterior longitudinal ligament is supporting the intervertebral disc as well as limiting flexion and extension movement of the spine (Clark, 2005).

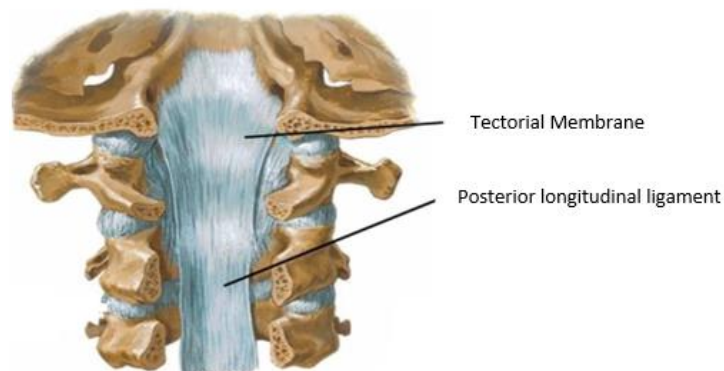


Figure 2.25. Posterior view of Posterior longitudinal ligament. From “Roof of neck,” by Megan L. 2014, <https://www.studyblue.com/notes/note/n/4-root-of-neck/deck/9360518>. Copyright 2014 by Megan L.

Ligamentum flavum: a long thick band of fibers made up from two lateral parts that run from axis down to the sacrum spine. They are located on the anterior surface of the laminae as they extend from root of articular process backwards to the point where laminae meet. The function of the ligamentum flavum is connecting vertebrae together and limiting the flexion of the spine (Clark, 2005).

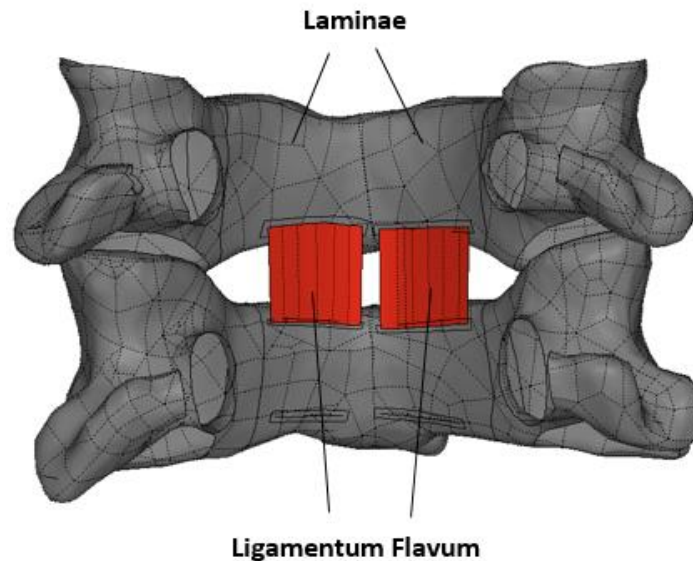


Figure 2.26. Frontal view of Ligamentum flavum.

Interspinous ligament: a thin layer of fibers that connect two adjacent spinous processes together. They join ligamentum flavum anteriorly and blend with supraspinous ligament posteriorly. Interspinous ligaments are active in flexion as they tend to limit the movement. Also, they contribute in limiting the rotational movement of the spine (Clark, 2005).

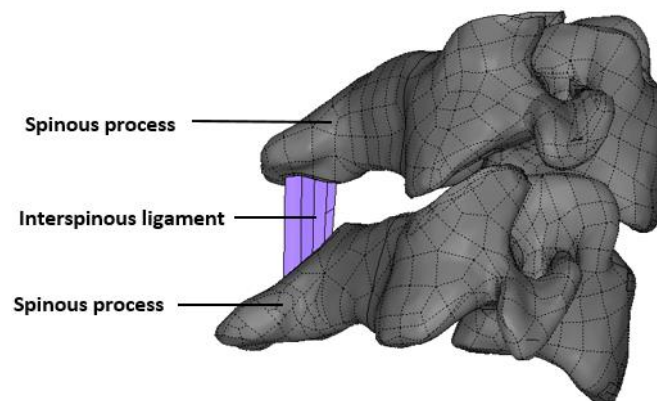


Figure 2.27. Side view of Interspinous ligament.

Nuchal ligament: thin layer of fibers running from inferior part of the occipital bone down to the last cervical spine vertebra (C7). It is attached to the interspinous ligament as well as the spinous process as it helps stabilizing vertebrae and limiting flexion (Clark, 2005).

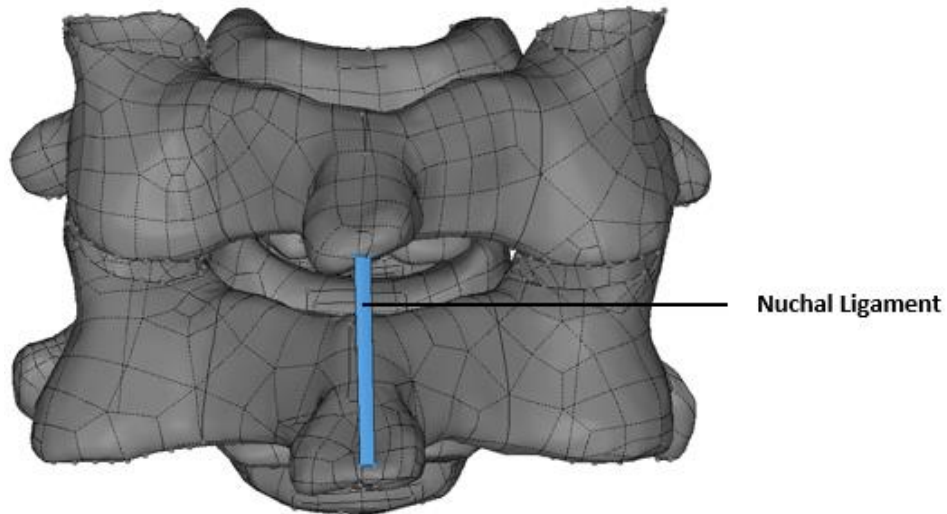


Figure 2.28. Posterior view of Nuchal ligament.

Intertransverse ligament: small straps of fibers that exist between transverse processes of vertebrae. They are disconnected at each vertebra. They play a role in resisting lateral flexion of the spine (Clark, 2005).

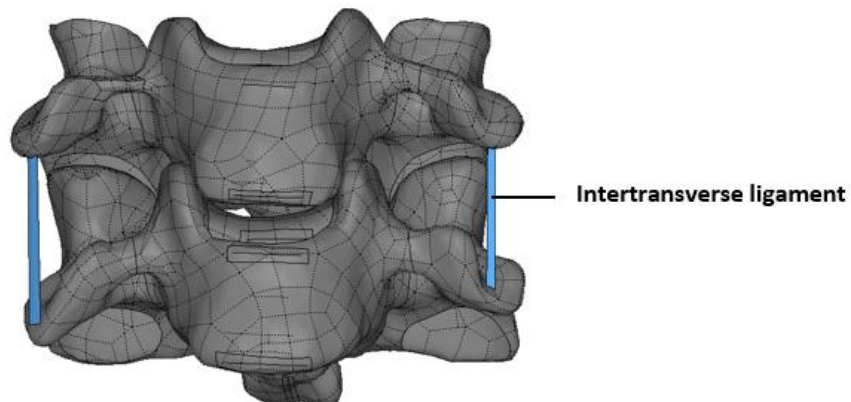


Figure 2.29. Frontal view of Intertransverse.

Capsular ligament: it forms a ring around the facet joint. Made up of small band of fibers that surround the facet joint on each side of motion segment and it is separated at each vertebra. It

helps in preventing the facets from sliding off each other as well as flexion and extension of the spine. It also plays a role in axial rotation and lateral flexion of the spine (Clark, 2005).

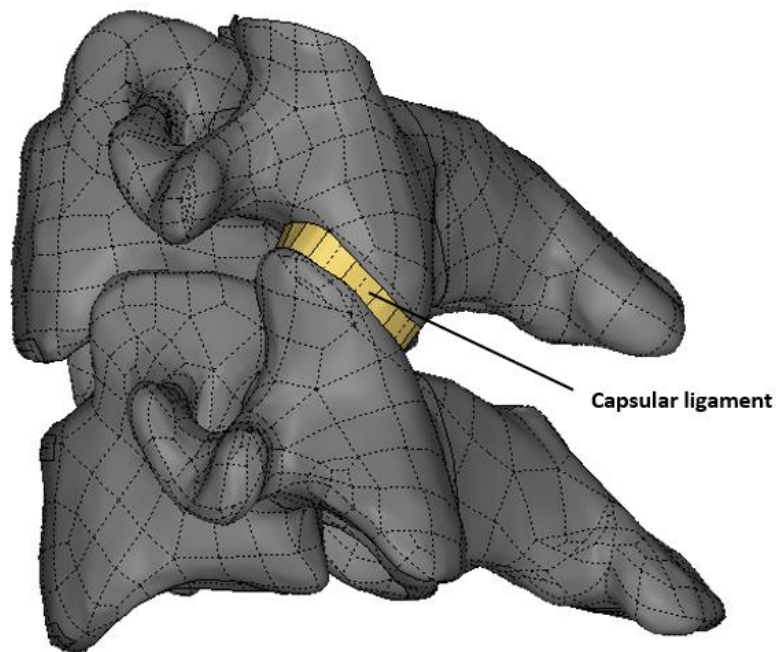


Figure 2.30. Side view of Capsular ligament.

2.3 Planes of Motion

In this study, three different planes were used to explain the position of the structures and the direction of the load as shown in the following Figure 2.31. The three different planes are sagittal (Median) plane, transverse plane, and frontal plane. Sagittal plane cuts through the body into two symmetric halves (left and right halves). Transverse plane runs through abdominal, separating the body into upper and lower parts. The last plane, frontal plane separates the body into front part and back parts. Figure 2.31 illustrates the three different planes.

Flexion and extension moments act in the sagittal plane. Flexion moment tends to force the spine to move forward in the sagittal plane while extension acts in the opposite direction making the spine move backwards. The second type of moment that acts in the transverse plane is axial moment. Axial moments force the spine to rotate axially to the left or right based on the applied moment. Moment in the other plane makes the spine lean to the left or to the right according to the applied moment.

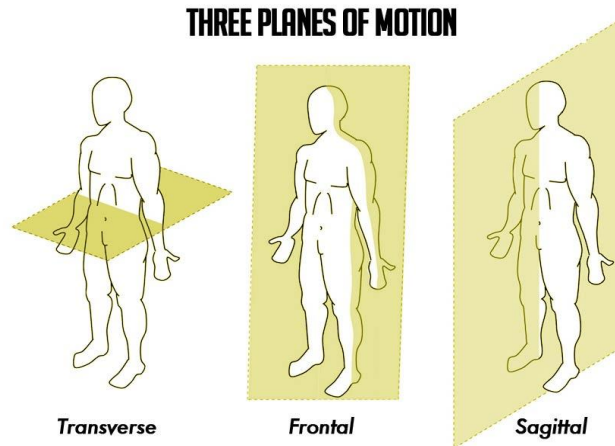


Figure 2.31. Three different planes used in the anatomy of the human body. From “Find your direction,” by Dyke, J., 2014, <http://www.crossfitsouthbay.com/find-your-direction/>. Copyright 2014 by Dyke, J.

2.4 Range of Motion of the Cervical Spine

Cervical spine has the ability to move in all directions due to its geometry. However, there is a limit to the movement that is exerted by the ligaments and muscles to avoid dislocation of the vertebrae.

There have been many studies on the range of motion under certain loading scenarios. Most of the studies conducted a 1 N·m of moment on the spine and reported the behaviour and rotation at each level. The applied moment was directed in 6 different directions on three different planes: flexion and extension in sagittal plane, axial rotation left and right on transverse plane while lateral flexion to the right and left on frontal plane. The following Figure 2.32 shows the different movement of the head according the three planes of motion.

Based on reported data, the average flexion and extension rotation of the spine under 1 N·m at each level is reported in the following table along with axial rotation and lateral flexion. In most of the studies, the spine consisted of T1 serving as the base for the model. While all the finite element models had modeled all the vertebrae, except for the experiments that had been conducted in lab, some samples had atlas and axis missing while others had only axis missing and some others had all the vertebrae from atlas down to T1 vertebra.

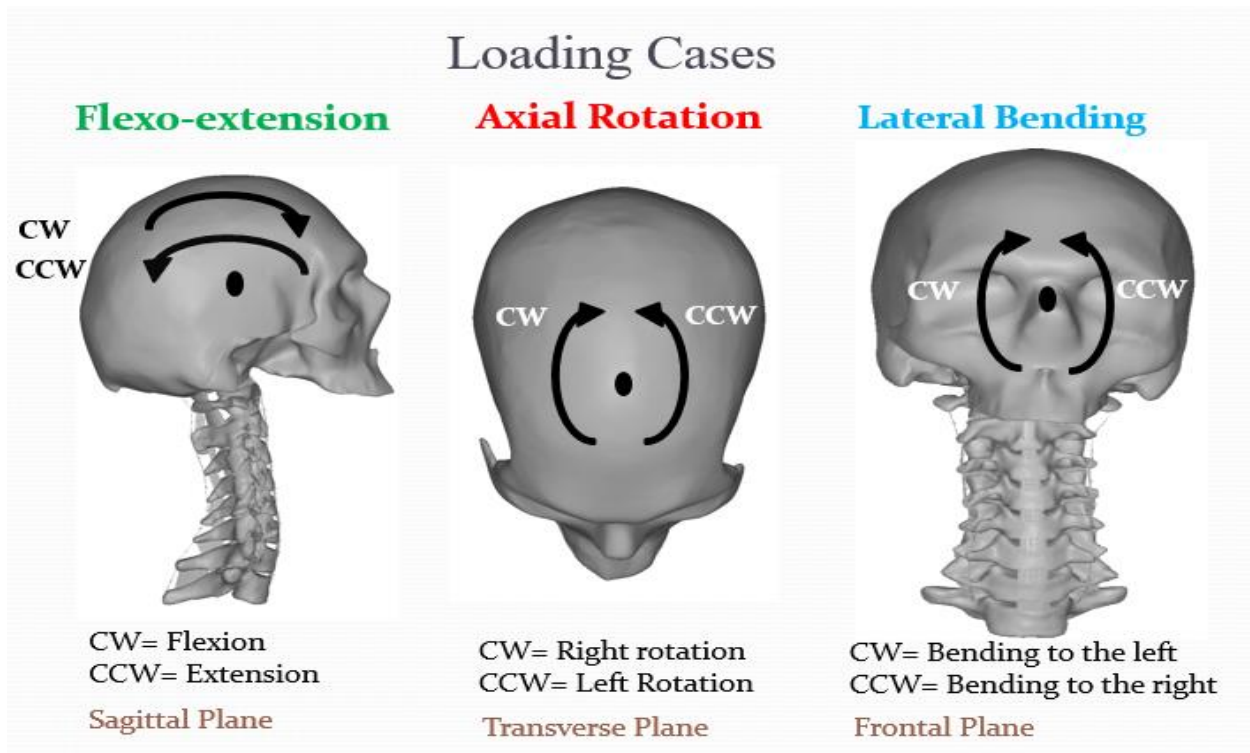


Figure 2.32. The three different rotations of head.

Table 2.1 Range of motion of the spine in response to different mechanical load. Flexo-extension combined the rotation of both flexion and extension movement, also, values for axial rotation and lateral flexion summate both right and left sides.

	Flexo-extension (°)	Axial rotation (°)	Lateral flexion (°)
C0-C1	25	10	7
C1-C2	25	51	6
C2-C3	11	7	5
C3-C4	10	6	5
C4-C5	10	7	4
C5-C6	10	6	3
C6-C7	7	5	3

In the table above

Table 2.1, the presented data are combination for all motions in the same plane; flexion and extension were added up as they both act in the sagittal plane, the same thing applies for the axial rotation and lateral flexion, the data summates both left and right side rotations.

In flexo-extension rotation, head, atlas and axis have the same range of motion and that is due to the fact that atlas and axis move together as one unit. From axis down to C6, all motion segments rotate the same degree with a little difference on the rotation angle. The C6-C7 has some rotation as well but insignificant comparing to the upper levels.

For the axial rotation, the movement of the spine is relatively low comparing with flexo-extension rotation. The reason behind that is due to the involvement of the ligaments in limiting the rotation. All motion segments rotate about the same angle except for the Atlanto-axial segment where they tend to move 51 degrees in both sides combined. That is resulted from the occipital joint mechanism that tends to make atlas rotate more and thus axis as Atlanto-axial joint move as one unit.

The least detectable rotation is in lateral flexion movement. Lateral bending of head to the left and right is very limited as the ligaments play a major role in restraining the vertebrae from moving. Also, facet joints have contribution as well as they experience high pressure when trying to transfer the load to lower spine regions. The skull rotates the most and rotation gets smaller as moving down the spine M. Shea et al., (1991); Nicole Kallemeyn et al., (2010); M. Haghpanahi et al (2012).

3 Literature Review

3.1 In-vitro Experiment

The study of spinal mechanism has been of scientific interest since at least the late 1970s and 1980s. In these studies, the cervical spine is shown to be the most complex as a result of unique geometry and pivotal role in load sharing and distribution Panjabi et al., (1988); Okawara S et al., (1974).

Early studies were performed on cadavers focused on the response of the cervical spine to various load cases, such as spinal rotation at each level as a result of an applied moment; flexion, extension, lateral bending, and axial rotation Panjabi et al., (1986); Panjabi et al., (1988); Moroney et al., (1988).

A notable in vitro experiment was carried out by Panjabi et al. (2001). The purpose of this study was to record the normal cervical spine motion patterns in response to an applied moment. In-vitro studies were chosen for this as they provide realistic response of real cervical spine under applied loads.

In his experiment, Panjabi et al. (2001) studied sixteen different samples, a few of which had some vertebrae missing. One sample had C0-C5, five samples had C0-C6, two samples had C0-C7, and eight samples had C2-C7 vertebrae. For proper preservation, all the samples had been kept in -20 degrees C, to stay fresh and to avoid degeneration of some parts due to dehydration. All non-ligamentous parts of the samples were removed, leaving bones, intervertebral discs and ligaments. To study the motion of the vertebrae, a 1.5 mm Plexiglas marker was attached to different parts of the vertebral body. The Plexiglas contained an 8 mm diameter steel ball, these balls served as position markers of the vertebrae as they moved, one marker positioned anteriorly, one posteriorly, and two laterally.

A total of 1 N·m was applied on the specimen in extension, flexion and lateral bending. The mechanism used to apply this force was made of pulleys attached to either the occipital joint of C1, or to the superior part of the uppermost vertebra for samples missing the atlas. Moment was generated by applying equal and opposite forces on the pulleys as shown in the Figure 3.1. A

force of 15 N was applied upward at the pulleys to counter the compression force applied by the pulleys on the specimens.

Three increments of loads were applied totalling 1 Nm. Between each increment 30 seconds of creep was allowed and three load-unload cycles were used to minimize viscoelastic effects. The measurements were taken on the third cycle. With that, two different readings were collected, the first one was a natural zone (NZ) reading from the second to last cycle to the final position of the vertebra, and the second reading was range of motion (ROM) measured from the motion of each vertebra from initial position to the final position. Data was obtained for each motion segment. The accuracy of the results depended on the plane of rotation; for example: -0.6 degrees for flexion-extension, -0.33 degrees in lateral bending, and -0.17 degrees in axial rotation. This paper was widely referred to for validation of finite element analysis models Zhang et al. (2006); N. Toosizadeh et al. (2011); Han et al. (2012); and Moglo et al. (2013)

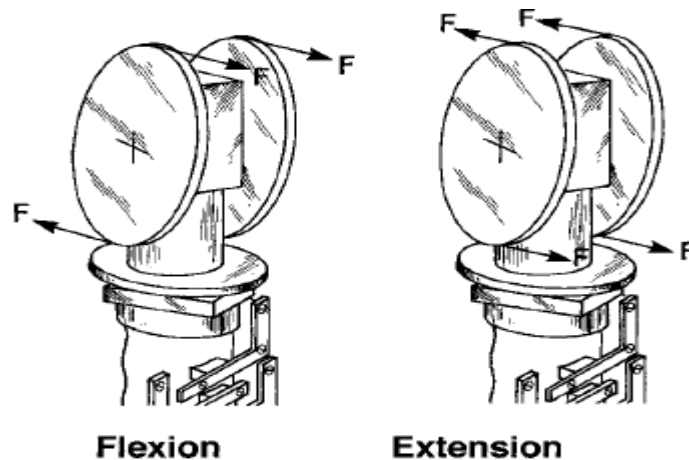


Figure 3.1. Pulley system used to translate force into moments. (Panjabi, M. 2001).

The limitation of this experiment was in the test subjects as some samples were missing parts of the spine, others did not have atlas and axis, or were missing atlas only, some were missing the bottom portion, and only a few had all the vertebrae present (atlas down to C7 vertebra).

Another limitation of the experiment was the sample preparation, which involved removing muscles to leave only ligament and bone intact. It is possible that the process of removing muscle could have affected the ligaments attachments as the ligaments are connected to each other as well as bonded to the bones.

In vitro experiments limit the obtained data that could be gathered. In the previous experiment, only rotation of the spine was obtained. Data such as stress in the intervertebral disc, ligaments and vertebrae are hard to collect and sometimes impossible and that is due to the lacking of the instruments that would enable to measure the stress. Thus, another method had to be established to gather these data as they are critical and beneficial in understanding the behaviour of the spine.

3.2 Finite Element Models (FEA)

Advances in computing have enabled models to be created that simulate cervical spine behaviour. Some of these use parametric studies of the spine instead of exact models in order to reduce geometric complexity, while other models construct precise bone shapes based on MRI scans M. Haghpanahi et al., (2012)

Using either the parametric or precise reconstruction approach will result in a reasonable simulation of spinal behaviour, and both methods have disadvantages, for example, the modified model ignores the true shape and complexity of the anatomy, but the outcome remains sufficiently reliable as they are validated. Other advantages to using parametric modelling software are good visualization, it is less time consuming than exact models, and it is easy to control different parameters like boundary condition, and geometric dimensions in case any correction are required.

On the other hand, an exact model with complex geometry can be limiting due to its time consuming nature, and it is still not an exact image of the spine because some geometrical features get eliminated in the construction phase, which can alter the results depending on the sample. In terms of the obtained results, the acquired data using bio-realistic geometry is more reliable than using parametric model.

An early model of the spine was created by Maurel N. et al., (1997). This model addressed composition of the lower cervical spine using parametrized geometry of vertebrae. Although the geometry was represented by 8-node elements, the model was lacking the detailed geometry of the cancellous bones. Figure 3.2 illustrates the shape of vertebra geometry in the model.

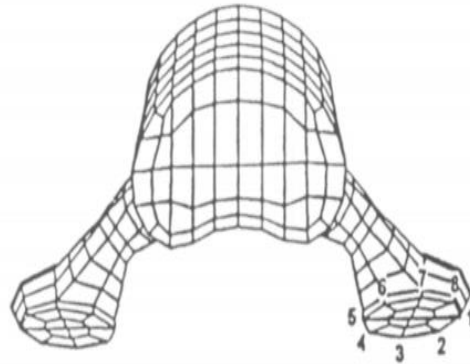


Figure 3.2. Parametrized vertebra (Maurel N., 1997).

Anatomical components of each vertebra were created separately based on their dimension and shape. Mathematical shapes were used to construct different morphologies of the vertebrae. For example, posterior articular shape was defined as an ellipse using 8 parameters. Same principle applied to the constructing the rest of the vertebrae components. With this, the geometry was assumed to be symmetrical around the sagittal plane.

Each component was created and meshed individually. Eight-node elements, cubical shape were used in meshing all parts of the vertebrae. The number of elements and nodes (vertebra body) was consistent at each level. To compensate for the difference in vertebra size on each level, the element size followed a pattern of ascending size going down the cervical spine. The number of nodes and element for each level is presented in the following Table 3.1.

Table 3.1. Number of nodes and 8-node elements for each vertebra component at each level.

Vertebra component	Nodes	elements
Vertebral body	345	112
Articular process	85	48
Pedicle	45	24
Laminae and spinous process	129	56
Transverse process	32	11

Having a consistent number of elements on each level was an important factor designing other spinal components, especially in the vertebral body area where the intervertebral disk is introduced in-between two adjacent vertebrae. The inferior surface of the superior vertebral body

along with superior part of the inferior vertebral body functioned as the end-plates for the intervertebral disk. With an additional two middle layers, the intervertebral disk was represented in four layers. Along with these four layers, 192 diagonally oriented cable elements (working in tension only) were represented fibers in the annulus; the intervertebral disk was made of 207 nodes and 224 three dimensional eight-node elements. Figure 3.3 part a and part b showing the intervertebral disk as well as fiber cables.

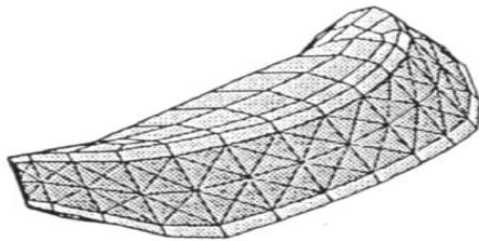


Figure a: intervertebral disk

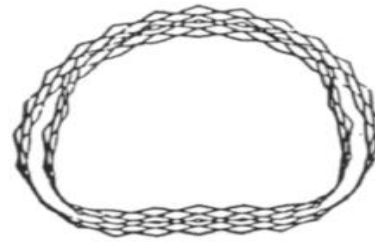


Figure b: Oriented fibers of the disk

Figure 3.3. Part “a” designed showing the intervertebral disc and “b” showing the annulus fibers (Maurel N., 1997).

Another set of cable elements were introduced in the model as ligaments. In each motion segment there were 5 different sets of elements represented by 41 cables. The ligaments were positioned according to the anatomical description.

Young’s modulus and Poisson’s ratio were implemented as all material properties were assumed to be elastic as the study did not include failure behaviour. Ligaments were represented by cables, and the material property included Young’s modulus and force displacement data obtained from previous in vitro studies. The test mechanism of the cervical spine, or functional unit, was quite simple. The lowest vertebral body was totally fixed in all directions and the load was applied on the most top vertebra. The load was applied to the whole body rather than a single point avoiding any distorted outcomes that may result from unevenly distributed force.

The complete model underwent bending moment loading cases, axial rotation, lateral bending, extension and flexion. The applied bending moment went from 0 to 2 N·m, and the results were validated against previously done tests by Pelker et al. (1991); and Moroney et al. (1988)

A limitation of this paper was the geometry; it was assumed that vertebrae were symmetrical along the sagittal plane, and modeled as flat surfaces, which is not the case in real spines due to irregular vertebrae.

Additionally, the ligaments were represented as beam members, i.e. 2-node elements, which would be unrealistic behaviour for the ligaments; as it was not possible to anticipate the high stress area and behaviour of the ligament under high stresses. Representing ligaments as beam members also limited the results because the number of used elements for each ligament affects the behaviour of the spine as more members make the model stiffer due to small load distribution among them.

Unlike the parametrized geometries, the recent studies had adopted the bio-fidelic geometry of the vertebrae. Software such as Mimic would enable the construction of vertebrae geometries based on the CT scans and intervertebral disc from MRI images. Most of the models of the cervical spine consisted of the skull as part of the cervical spine region; Zhang et al. (2006); N. Toosizadeh et al. (2011); Han et al. (2012); and Moglo et al. (2013) while other models had C1 as the top most vertebra such as the model created by Palomar et al. (2007). All the models mentioned earlier had C7 as the bottom vertebra except for Moglo et al. (2013), which had T1 vertebra serving as the bottom vertebra.

Vertebrae are made of two types of osseous tissues, cortical bone is the stiff outer layer covering the inner tissue, cancellous bone. Depending on the scope of the study, some models had vertebrae constructed of both bone tissues; N. Toosizadeh et al. (2011); and Han et al. (2012), while other models had cortical bone only; Palomar et al. (2007); and Moglo et al. (2013). The latter two models treated vertebrae as rigid bodies.

Palomar et al. (2007) meshed cortical bone with 4-node shell elements for the most parts and 3-node shell elements for the areas connected to intervertebral discs. Similarly, Moglo et al. (2013) also had bony parts of the spine meshed using 4-node shell elements. Since N. Toosizadeh et al. (2011) modeled both cortical and cancellous bones, 10-node tetrahedral (solid) elements were used for meshing both tissues. Han et al. (2012) on the other hand used two types of elements to mesh the vertebrae, 4-node shell elements for the cortical bone and 8-node solid elements for cancellous bone. The model constructed by Zhang et al. (2006) used 8-node solid elements for

both cortical and cancellous bones. The different element types used in each model did not affect the obtained results.

For most of the models, the intervertebral discs were created from MRI images except for Palomar et al. (2007). In this model, the surfaces of the vertebral bodies on two adjacent vertebrae were used to define the size of the intervertebral disc. Solid volumes elements were used to construct the intervertebral disc. The created disc was divided into nucleus and annulus and having annulus fibers imbedded in annulus. The disc size varied along the spine as the nucleus area ratio to the total disc area varied from 50 to 80 percent.

Other models used MRI images of intervertebral discs to construct the discs. Similar to Palomar et al. (2007), the discs were divided into two regions; nucleus and annulus. The created disc geometry by Moglo et al. (2013) was divided into two equal halves at all levels of the cervical spine; annulus and nucleus. The obtained intervertebral discs were meshed using hexagonal solid elements. N. Toosizadeh et al. (2011) created disc using two different types of elements. 10-node tetrahedral solid elements were used to model annulus while 10-node tetrahedral hyper-elastic solid elements used for nucleus. Annulus was assigned elastic elements while nucleus behaved more like hyper-elastic materials. Han et al. (2012) used 8-node solid elements for meshing both annulus and nucleus but they had different material properties.

For the annulus fibrosus, some models created by Palomar et al. (2007); and N. Toosizadeh et al. (2011) used tension only members. While other models created by Zhang et al. (2006); and Han et al. (2012) used truss members as fibers that would work in tension only. On the other hand, the model constructed by Moglo et al. (2013) was lacking fibres in the annulus.

The previously mentioned models had ligaments modeled with tension only members. Han et al. (2012) used nonlinear tension-only truss elements for all the ligaments in the cervical spine region. While N. Toosizadeh et al. (2011) also used nonlinear tension only members represented by springs. (Moglo et al. (2013) also used tension only members by using nonlinear uniaxial spring elements. Palomar et al. (2007) created ligaments using nonlinear truss elements that would work in tension only. Although the ligaments were constructed differently in each model, they behaved similarly as they only worked in tension only and the obtained results for the

models

were

matching.

3.3 The Current Study

This thesis follows similar steps in modeling the cervical spine as was done in the works mentioned earlier, however, the method used to model the ligaments is different.

In all the previously mentioned works, ligaments were modeled either by using spring elements, which work in tension only, or beam members, used with the compression effect being neglected or disabled. The advantage of this was they would serve as real ligaments in resisting tension forces. Disadvantages are the lack of stress distribution along the ligament and the failure mode of the ligament.

The stress distribution would aid in understanding the behaviour of the ligament when loaded to the injury level. The study conducted by (El-Rich et al., 2009) showed that in the impact loading conditions, stress in the spinal ligaments is not uniform. El-Rich et al., (2009) had ligaments modeled from shell elements. The current study used the same methodology in creating the ligaments.

The failure mode happens when the elements of the ligaments were deleted as critical values of strain in the ligaments were reached. In spring elements, it happened simultaneously and symmetrically in all the ligament members (DeWit et al., 2012). It was proven by experiments that failure in ligaments does not happen abruptly, it starts with a gradual tear and propagates along the ligament (Mattucci et al., 2012). Using the created ligaments in the herein study would allow the gradual stress distribution and propagation along the ligament elements. From the obtained data from the current study, it was shown that the stress distribution was not symmetric along the ligaments due to asymmetric geometry of the spine.

4 Finite Element Model Creation

4.1 Geometry Acquisition

The original model was based on CT scans and MRI images of a 39 year old man, which was donated by National Library of Medicine's Visible Human. The model consisted of bony structures constructed from CT scans, and intervertebral discs constructed from MRI images. The modeling was done using Mimics software. The ligaments were also included in the geometry as 2 node lines, and the insertion points were based on histological and anatomical studies. Figure 4.1 shows the raw state of the model. Later, these lines were used to construct 2 dimensional surfaces ligaments.

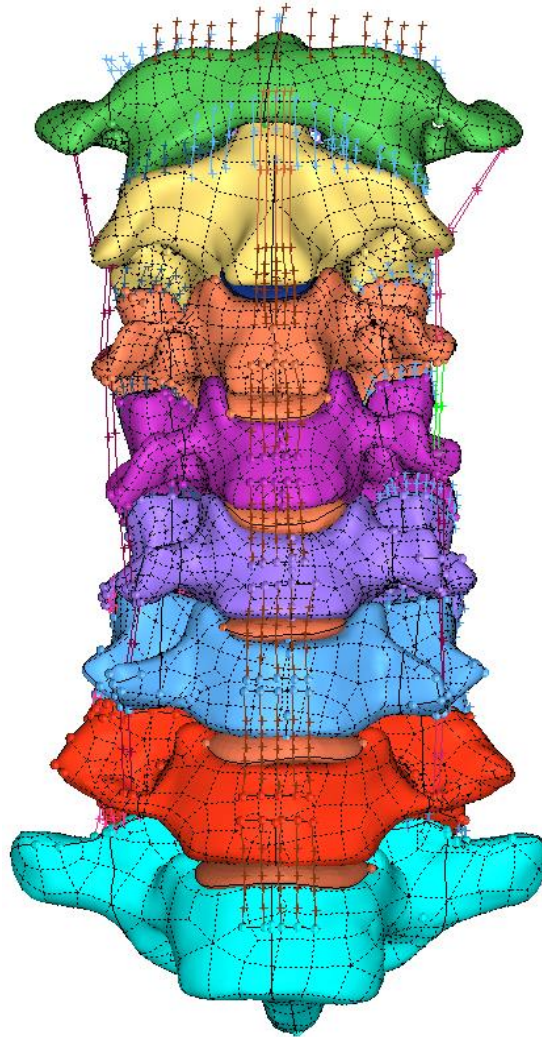


Figure 4.1. Showing the raw state of the model, without skull (C0).

Bony structures were imported from CT scans. Mimics software was used to create and clean the geometry of the vertebrae. Once all vertebrae were created, they were exported into Hypermesh software. It was noticed there were some penetration at some levels and they had to be cleaned before proceeding with modeling. Figure 4.2 showing a penetration area between (C6-C7) vertebrae.

Later, the ligament lines were used to create 2 dimensional surfaces. Hypermesh software was used to fix the geometry, and create the ligaments. Once all the penetrations and intersections were fixed, and ligaments were created, next the model was imported into Abaqus (Finite Element Analysis) software.

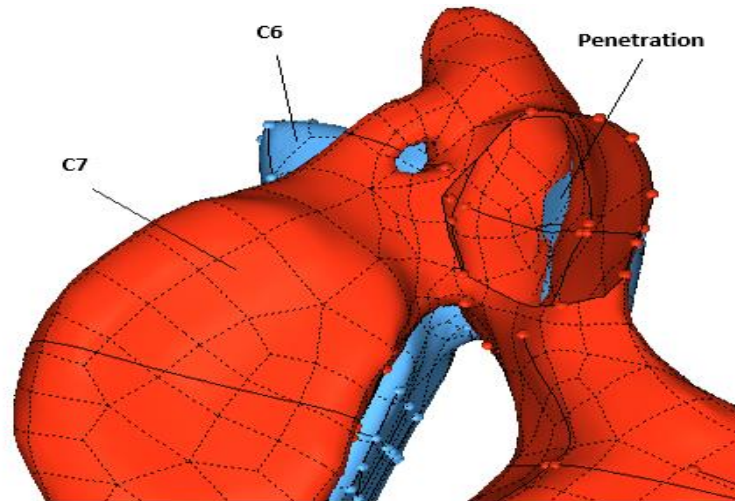


Figure 4.2. Showing the penetration between C6-C7.

4.2 Modeling

4.2.1 Hypermesh

The raw model was first imported into hypermesh for modification. The model consists of all bony structures from C0 (skull) down to the first thoracic vertebra T1, created using CT scans, and also included intervertebral discs, constructed from MRI images. The ligaments are represented by 2-node ligaments.

The first step was to create two dimensional ligaments using the already existing ligament lines and insertion points. For each ligament, these lines were used as boundaries for the surfaces. The ligaments were divided into smaller surfaces to sit adjacent to the bone surface irregularity, and to prevent surface penetration between the ligament surfaces and the bones. Thus, each ligament surface had two lines, and bony structures defining its surface boundaries. Figure 4.3 shows the steps for creating ligaments, Figure 4.3-a shows lines defining the insertion area, and Figure 4.3-b illustrates the ligament after constructing the ligament surface using the lines and bony surfaces as boundaries.

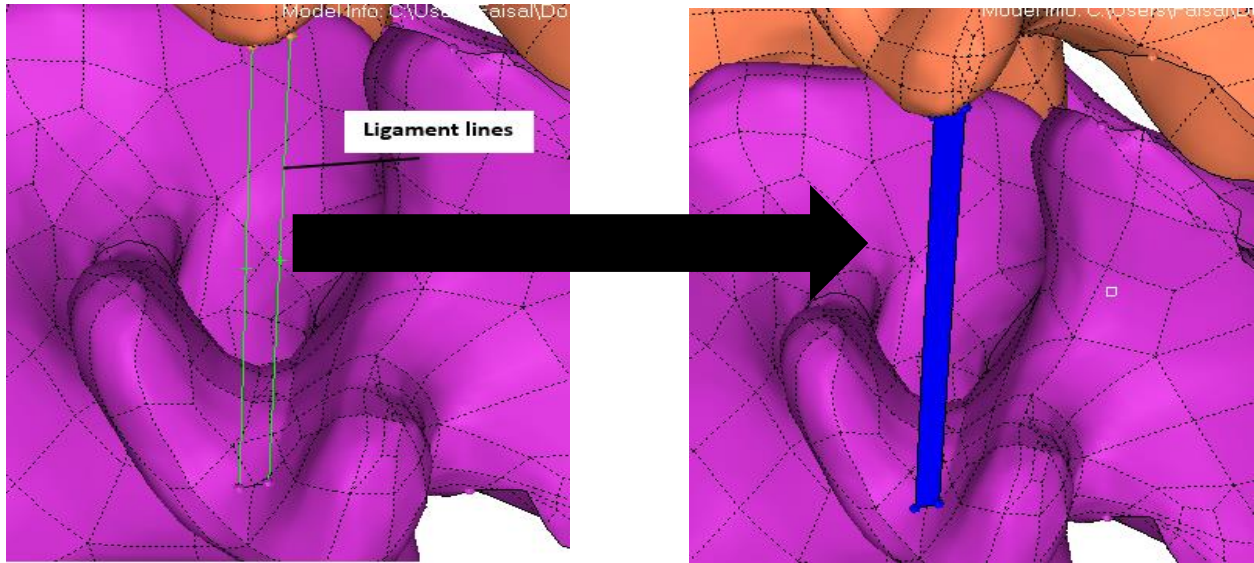


Figure 4.3. a) Ligament lines b) Ligament surface.

Once all the ligaments were created, intervertebral discs were to be modeled next. First, end-plates on each vertebral body was created using the imported discs. This was done by splitting the surface of the vertebral body that is in contact with the imported discs as shown in Figure 4.4.

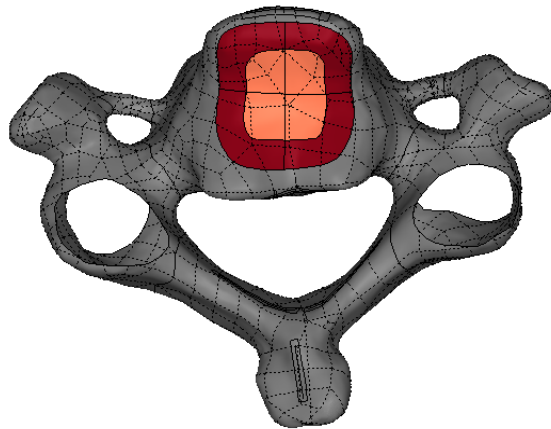


Figure 4.4. Showing the end-plates at the inferior surface at the vertebral body.

Once the end-plate areas were established, they were divided into two regions, nucleus and annulus. Pooni et al., (1986) reported the area of the intervertebral discs based on analysis of four specimens. The intervertebral area along with nucleus pulposus areas indicated the nucleus area ratio to the whole intervertebral area. Using these data, the nucleus to annulus area was determined, and used in the model. Table 4.1 summarizes the ratios and reports the annulus and

nucleus areas used in the model. In this model, the annulus thickness was considered equal in all directions: anteriorly, posteriorly, and bilateral directions.

Table 4.1. Showing the disc area and the ratio of nucleus to the total area as well as annulus and nucleus areas. All units are in mm².

Segment	Disc area	Nucleus area ratio	Annulus area	Nucleus area
C2-C3	214	0.510	104	109
C3-C4	208	0.314	142	65
C4-C5	218	0.25	164	54
C5-C6	218	0.367	138	80
C6-C7	249	0.408	147	102
C7-T1	275	0.442	153	121

After establishing the areas, penetrations had to be solved. All the penetrated areas were divided into two parts; simple and severe penetrations. Simple penetrations were fix as the penetrated area was small, and the surfaces were not penetrating deep into each other. Element offset option was used to separate the simply penetrated areas. Using this method gives more flexibility, as only a few elements were involved, and there was no need for the surface reconstruction. Also, offsetting a small number of elements does not affect the overall geometry of the structure. This is done after meshing the model because only meshed elements can be offset.

In instances of severe penetration, the penetrated surfaces had to be reconstructed due to element offsetting, which results in a large number of elements being moved, and the structure losing its original geometry. In this process, the penetrated areas are deleted after being separated from the rest of the geometry. Then, using the surrounding areas, a similar surface is created that would hold the similar geometry to the ones that had been deleted. The advantage of using this process is that a gap was left between the original penetrated surfaces, solving the penetration problem.

Once all the penetrations had been fixed, the model was meshed. End-plates were meshed first because these elements were used to create intervertebral discs. Figure 4.5 showing a meshed end-plate. First, the end-plates were meshed using 4-nodes shell elements (S4). Opposing sides were meshed with the same number of elements, because they were used to construct the annulus and nucleus pulposus. Every two opposing sides were mapped together using five layers of 8-

node hexahedral cubic elements (C3D8R) Mustafy et al., (2014) for both annulus pulposus and nucleus pulposus.

Along the nucleus pulposus and annulus pulposus, the annulus fibrosus was added to the intervertebral disc as a third component. Fibers are represented by 2-node nonlinear spring elements that work in tension only; SpringA elements. The springs were organized in diagonal pattern on the front surface of each of the hexahedral cubic element of annulus pulpous. Figure 4.6 showing annulus pulposus with annulus fibrosus. The fibers formed ± 35 degrees on average with longitudinal axis (Schmidt et al., 2007).

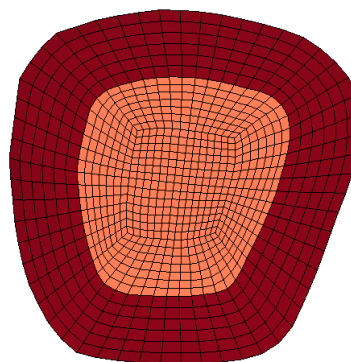


Figure 4.5. Meshed end-plate.

After constructing the intervertebral discs, each of end-plates elements was divided into two 3-node shell (S3) element. The purpose of that was that these elements were used later in constructing Cancellous bone, which were made from tetrahedral elements.

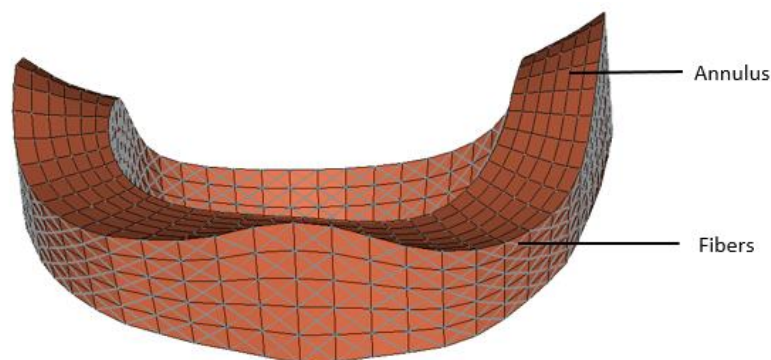


Figure 4.6. Annulus fibrosus elements.

The next component to be meshed was the ligaments. Shell elements (S4R) were used to mesh the ligaments.

Vertebrae are made up of two types of osseous tissues. Cortical bone is the outer surface while cancellous bone is the soft and flexible inside part. Cortical bone is the solid part of the bone, it is very stiff and provides protection for the cancellous part. Cancellous bone is contained inside cortical bone, and it makes up most of the bone volume.

Because cortical bone is the solid surface, it was meshed using 3-node shell elements (S3). Cancellous bone was constructed from cortical bone elements. Cancellous bones were created using 4-node tetrahedral elements (C3D4). Figure 4.7, cortical and cancellous bones after meshing.

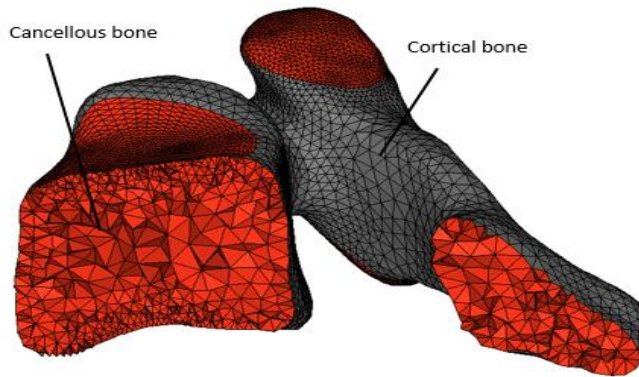


Figure 4.7. Cortical and cancellous bones.

Table 4.2. Element type and number of elements used for each part.

	Segment	Elements Type	Number of Elements
Bone	Cortical bone	Shell elements S3	250079
	Cancellous bone	Tetrahedral elements C3D4	1353476
Ligament		Shell elements S4R	173313
Intervertebral Disc	Annulus	Hexahedral elements C3D8R	10080
	nucleus	Hexahedral elements C3D8R	17640
	fibers	2-node SpringA elements	82412

Figure 4.8 shows C3-C4 motion segments; two vertebrae along with all the ligaments bonding them together as well as the intervertebral disc in-between the two vertebrae.

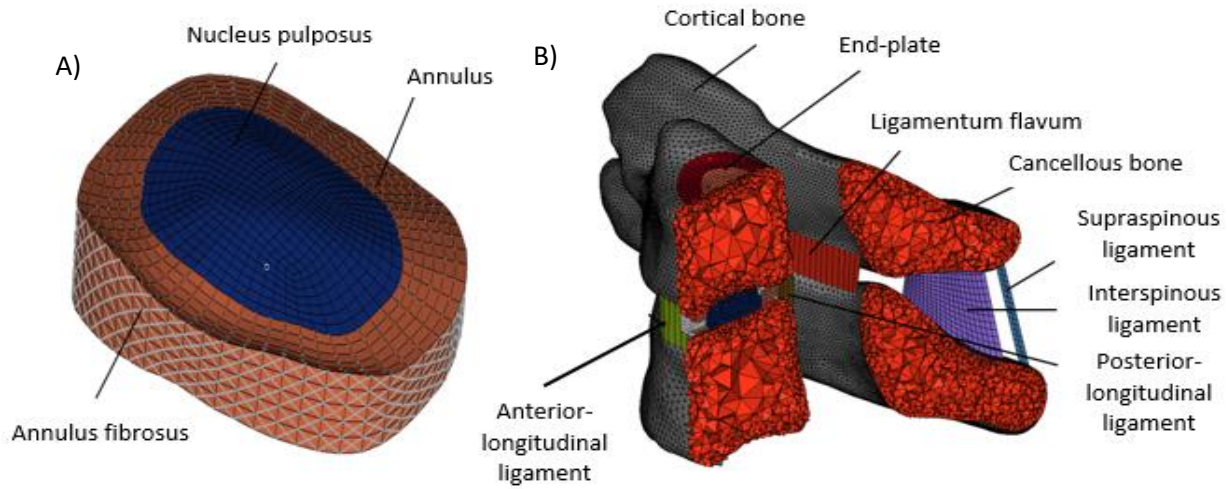


Figure 4.8. C3-C4 motion segment with all the soft tissues a) intervertebral disc, b) motion segment.

4.2.2 Finite Element Analysis (Abaqus)

The meshed geometry was next imported into the finite elements analysis software (Abaqus) to analyse and validate the geometry. In Abaqus, material properties were assigned to each section and all the parts were assumed to be elastic and isotropic except for the annulus fibrosus. Ligaments were modeled as membrane sections with 1 mm thickness (Mustafy et al., 2014). The Poisson's ratio for ligaments ranged from 0.3 to 0.4. For the bony parts, both cortical and cancellous bones were assumed as homogeneous isotropic elastic material with different material properties. Cortical bone was divided into three sections: vertebral body, end-plates, and facet joint.

Intervertebral discs were also considered linear elastic materials, both annulus and nucleus. However, the collagen fibers were assumed as nonlinear elastic, and their behaviour was determined from nonlinear curve obtained from Shirazi-Adl et al. (1986). Table 4.3 shows all the geometry parts with their material properties.

Table 4.3. Material properties of the created model.

		Young's modulus (MPa)	Poisson's ratio	Source
Bone	Cortical bone	10000	0.29	Mustafy et al., 2014
	Cancellous bone	100	0.29	Mustafy et al., 2014

	End-plate	500	0.3	Han et al., 2012
	Facet joint	500	0.4	Mustafy et al., 2014
Disc	Annulus	7	0.4	Moglo et al., 2012
	Nucleus	7	0.49	Moglo et al., 2012
Ligaments	Alar ligament	5	0.3	Panjabi et al. 1998
	ALL	30	0.3	Zhang et al., 2006
	CL	10	0.3	Zhang et al., 2006
	ISL	10	0.3	Zhang et al., 2006
	ITL	17.1	0.4	Mustafy et al., 2014
	LF	1.5	0.3	Zhang et al., 2006
	PLL	20	0.3	Zhang et al., 2006
	SSL	1.5	0.3	Zhang et al., 2006
	TL	20	0.3	Zhang et al., 2006
	APL	20	0.3	Zhang et al., 2006

ALL=anterior-longitudinal ligament; CL=capsular ligament; ISL=interspinous ligament; ITL=intratransverse ligament; LF=ligamentum flavum; PLL=posterior-longitudinal ligament; SSL=supraspinous ligament; APL=apical ligament; TL=transverse ligament

Material properties for collagen fibers were obtained from nonlinear elastic stress strain curve Shirazi-Adl et al. (1986). From this, the force vs. displacement curve was determined for each intervertebral disc. Force was determined from the stress, and deformation was from strain.

Based on the annulus fibrosus area in each level, the forces in the fibers were determined. Fibers made about 20 % of the total area of the annulus (Han et al., 2012). Using these data, annulus fibrosus area was calculated at each level. Table 4.4 summarizes the fibers area in each level of the cervical spine.

Table 4.4. Annulus and fibers area at each level.

Segment	Annulus area mm ²	Fibers area mm ²
C2-C3	104	20
C3-C4	143	28
C4-C5	163	32
C5-C6	138	27
C6-C7	147	29
C7-T1	153	31

Due to intervertebral discs area variation at each motion segment, force deformation data were obtained for each individual level. Also, it was noticed that fiber length also varied at each single

disc going from anterior part of the disc to the posterior area, but because this variation is small, an average length was used in calculations.

Using the annulus fibrosus area at each level, forces were determined by multiplying the area by the stress to produce average force. Deformation was calculated using the average length of the fibers. The force and deformation curve is illustrated in Figure 4.9.

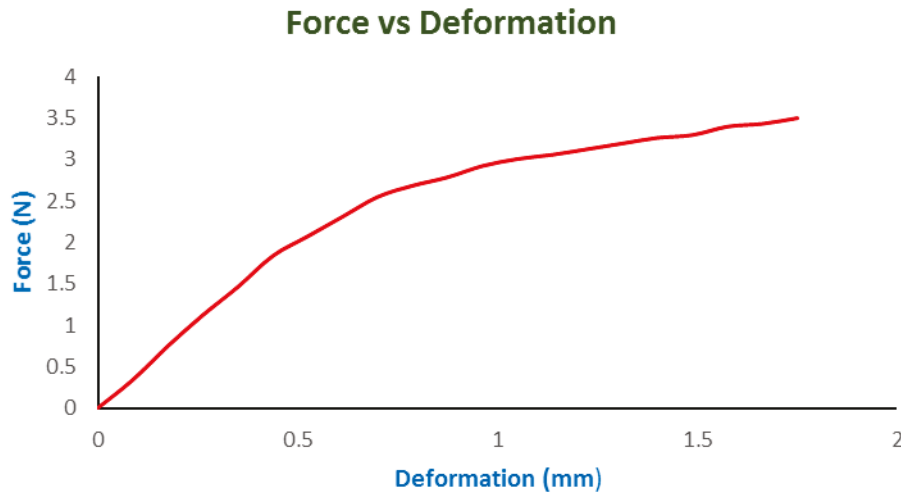


Figure 4.9. Force vs deformation of annulus fibrosus.

Once the material properties had been assigned to each section, the next step was defining rigid bodies. The purpose of this is to reduce the calculation time and speed up running time. The way rigid body calculations work is by assigning a number of elements nodes to a single governing node, which makes all the selected nodes follow that specific (reference point) governing node in motion, and load response. Also, defining a rigid body made it easier to restrain elements by applying boundary conditions as well as assigning an external load. Another reason for selecting bony parts to be represented as rigid body was that the bones are stiff compared to the soft tissues (intervertebral disc and ligaments). Figure 4.10 shows a group selected nodes being assigned a single reference node. Both cancellous bone and cortical bone were made rigid.

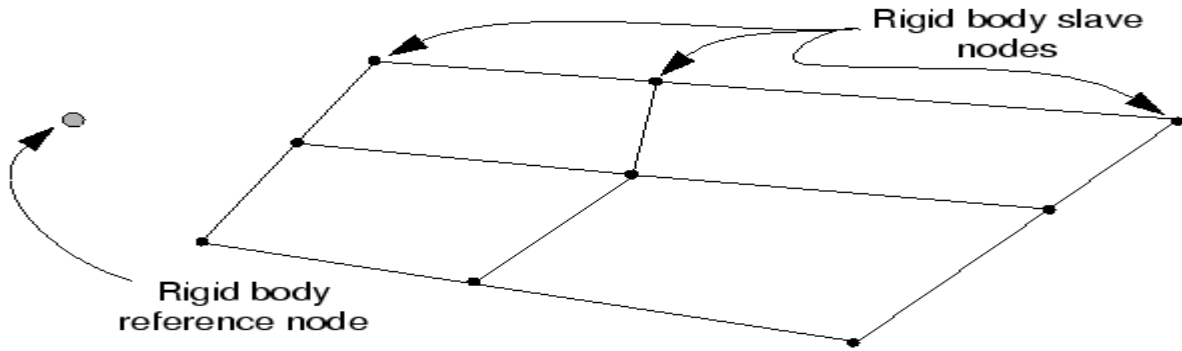
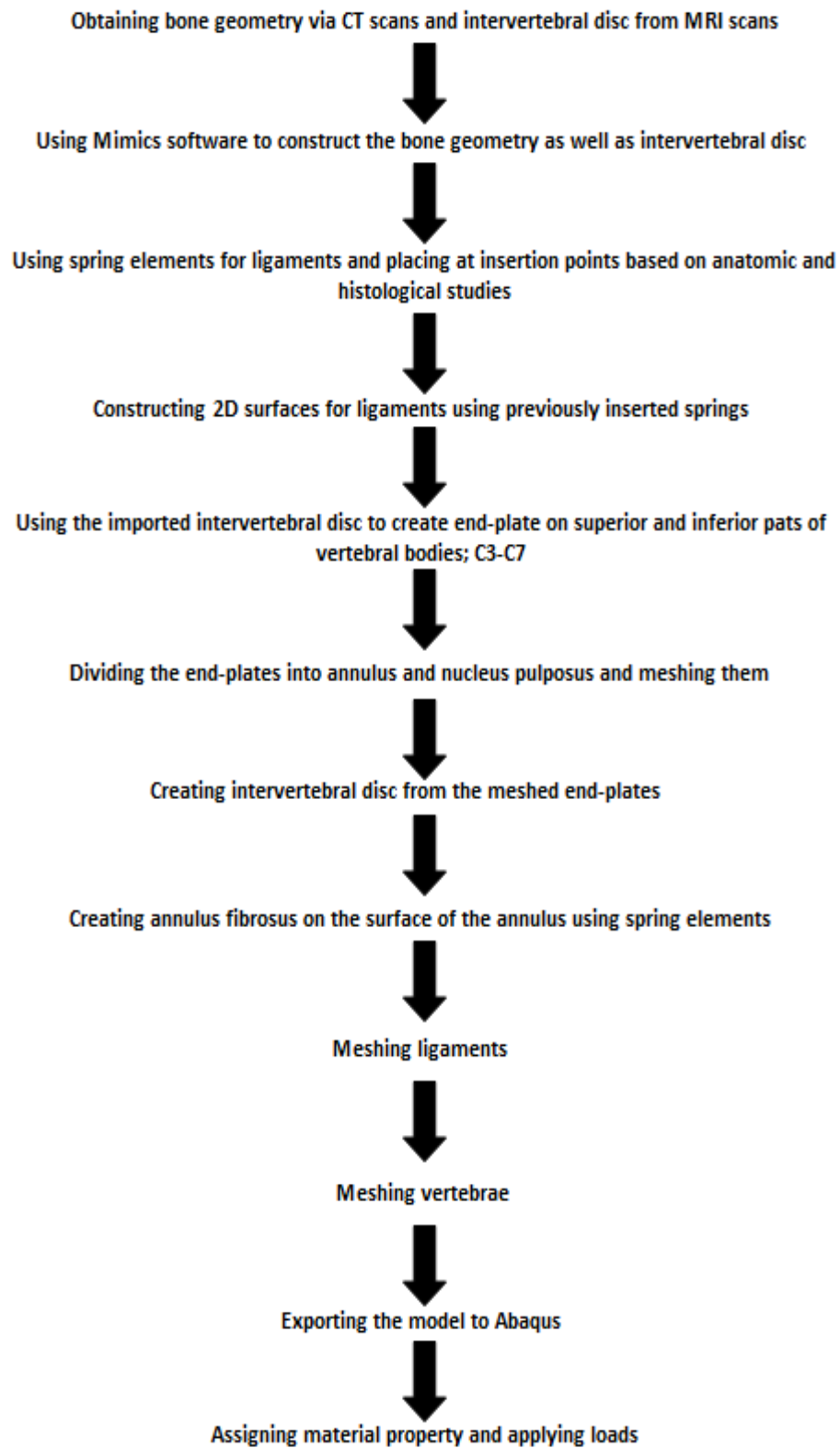


Figure 4.10. Nodes tied to a single reference node. From “Rigid body,” by Abaqus 6.14, 2015, <http://ivt-abaqusdoc.ivt.ntnu.no:2080/v6.14/books/gsa/default.htm?startat=ch03s02.html>. Copyright 2015 by Abaqus 6.14.

The synovial joint holds two adjacent facet joints together, preventing them from slipping and gridding against each other by providing a smooth surface that acts a lubricant. In the current model, a contact option was established between the facet joints that rub against each other. That contact option provides smooth sliding on the surfaces of the facet joint, as well as preventing them from penetrating one another. Penetration was a critical component to the model as they play major role in whether transferring loads between different motion segments as well as stabilizing the spine as they limit the movement of the spine in certain directions. The following chart summarizes the steps of constructing the model.



5 Validation

To validate the created model, the model's static response to a 1 N·m. moment was compared to the reported experimental results, as well as other finite element models. The in vitro experiment done by Panjabi et al. (2001), was used to validate the results from the current model. The data were also compared against other finite element models: Palomar et al. (2007); Toosizadeh et al. (2011); Moglo et al. (2012); Zhang et al. (2006); and Han et al. (2012).

In the current study, a load of 1 N·m. moment was applied in 6 different directions. It was applied at the bottom of the skull, at Atlanto-occipital joint. For the boundary conditions, only the bottom vertebra was restrained from moving or rotating in any direction, the other vertebrae were left free to move or rotate. The rotation at each motion segment was the average between the rotations of the two adjacent vertebrae.

5.1 Experimental data (in vitro)

In the experiment that was conducted by Panjabi et al. (2001), the samples were fixed at the bottom from moving or rotating. The external load was applied on the upper most vertebra using a pulley that transfers equal and opposite forces into moments as shown in Figure 3.1.

The experiment was carried out by applying six moments of a value of 1 N·m. each on three different planes on the samples. Two moments were applied on the sagittal plane (flexion and extension), two along the transverse plane (axial rotation; left and right), and two along frontal plane (lateral bending; spine bending to the left and to the right). The following charts compare the data from the model against those recorded in the experiment by Panjabi et al. (2001). In the charts, the rotations in same planes were combined together; extension with flexion, called flexo-extension, and the lateral bending and axial rotation charts summate both right and left sides.

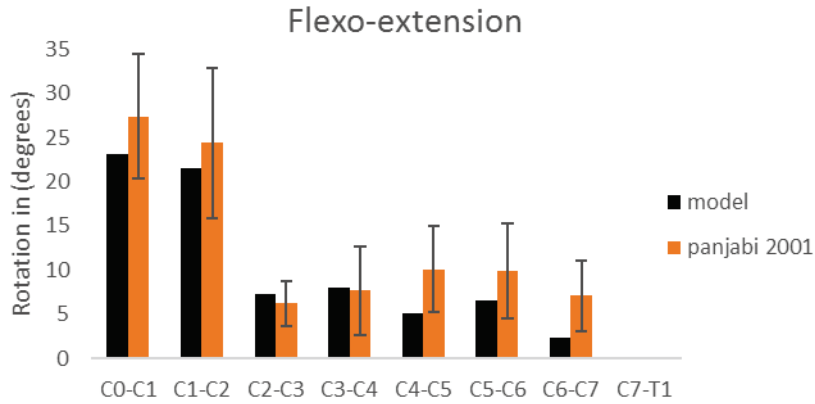


Figure 5.1. Flexo-extension of Panjabi 2001 and the current FEA model.

In a comparison of results, the model and the in vitro experiment produce similar outcomes for most parts of the spine. In Panjabi et al. (2001)’s experiment, Atlanto-occipital joint has the highest rotation, followed by Atlanto-axial joint. The current model shows the same results: Atlanto-occipital joint going through the highest rotation, and next Atlanto-axial joint. C2-C3, C3-C4 and C5-C6 segments are within one standard deviation specifically, C3-C4 has the same rotation degree as that reported by Panjabi et al. (2001). However, the observed rotation at C4-C5, as well as the C6-C7 segment, do not match or fall within the same range as those in Panjabi et al. (2001)’s experiment. The last set of bars in Figure 5.1 indicate zero degrees of rotation for the last segment, as it was fixed in place, and thus no rotation was reported.

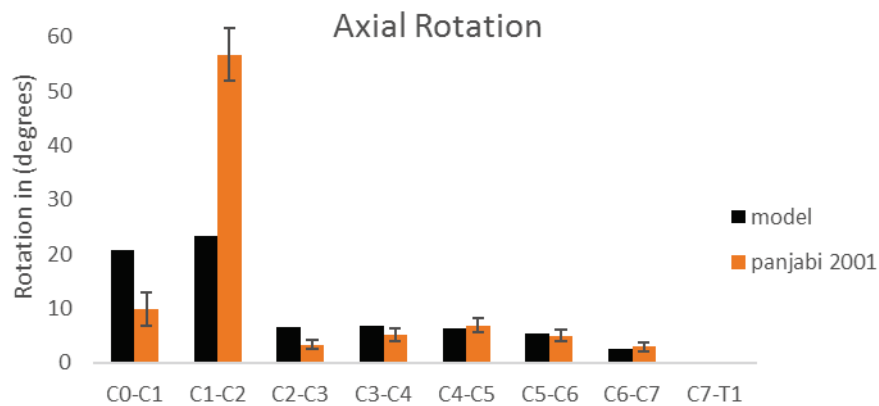


Figure 5.2. Axial rotation of Panjabi 2001 and the current FEA model. Values summate both right and left sides.

For axial rotation, Atlanto-axial motion segment has the highest degree of rotation observed during the test, reaching 56 degrees, indicating a high flexibility of the joint. The next highest rotation was noticed at Atlanto-occipital joint. For the rest of the spine, the rotation is relatively small as compared to the first two segments. Starting at the C2-C3 level, the rotation angles goes up till C4-C5 motion segment, and then drops down for vertebrae below this. The difference in the upper cervical spine rotation is a result of ligaments playing a role in resisting the applied load as well as limiting the rotation.

The created finite element model agrees with the Panjabi et al. (2001) results in terms of the rotation pattern between the different motion segments. Atlanto-axial segment has the highest degree of rotation, followed by Atlanto-occipital joint. Also, same pattern of rotation could be observed down the spine as the rotation angles goes up from C2-C3 segment down to C4-C5 and then drops again to zero at the very bottom of the spine. Although the model shows the same response to the applied moment, the rotation degrees are discrepant. Atlanto-occipital joint indicates that the rotation at this level is higher than the one reported by Panjabi et al. (2001), and this is due to the moment being applied on the skull. Atlanto-axial joint has the highest rotation degree, but it still does not match the in vitro reported rotation degree. For the rest of the spine, the rotation degrees are within the same range as the in vitro results.

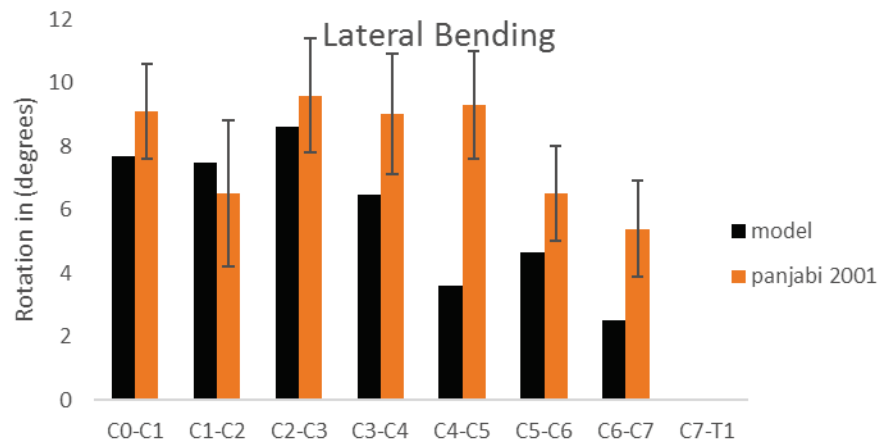


Figure 5.3. Lateral bending rotation of Panjabi 2001 and the current FEA model. Values summate both right and left sides.

For the lateral bending, the finite element model results are similar and within range of the in vitro for the top three segments. However, moving down the spine, the model seems to be stiffer due to the effect of the ligaments. The greatest discrepancy is observed at the C4-C5 level. At

this point the model indicates the least rotation after C6-C7 segment, while the in vitro report shows that the rotation is relatively high compared to the other regions of the spine.

5.2 Numerical Data (Finite Element Models)

Along with in vitro comparison, the current finite element model was compared to other previously constructed models. The models the current will be compared against are Zhang et al. (2006); Palomar et al. (2007); Toosizadeh et al. (2011); Han et al. (2012); and Moglo et al. (2012). All models consisted of skull (C0) down to C7 vertebrae.

The testing mechanism of the finite elements models was similar. All the models went under 1 N·m. moment at different directions, making the model undergo flexion, extension, bilateral bending and axial rotation in both directions. The applied moment was on Atlanto-occipital joint because some of the models did not contain a full skull, only the lower portion of the skull (occipital bone) was modeled to save time. The C7 vertebra was fixed. The following graphs compare the results from the current model with the ones provided by the earlier finite element models.

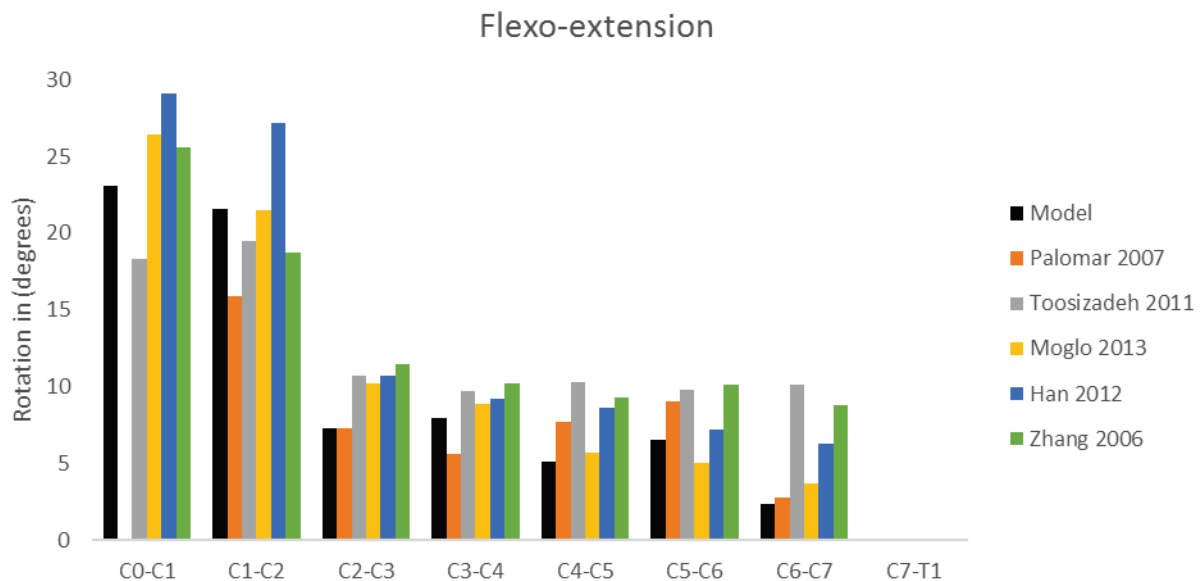


Figure 5.4. Flexo-extension of the current FEA model and other FEA models.

The results of the created finite element model concur with the majority of the other models. For the top two motion segments, this model is approximately the average of all the other models. For the C2-C3 segment, the models rotates approximately the same as the model from Palomar et

al. (2007), but compared to all other models it indicates less rotation. Also, the C4-C5 and C6-C7 segment results of the created model are lower. For the C5-C6 segment, it is about on par with the other models.

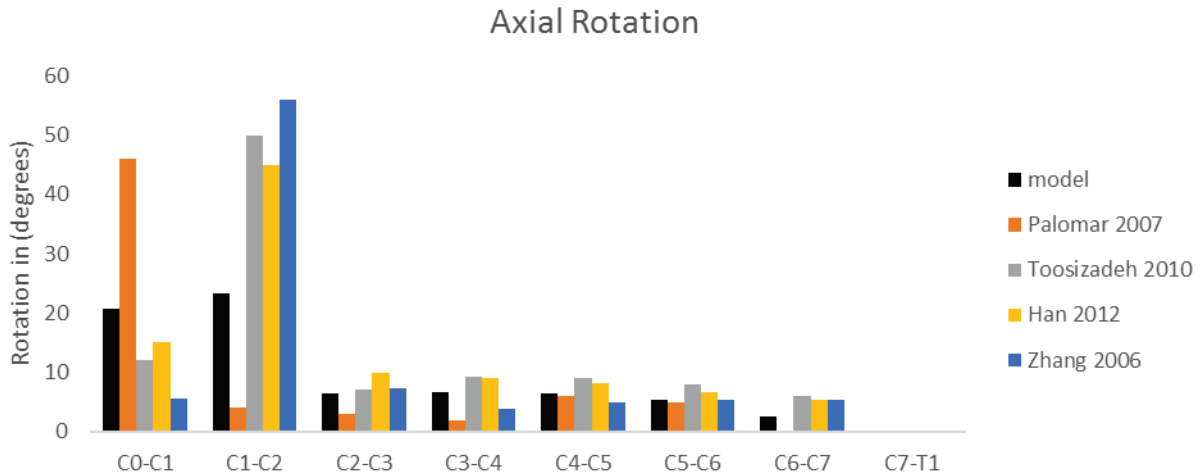


Figure 5.5. Axial rotation of the current FEA model and other FEA models. Values summate both right and left sides.

For the axial rotation, the data obtained is very similar to the other reported results by other models. The lower cervical spine rotation is close to the output from other papers under the same applied load. However, for the first two segments of Atlanto-occipital joint, the current finite element model rotates more than the others, with the exception of the Palomar et al. (2007) model. In contrast, the second motion segment; Atlanto-axial segment, seems to be stiffer than the other models, with the exception of Palomar et al. (2007).

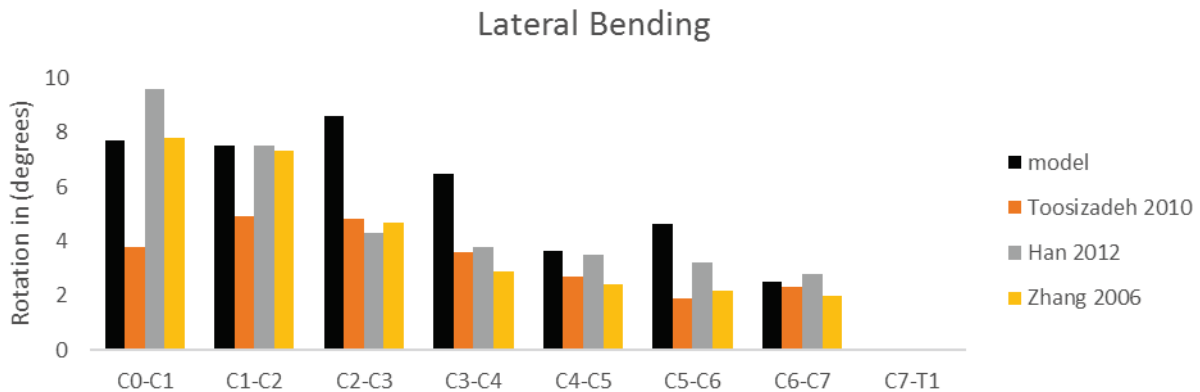


Figure 5.6. Lateral bending of the current FEA model and other FEA models. Values summate both right and left sides.

Comparing the data obtained in the currently created finite element model and the reported results from the other models, it could be concluded that the data are similar in some of the segments of the spine, while it contradicts past results in other areas. For example, the first two motion segments, the results are almost identical to the ones reported by Zhang et al. (2006). However, the rotation in this model is the average for the first segment, but rotates more than others in the second segment. The C2-C3 segment and other segments all experience higher rotations than the other models except for the C4-C5 level, which rotates approximately the same amount. The difference between the obtained results in the herein study and the previous studies comes from the different material properties used as well as symmetrical geometry assumption that was acquired in the earlier mentioned papers.

6 Model detailed Output

When the spine rotates, the ligaments stretch to limit movement and prevent injury. Different ligaments are distributed all around the vertebrae, on the anterior and posterior surfaces, the sides, and in-between the vertebrae. All the ligaments play a role in limiting the rotation and movement of the vertebrae, however, some of them contribute more to resisting certain loads due to their location. For example, anterior ligaments bear most of the stress in extension rotation, while posterior ligaments limit most of the flexion rotation of the spine. Figure 6.1 shows a theoretical longitudinal transection of the vertebrae and ligaments into anterior and posterior parts. Anterior ligaments are mostly active in extension while posterior ligaments are active in flexion rotation.

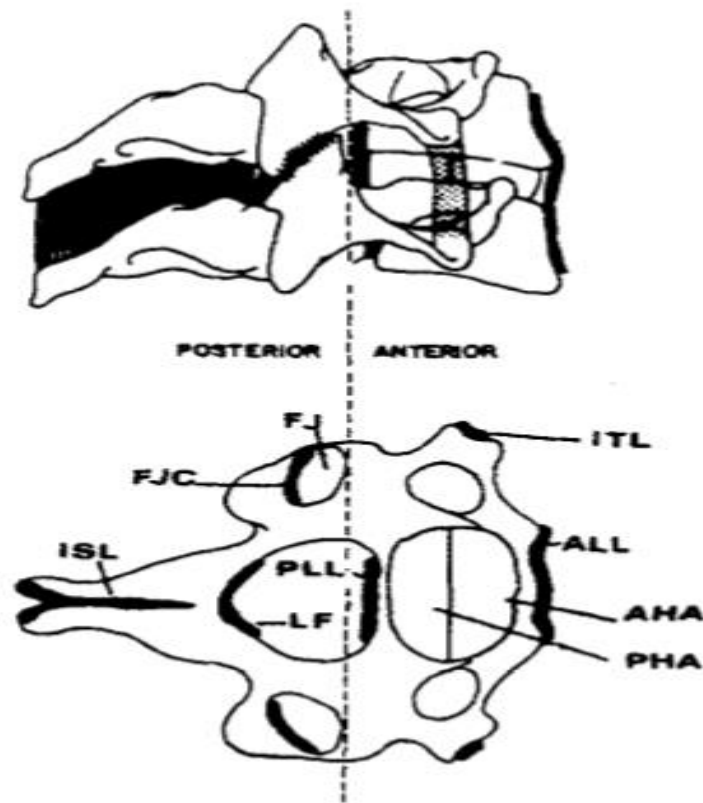


Figure 6.1. Transection of the ligaments into anterior and posterior sections in flexo-extension rotation. (Panjabi, M. 1978). Used with permission.

In Figure 6.1, the anterior ligaments are anterior longitudinal ligament (ALL), intertransverse ligament (ISL), annulus fibrosus; both anterior and posterior halves (AHA and PHA), and posterior longitudinal ligament (PLL). The posterior ligaments are ligamentum flavum (LF), interspinous ligament and nuchal ligament (ISL), facet joint capsule (FJC), as well as facet joints, all contribute to limiting the movement.

For lateral bending, the spine sways left and right based on the applied load. When the spine rotates to one side, the ligaments of the opposite side stretch, limiting the movement, and making all the ligaments on the opposite sides active. In this case, the spine is split symmetrically in the middle through the sagittal plane as shown in the following Figure 6.2. Axial rotation is resisted by all the ligaments activated at the same rate whether the spine is rotated in either direction. In the following section, the stress development along each ligament will be presented in all six different rotations. In the following sections, the development of Von Misses stress is presented in the upper cervical spine ligaments

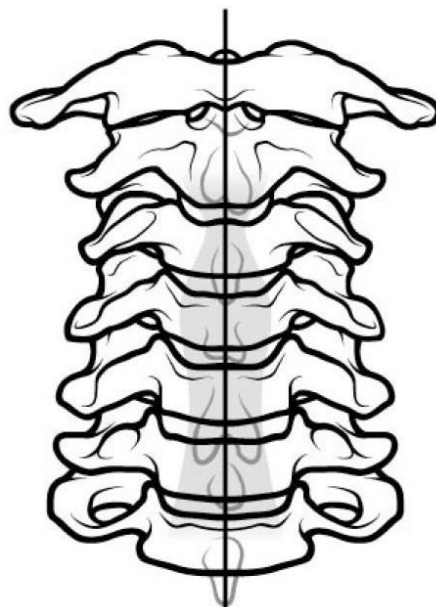


Figure 6.2. Transection of the spine into two symmetrical halves. From “Which X-Ray Views Should Be Obtained?,”2015, http://www.ebmedicine.net/topics.php?paction=showTopicSeg&topic_id=51&seg_id=936; Copyright 2015.

6.1 Ligaments

6.1.1 Flexo-extension

When the spine rotates anteriorly in the sagittal plane, it is called flexion, and when it rotates backwards or posteriorly in the sagittal plane, it is called extension. For either of these two rotations, there are certain ligaments that play critical roles in limiting the movement. Applying a moment of a value of 1 N·m developed stress in the ligaments as they were trying to limit the movement, and the stress values ranged based on the applied moment, and their position on the spine. The data from this work presents the stress in all of the ligaments in the cervical spine region. The following graphs show the top three motion sections, all other graphs can be found in the appendices.

The anterior longitudinal ligament (ALL) is located on the anterior surface of the vertebral body. As the spine rotates in extension, the ligament stretches and thus develops stress, while in flexion it does not have any contribution and buckles, and very small stresses develop in the ligament at the connection point with the vertebra. Figure 6.3 shows the stress development in the ALL at top three motion segments.

From Figure 6.3, it can be noticed that ALL is very active in extension rotation, while it has almost no contribution to resisting flexion moment. The highest detectable stress is at the C1-C2 level, then C0-C1 and C2-C3 respectively. The stress in the ALL decreases as going down the spine until it approaches zero at the C7-T1 junction. Some stress is detected in the flexion rotation and that is due to the distal and proximal translation of the vertebrae.

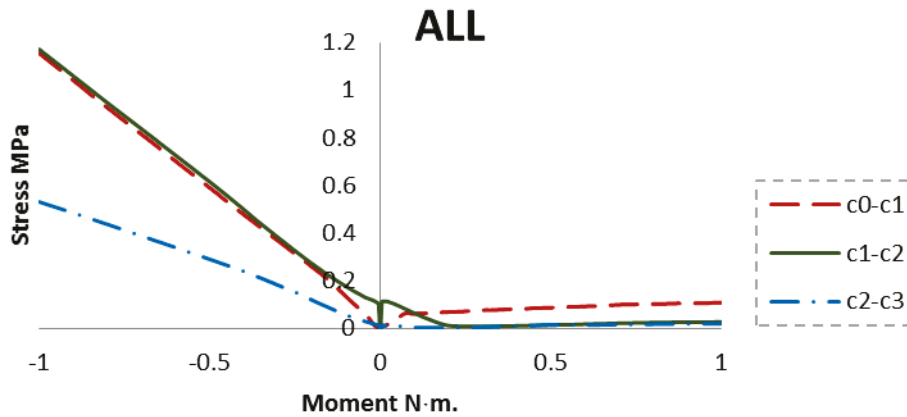


Figure 6.3. Stress development along the ALL for all the motion segments from C0-C1 ligament down to C2-C3 section. Negative moment is extension while positive moment is flexion.

Another ligament that resists flexion rotation is the intratransverse ligament (ITL), located on the anterior section of the vertebra. It is made of two strips on either side of vertebra joining two adjacent transverse processes on two different vertebrae. The following Figure 6.4 shows the stress development in the ITL in flexo-extension rotation.

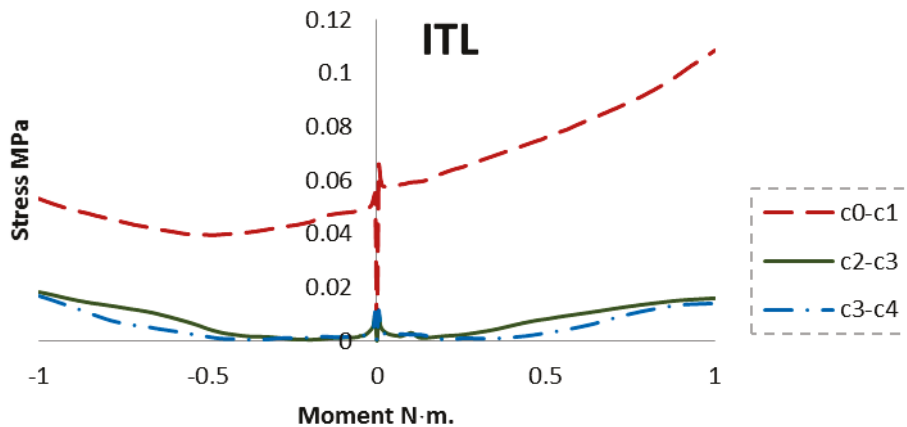


Figure 6.4. Stress distribution along ITL. Negative moment is extension while positive moment is flexion.

ITL picks up a high stress at the beginning due to proximal and distal translations at all levels. C1-C2 segment detects higher stress in flexion compared to the rest of the levels. However, in extension, the stress decreases as the moment increases but then picks up again as the moment reaches 1 N·m. C2-C3 and C3-C4 segments have no contribution to resist the applied moment either in extension or flexion rotations except at the end as the applied moment reaches 1 N·m.

The next ligament to be investigated is the posterior longitudinal ligament (PLL). From Figure 6.1, it is located on the posterior surface of the vertebral body, near the longitudinal line that transects vertebrae into posterior and anterior sections. Theoretically, it helps in resisting both flexion and extension moment but it is more predominant in flexion. Figure 6.5 shows the stress on PLL in flexo-extension rotations.

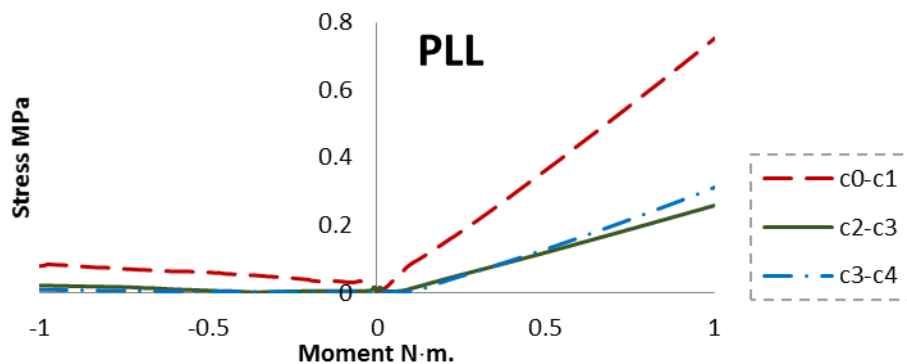


Figure 6.5. Stress distribution along PLL. Negative moment is extension while positive moment is flexion.

From Figure 6.5, PLL helps in limiting the flexion rotation while it barely has any contribution in limiting the extension rotation, even though it lies in the anterior section of the vertebra. The highest stress is in Atlanto-occipital motion segment (C0-C1) where the stress reaches up to 0.8 MPa, and this is because the skull (C0) has the highest rotation when compared to the rest of vertebrae. The reported stress in PLL drops significantly, and the inferior motion segments, as shown in Figure 6.5. The C2-C3 and C3-C4 segments behave similarly in both flexion and extension, although C3-C4 experiences slightly higher stress in flexion.

Capsular ligament (CL) is located around the facet joint on the superior and inferior surfaces of a vertebra. Based on Figure 6.1, it lies on the line that transects the vertebra into two halves. Theoretically, it is involved in limiting both flexion, and extension rotations.

As anticipated, the CL is active in both flexion and extension. The most stress is developed in C1-C2 segment with being more involved in flexion resisting. C0-C segment is more contributing to the extension resisting than being involved in flexion resisting. C2-C3 is opposite to C0-C1 segment as being more active in flexion as the stress in this region exceeds C0-C1 while it is much less involved in resisting extension. The stress level drops as moving down the spine as it can be seen from the graphs in the appendix.

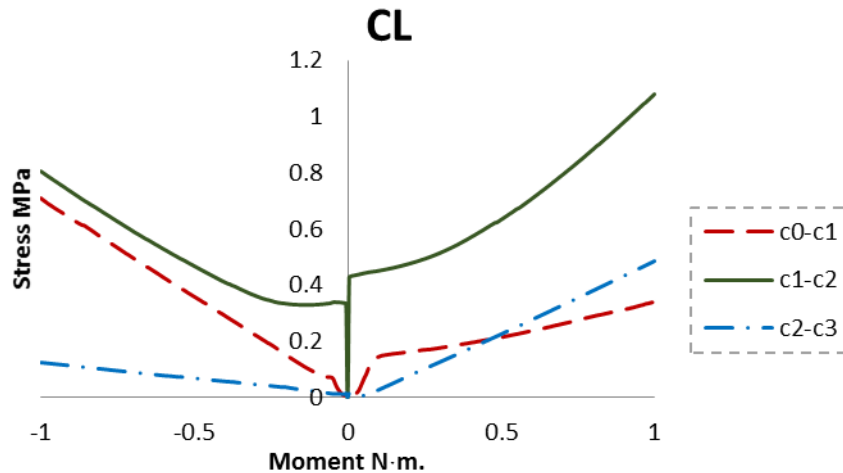


Figure 6.6. Stress distribution along CL. Negative moment is extension while positive moment is flexion.

Ligamentum flavum (LV) also is located in the posterior region on the vertebra, within a close distance from the longitudinal transection line. Based on its location, LV is mostly active in limiting flexion rotation. The following Figure 6.7 shows the stress distribution along each ligament on C1 through C4 levels.

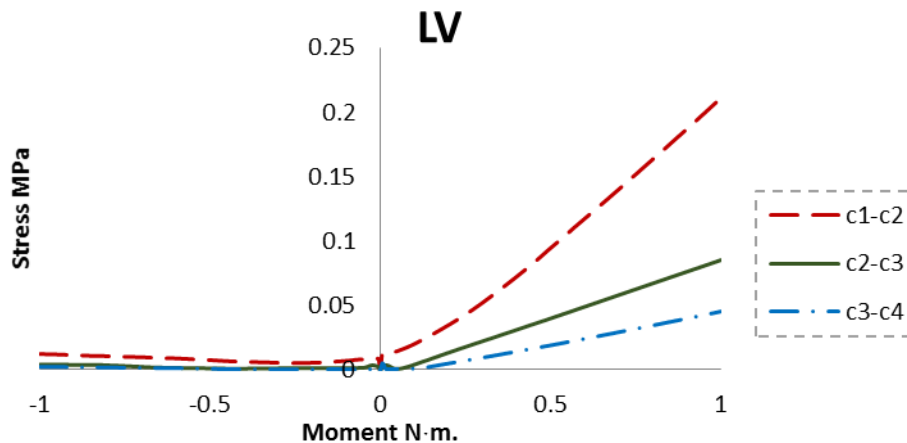


Figure 6.7. Stress distribution along LV. Negative moment is extension while positive moment is flexion.

Similar to PLL, LV is mainly active in resisting flexion and has a minimal assistance in resisting extension moment. Similar to ALL and PLL, superior ligaments are more involved than the inferior ones as upper vertebrae rotate more than the bottom vertebrae. However, comparing to

PLL, LV is not highly involved in resisting flexo-extension rotations although it is more active in flexion than extension. The highest stress value in flexion is about 0.22 MPa whereas 0.8 MPa for PPL, and its contribution decreases as moving down the spinal column.

Interspinous ligament (ISL) is located at the posterior margin of the vertebrae connecting two adjacent spinous processes together. Because of its location, ISL is only involved in flexion and has no contribution to extension. Figure 6.8 shows the stress distribution on ISL in both flexion and extension rotations on the top three levels.

As the spine rotates in flexion, ISL stretches as trying to hold the vertebrae in position and limiting the movement. This imposes a high stress on the ligament as it can be noticed in Figure 6.8. A stress of a value of 0.3 MPa can be noticed on the superior ligament C1-C2 and it deteriorates as moving to lower levels until the model detects almost a zero stress at the bottom segment C7-T1. C2-C3 and C3-C4 segments respond similarly to the moment in flexion as the stress in these two ligaments is about 0.08 MPa in flexion. In extension, all three ligaments have the same response as very small stress is detected in the ligaments.

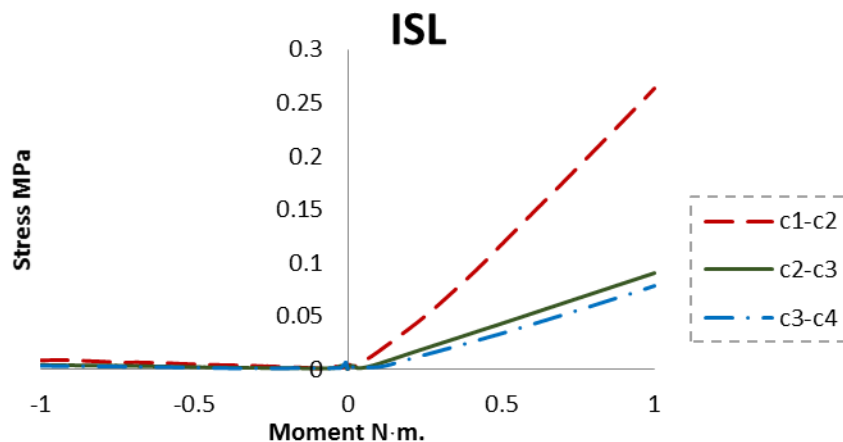


Figure 6.8. Stress distribution along ITL. Negative moment is extension while positive moment is flexion.

At the tip of the spinous processes where the two laminae join, a thin and long ligament joins each two adjacent vertebrae and it is called supraspinous ligament (SSL). It extends all the way from occipital bone down to T1 vertebra. Similar to ITL, it is stretched in flexion as shown in the following graphs.

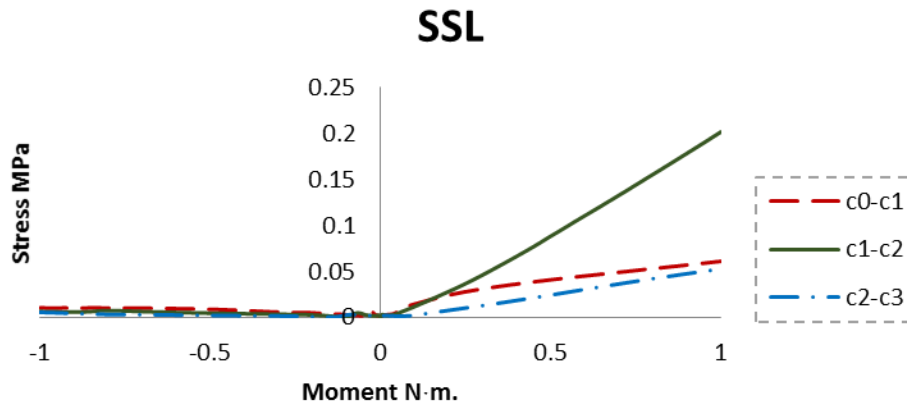


Figure 6.9. Stress distribution along SSL. Negative moment is extension while positive moment is flexion.

From Figure 6.9, SSL on level C1-C2 stretches the most and thus developing the highest stress comparing to the rest SSL on the other levels. The stress on SSL at C0-C1 is lower than C1-C2 level because in flexion rotation, the ligaments are the only organs holding C1 to C2 as there is no intervertebral disc between the two vertebrae. Thus, high stress is applied on the ligaments in-between atlas and axis as trying to keep them connected. Being on the posterior section of the spine, it is only active in flexion rotation and does not involve in resisting extension rotation as it was anticipated.

Three more ligaments that are only exists in the cervical region that also have contribution in resisting flexion and extension rotations. Alar ligament secures odontoid in position by tying it to lower portion of the occipital bone. It is mainly active flexion as well as axial rotation. Another ligament plays a critical role in holding the odontoid in position and that is transverse ligament. This ligament stretches from one side of atlas on the inner surface to the other side passing odontoid from behind. Similar to alar ligament, it helps keeping Odontoid in position when the spine rotates in flexion. One more ligament also holds Odontoid in position and that is apical ligament. It is attached to the Odontoid from top and it extends upward to the occipital bone. It helps in keeping Odontoid in position. Any movement of Odontoid stretches Apical ligament, and thus stress is developed in the ligament. The following Figure 6.10 shows the stress distribution along the three ligament in flexo-extension rotation.

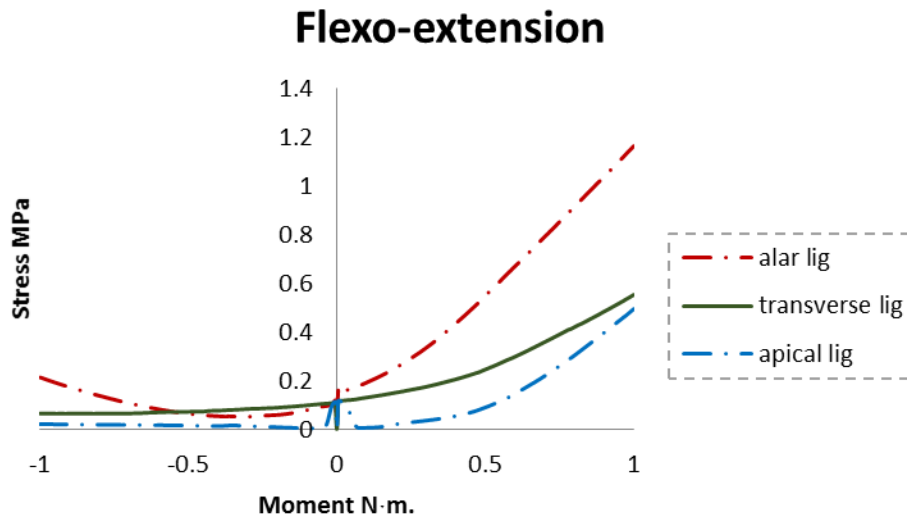


Figure 6.10. Stress distribution along Alar ligament, Transverse ligament and Apical ligament. Negative moment is extension while positive moment is flexion.

When the spine goes in extension, the back face of the anterior arch pushes on Odontoid and thus Alar ligament experiences a tensile stress. On the other hand, when the spine goes on flexion rotation, Atlas pulls on Alar ligament and in turn, it pulls on Odontoid. This stretching puts a high stress on Alar ligament as it can be noticed from Figure 6.10. The stress continues rising as the applied moment increases. From the previous Figure 6.10, the stress on transverse ligament is relatively higher in flexion comparing it to the extension. In extension rotation, there is a sudden increase at the beginning but it decreases as the load increases and that is due to the proximal-distal transition effect on the model. However, in flexion, it keeps rising as the applied moment increases. Comparing transverse ligament to Alar ligament, Alar ligament experiences higher stress in flexion, almost twice the stress comparing to transverse ligament and this indicates the critical role in keeping Odontoid in position during flexion rotation. Also from Figure 6.10, it can be concluded that Apical ligament is very active in resisting flexion rotation while a minimal contribution in extension rotation. In flexion, it starts with a small peak and then drops down to zero. But, then the stress picks up going up to 0.5 MPa at 1 N·m moment. In extension, similarly to flexion there is a small peak and then the stress decreased to zero. A small stress develops in the ligament as a higher moment is applied but it is very small comparing to the stress in flexion rotation.

6.1.2 Axial Rotation

Another test that was conducted on the finite element model was an axial moment. Two Rotational moments were applied on the model, one making the model rotate in positive direction (turning head to the right) while the second moment made the model rotate to the left. Theoretically, as the vertebrae rotate in either direction, all the ligaments attached to the moving vertebra are engaged in resisting the rotation. In the following section, graphs show stress distribution along all the ligaments in the cervical spine.

Starting with anterior longitudinal ligament (ALL), it is a thin board strip running vertically along the anterior surface of the vertebral body. When the spine rotates in axial rotation, ALL goes under torsion effect. Figure 6.11 shows the average distributed stress along ALL.

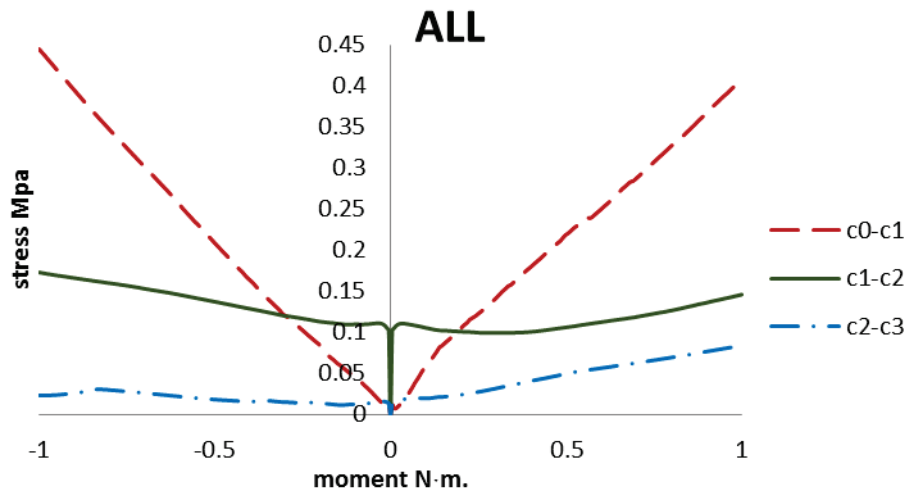


Figure 6.11. Stress distribution along ALL. Negative moment indicates rotation to the left side while positive indicates right side rotation.

From figure 5.1.2.1, C0-C1 and C1-C2 motion segments respond similarly to the applied axial rotations, both positive and negative. C0-C1 has the highest stress as it reaches 0.45 MPa in both directions. C1-C2 segment experiences the highest stress with about 0.15 MPa. It starts with a peak then continues to rise to reach the maximum value at 1 N·m. moment. C2-C3 does not respond symmetrically to axial rotation, it is more active in positive rotation than negative rotation as its contribution is minimal.

ITL are two thin small strips join two adjacent transverse processes on two different levels. When they go under axial rotation, the ligament goes under torsion and tension effect simultaneously. The following Figure 6.12 shows the effect of axial rotation on ITL.

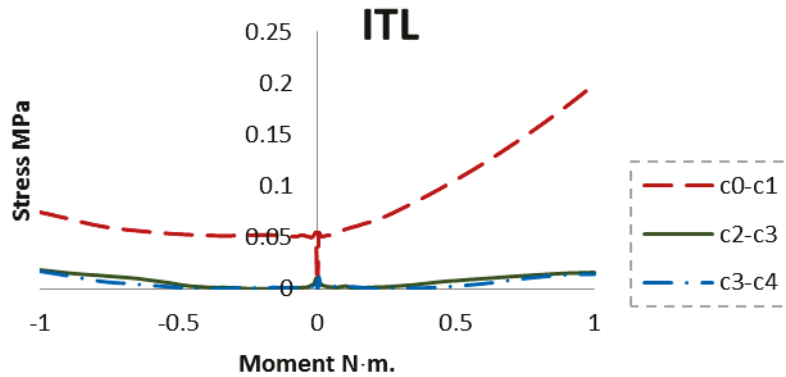


Figure 6.12. Stress distribution along ITL. Negative moment indicates rotation to the left side while positive indicates right side rotation.

Comparing to ALL, the stress in ITL is lower as it can be noticed from Figure 6.12. The response of the ligament C1-C2 segment is unsymmetrical to each sides as the detected stress in positive rotation is higher than negative rotation. From the previous Figure 6.12, the reported stress in ITL is 0.2 MPa in positive rotation while it is 0.08 MPa in negative rotation. The response in the lower levels is identical as C2-C3 and C3-C4 segments have the same stress flow in the graph, but compared to the most superior segment, they have a very small limitation of the axial rotation of the spine and the reason behind this is that the two upper most motion segments have the highest rotation comparing to the other segments as it was reported in chapter 4.

PLL is a wide ligament that runs downward on the posterior surface of the vertebral body. When PLL goes under axial rotation, stress developed in the ligament as shown in Figure 6.13.

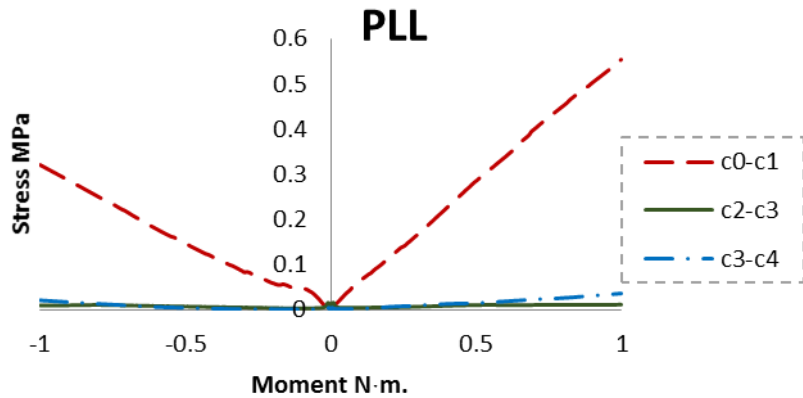


Figure 6.13. Stress distribution along PLL. Negative moment indicates rotation to the left side while positive indicates right side rotation.

Similar to ALL and ITL, the C0-C1 segment has experienced the highest stress compared to the lower segments as it reaches 0.6 MPa in the positive rotation. Unsymmetrical behaviour is noticed as the negative rotation stress is about half of the positive rotation as that is because of the irregular geometry of the model. Stress level drops significantly in the lower segments as it can be seen in Figure 6.13.

Capsular ligament (CL) is a circular ligament that surrounds facet joint. When the model goes under axial rotation, CL experiences torsional effect. With that, some area experience relatively high stress and some other area very low stress. The following Figure 6.14 shows the stress along CL.

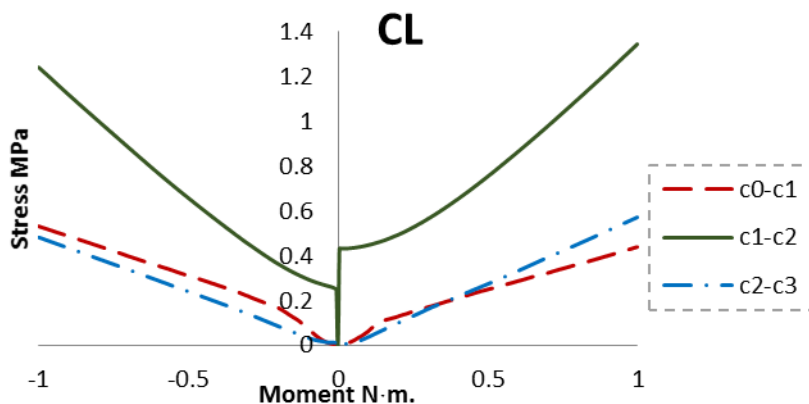


Figure 6.14. Stress distribution along PLL. Negative moment indicates rotation to the left side while positive indicates right side rotation.

The highest rotation degree in axial rotation is at C1-C2 segment and that reflects the amount of stress in the ligaments in that segment experience. The highest stress in CL is in the C1-C2 region due to high rotation in that region, followed up by C0-C1 segment in the negative rotation (spine rotating to the left) while C2-C3 has higher stress rotating in the other direction (positive rotation). Although C1-C2 has unsymmetrical response, but the stress values at 1 N·m moment are similar.

LV runs along the laminae process to the joining point. LV is a broad ligament that holds two adjacent vertebrae together. The following Figure 6.15 shows the stress along LV for the applied 1 N·m.

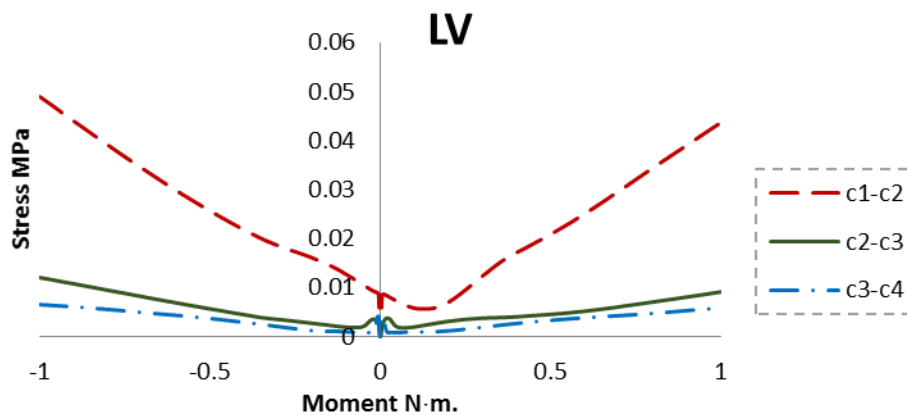


Figure 6.15. Stress distribution along PLL. Negative moment indicates rotation to the left side while positive indicates right side rotation.

When the spine rotates, LV has a minimal contribution in resisting the applied moment comparing to ALL, ITL, PLL and CL. Similar to the previously mentioned ligaments, C1-C2 has the highest resistance due to the rotational degree of the spine. The lower ligaments experience very low stress as the stress decreased to zero at the very bottom motion segment. C2-C3 and C3-C4 segment have symmetrical behaviour on both sides unlike the very top ligament where behaviour and stress are distinct on both sides.

ISL connects the spinous process of two adjacent vertebrae together. When the spine goes in axial rotation, ISL experiences tension and rotational stresses. Figure 6.16 shows the stress distribution along the ligament.

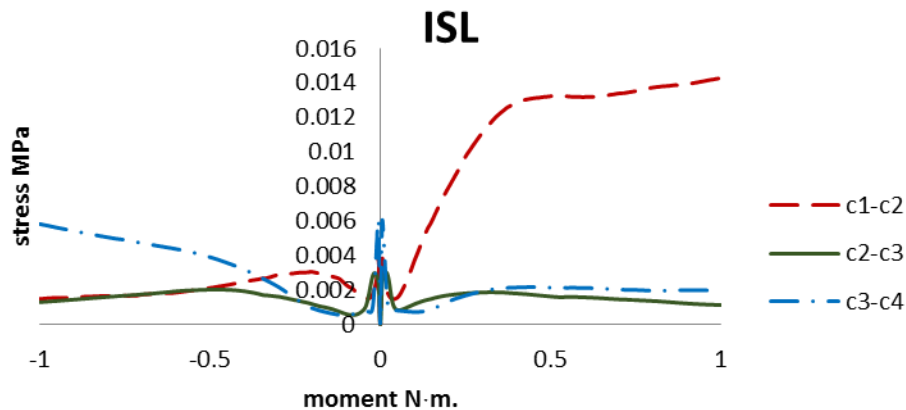


Figure 6.16. Stress distribution along ISL. Negative moment indicates rotation to the left side while positive indicates right side rotation.

The stress in ITL is different at each level. C1-C2 is more active in positive rotation than negative rotation. In the positive direction, the stress in C1-C2 is the highest as it is 0.014 MPa while it is the lowest among the top three in the negative direction. C2-C3 segment has a symmetrical response in both axial rotations. The stress in this segment is lowest in positive direction and it is a little higher in the negative direction. Just like the most top segment, the stress C3-C4 is asymmetric as the stress is highest in the negative direction while the stress is lower than C1-C2 segment in the positive direction.

Along with ISL, there is SSL that joins the tip of spinous process together. They are thin long ligaments that run from the skull (C0) down to T1 vertebra. In axial rotation, it develops torsional effect and goes under tension stress in some areas. Figure 6.17 shows the stress along the ligament.

From Figure 6.17, it can be noticed that SSL did not get significantly affected by the applied rotational moment on the spine. C1-C2 segment has the highest stress in positive rotation. While in negative rotation, the top three segments have the same stress at 1 N·m C0-C1 and C2-C3 have the symmetrical response to the applied moment. However, C1-C2 segment has distinct response to either moment as shown in Figure 6.17.

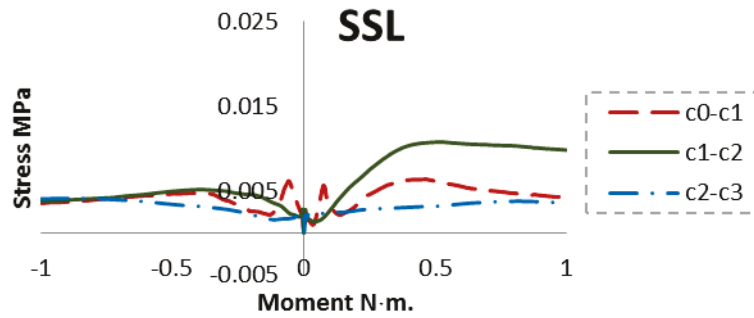


Figure 6.17. Stress distribution along SSL. Negative moment indicates rotation to the left side while positive indicates right side rotation.

The three unique ligaments at Odontoid junction also develop some stress as they try to keep odontoid in contact with Atlas. The three ligaments are Alar ligament, Transverse ligament and Apical ligament. The first one is made up of two portions on both sides of tip of odontoid holding to the atlas. The second one is a long band like ligament running on the posterior surface of the odontoid. The third one joins the tip of Odontoid to the Occipital bone. The stress along each ligament is shown in the following Figure 6.18.

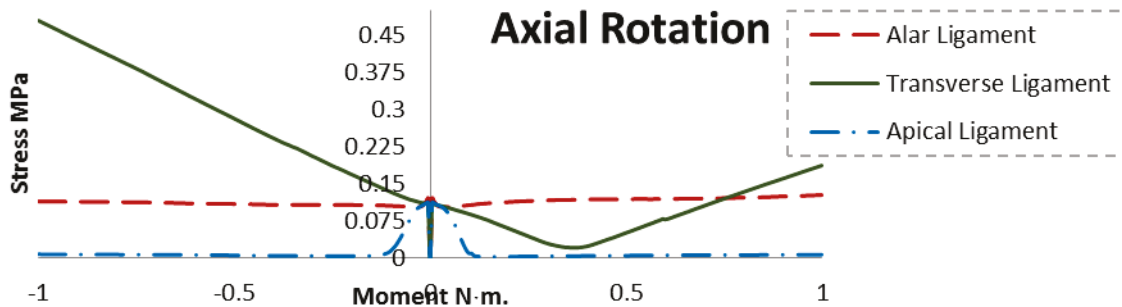


Figure 6.18. Stress distribution of Alar ligament, Transverse ligament and Apical ligament. Negative moment indicates rotation to the left side while positive indicates right side rotation.

Apical ligament has no contribution in resisting axial load as it can be concluded from Figure 6.18. Although there is a small peak at the beginning, Alar ligament has a steady and symmetrical behaviour to the rotational moment in both directions. However, Transverse ligament has unsymmetrical response to axial rotation in both directions as the stress increases in the negative rotation while there is an immersion near 0.5 N·m and then the stress starts increasing in the ligament.

6.1.3 Lateral Bending

Another test was performed on the spine and that was lateral bending on both directions. 1 N·m moment was applied on both directions making the spine rotate in frontal plane. When the spine rotates in either direction, ligaments tend to limit the movement and thus develop stress. Figure 6.2 divides spine into two halves; when the spine rotates to the right, the ligaments on the opposite side are stretched and tend to resist the moment and vice versa.

In Figure 6.2, ALL is divided into two equal halves; each half is stretched in each direction. When the spine rotates to the left, the right portion of ALL is activated in order to resist the rotation and when the spine rotates to right, the left portion is activated and develops stress.

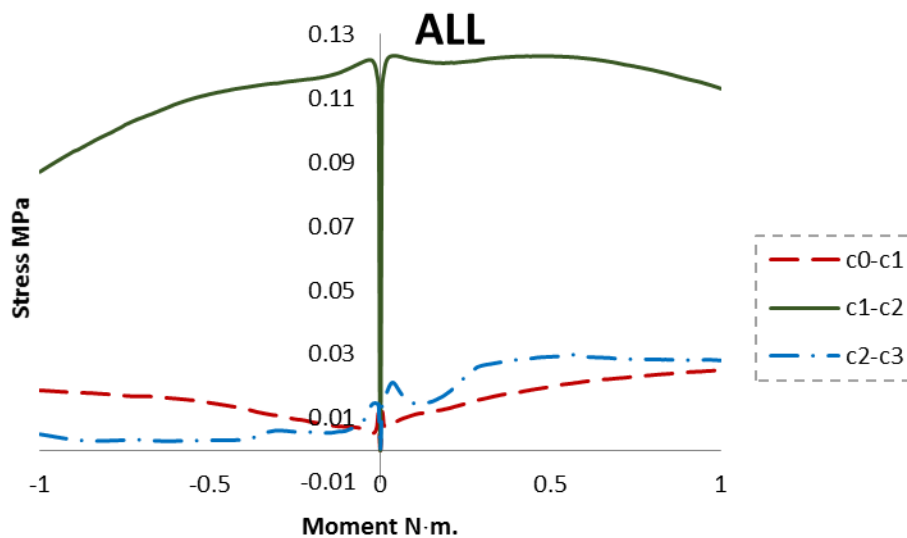


Figure 6.19. Stress distribution along ALL. Negative moment indicates the spine rotates to the left side while positive indicates the right side rotation.

From Figure 6.19, C0-C1 motion segment is barely involved in resisting the lateral bending. That is due to the fact that the skull (C0) and Atlas stick together and act as one unit when the spine rotates in lateral bending. On the other hand, C1-C2 segment has the highest stress. It starts with a peak due to proximal-distal translation and then the stress decreases as the load is increasing and the spine starts to rotate. C2-C3 segment also has a relatively small stress and it behaves unsymmetrically. The rest of the ligaments experience low stress comparing to C1-C2 segment.

ITL have two strips on each side of the vertebra, when the spine rotates one direction, ITL on the other side stretches while ITL on the same side buckles with a minimal stress. The following Figure 6.20 shows the stress in each ITL at the top three levels.

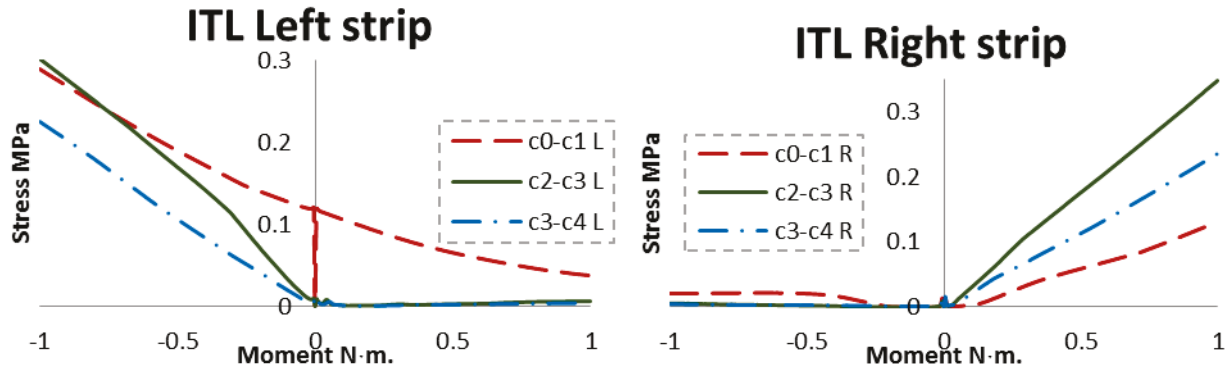


Figure 6.20. Stress distribution along ITL. Negative moment indicates the spine rotates to the left side while positive indicates the right side rotation.

From Figure 6.20, when the head rotates to the right side, the right side strip stretches and stress increases in the ligament as it can be noticed in the ITL right strip graph and on the other side, there is no stress in the ligaments except on the C1-C2 segment. Similarly, when the head sways to the left, the left side strips stretches and develops stress and on the other side, no stress in the left side ligaments except for the C1-C2 strip which predicts a small value of stress. In the left side rotation, the highest stress is developed in the C2-C3 segment then C1-C2 and followed by C3-C4. On the right side, the highest stress is in the C2-C3 segment then C3-C4 and then C1-C2 segment.

Similar to ALL, PLL is also divided into two halves when it comes to lateral bending. Stress is spread accordingly to the applied moment, when the spine rotates to the left, the right side is stretched and when the spine sways to the right, the left side is stretched. Figure 6.21 shows the stress distribution of the stress along PLL.

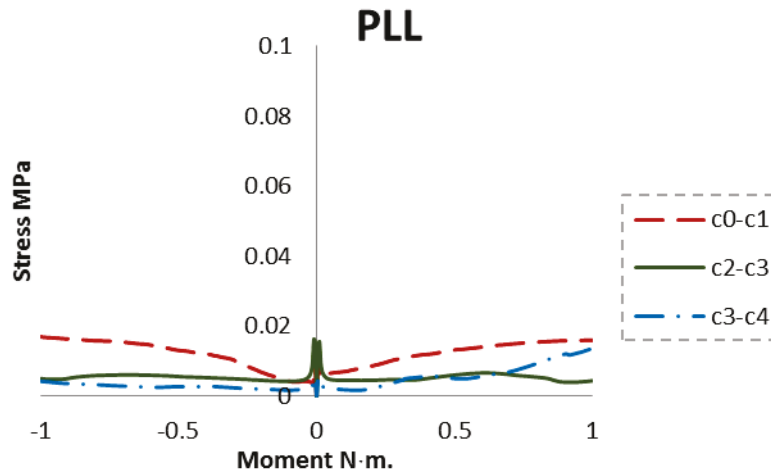


Figure 6.21. Stress distribution along PLL. Negative moment indicates the spine rotates to the left side while positive indicates the right side rotation.

C0-C motion segment experiences the highest stress as the spine sways to either left or right at it reaches about 0.018 MPa. Although the behaviour is asymmetric at the beginning, but then the ligament adopts the same response to the applied load specifically after 0.5 N·m. followed by symmetrical behaviour by C2-C3 segment. The third segment C3-C4 segment has unsymmetrical response as the stress in right rotation is higher than left rotation.

CL also has two separate ligaments, one joining the right facet joint and the other joining the left facet joint. Under lateral bending moment, one side goes under tension force and thus stretches while the other one experiences compression force and thus buckles. Figure 6.22 shows the left and right ligaments under lateral bending in both directions.

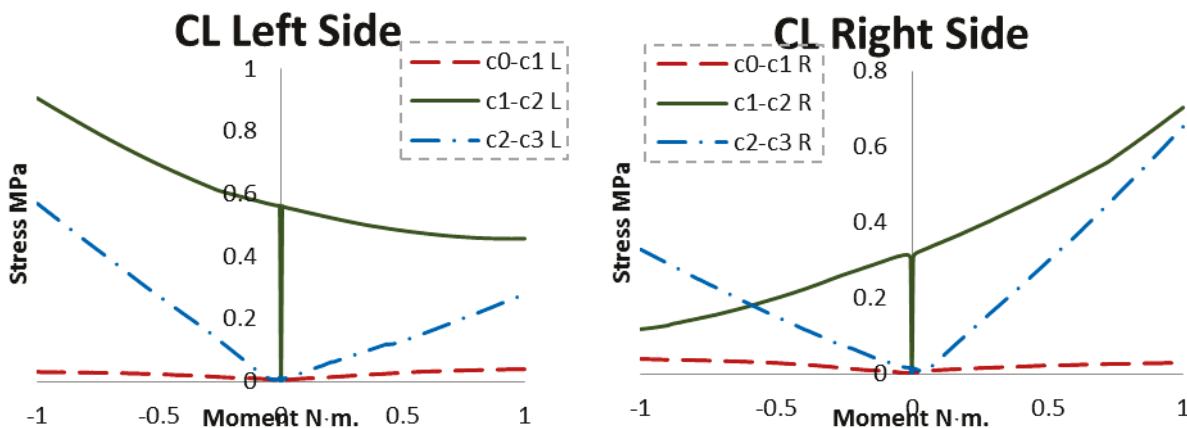


Figure 6.22. Stress distribution along CL. Negative moment indicates the spine rotates to the left side while positive indicates the right side rotation.

From Figure 6.22, CL at different levels experience different stress. C0-C1 segment has very low stress developed as the C0-C1 translates as one unit. The highest stress is in the C1-C2 segment in both directions. The left side ligament has 0.9 MPa stress in the left rotation while 0.5 MPa in right rotation, while the right side ligament has 0.15 MPa in the left rotation and 0.75 MPa in the right rotation. Similarly, C2-C3 also contributes in limiting lateral bending rotations in both directions as the stress is 0.55 MPa and 0.3 MPa for the left side and 0.3 MPa and 0.6 MPa for the right side.

LV has similar characteristic to PLL as being a thin broad layer of ligament. In lateral bending, LV stretches and thus stress increases in the ligament. Depending on the applied load, some part of the ligament has a high stress while the other part barely stretches.

From Figure 6.23, LV has a minimal contribution comparing to the other ligaments when it comes to 1 N·m. moment. C1-C2 is more involved in resisting negative rotation as resisting positive rotation. In negative rotation, C1-C2 ligament has the highest stress then C2-C3 and C3-C4 segments having the same response. In the positive rotation, C1-C2 and C2-C3 behave similarly and the stress is 0.01 MPa. C3-C4 segment experiences a lower stress in the same loading scenario as the stress reaches 0.005 MPa. The highest stress is reported at the C5-C6 segment while it is very low at the other levels.

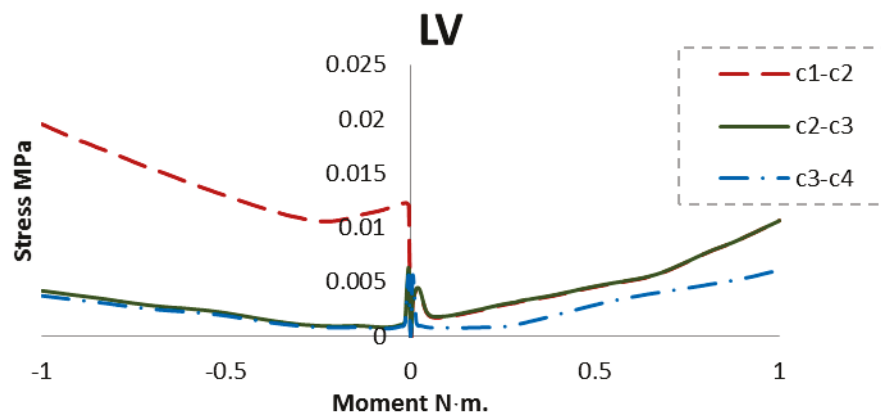


Figure 6.23. Stress distribution along LV. Negative moment indicates the spine rotates to the left side while positive indicates the right side rotation.

ISL lies along the transecting line in Figure 6.2. This makes it susceptible to lateral bending moment in both directions. The following Figure 6.24 shows the stress in ISL in both positive and negative directions.

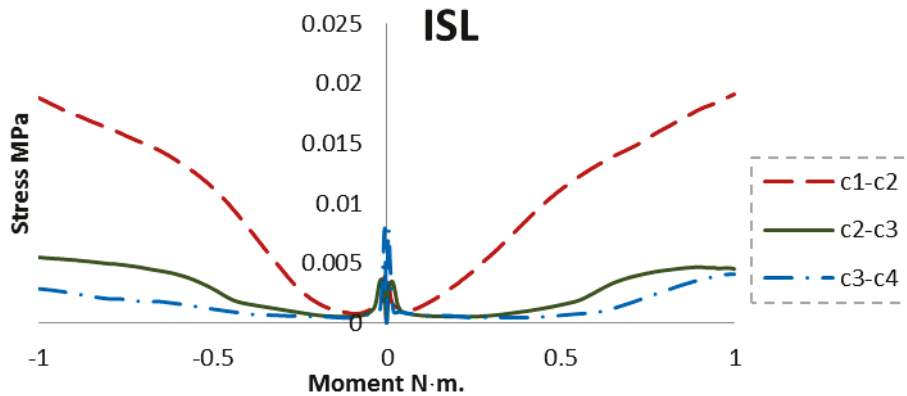


Figure 6.24. Stress distribution along ISL. Negative moment indicates the spine rotates to the left side while positive indicates the right side rotation.

The stress in ISL is symmetrical in both directions indicating that ISL responds symmetrically to lateral bending moment in both directions. C1-C2 segment has the highest stress among the top three levels as the stress reaches 0.02 MPa. The next most influential segment is C2-C3 segment as the stress is about 0.005 MPa and the least stress detectable is in the level C3-C4 segment. The stress in the other segments is lower as it can be seen from the graphs in the attached appendices.

When the spine goes in lateral bending, the vertebra tends to move away from the adjacent vertebra. As this happening, ligaments tend to hold vertebrae together. SSL joint the tip of spinous process of two adjacent vertebrae. As the spine is going through lateral translation, SSL stretches and thus stress is detected in the ligament. The stress distribution in the ligament is presented in the following Figure 6.25.

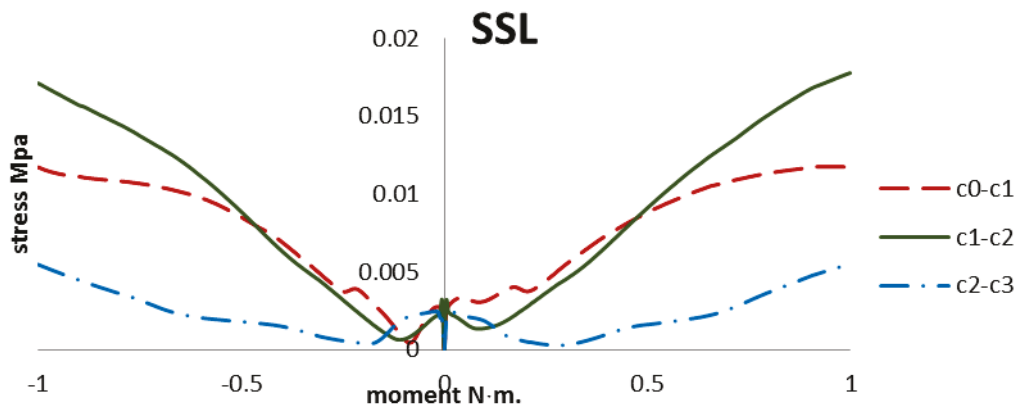


Figure 6.25. Stress distribution along SSL. Negative moment indicates the spine rotates to the left side while positive indicates the right side rotation.

Although the stress in SSL is relatively low compared to the other ligaments, the response is identical in all levels. From the Figure 6.25, a peak could be noticed as the spine goes in proximal-distal translation at early stage of loading. The stress drops later but then picks up for C1-C2 segment to reach 0.018 MPa on both rotational directions. However, for the lower segment, there is also a drop in the stress and then the stress starts increasing to reach 0.015 MPa for C0-C1 segment and 0.006 MPa for C2-C3 segment.

Skull (C0) and atlas act as one unit, so as the lateral bending moment is being applied, the spine tends to sways to either direction based on the applied moment. As C0-C1 segment is rotating, Odontoid tends to separate from Atlas, however, Alar ligament, Transverse ligament and Apical ligament tend to hold Odontoid in place. By doing so, stress is stress detected in the three ligaments as shown in the following Figure 6.26.

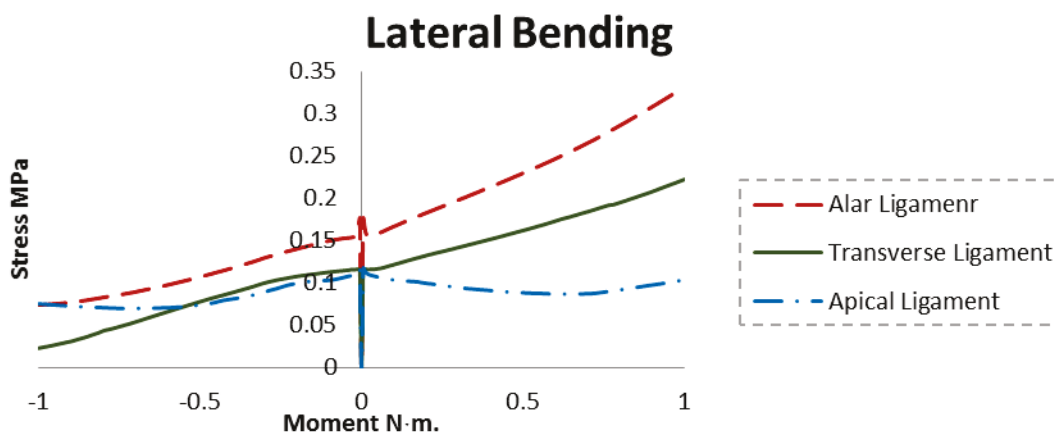


Figure 6.26. Stress distribution of Alar ligament, Transverse ligament and Apical ligament. Negative moment indicates the spine rotates to the left side while positive indicates the right side.

When the spine sways to the left, the three ligaments do not have a critical effect on resisting the load as they have an influence when the spine rotates to the right. In the left bending, Alar and Apical have the same stress which is about 0.08 MPa while Transverse ligament has a lower stress, 0.05 MPa. However, for the right rotation, the stress in Alar ligament is the highest as it is 0.035 MPa while it is 0.02 MPa and the lowest stress is along Apical ligament which is about 0.1 MPa.

6.2 Facet Joint

Another component that plays a major role in limiting the spine movement is called facet joint. Facet joints are extensions from pedicle and lamina connection. Each vertebra has four facet joints, two on the superior surface and two on the posterior surface. As the spine rotates, facets on the superior surface push against the facet joints on the inferior surface of the superior vertebra, this provides stability for the spine as well as resisting and limiting movement of the spine. The contact force presented here is the magnitude of all the force components in each direction.

6.2.1 Flexo-extension

Facet joints play a critical role in resisting flexo-extension rotation. When the spine rotates in flexion, the facet joint surfaces move away from each other except for the top two joints where they still push onto each other. For Atlanto-occipital joint, the condyle of occipital bone glides against the posterior wall of the concave atlantal facet. For Atlanto-axial joint arthrokinematic, the facet joints on the two vertebrae glide on each other in all direction movement. The following Figure 6.27 shows the contact force between facet joints at different levels for flexion and extension rotations.

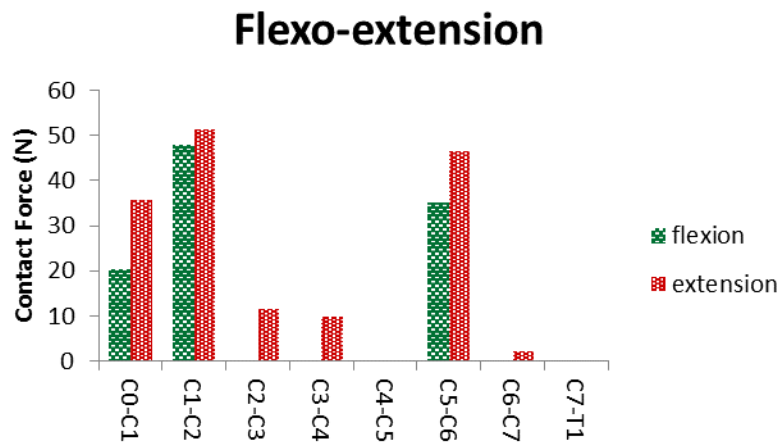


Figure 6.27. Contact force between facet joints at all levels of cervical spine in flexo-extension rotation.

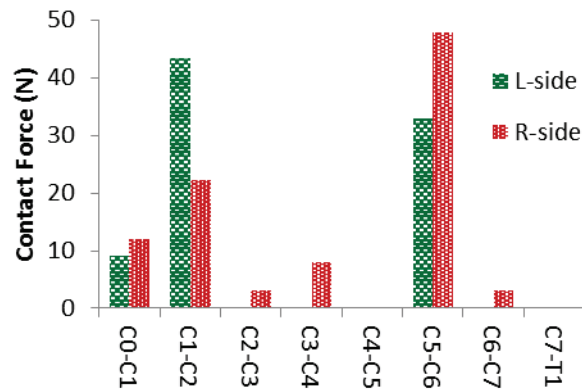
When the spine rotates in flexion, every couple facet joint move apart from each other, except for Atlanto-occipital and Atlanto-axial joints. From Figure 6.27, the contact force on the upper most joint is about 20 N while it is higher at the C1-C2 segment and it is about 50 N. the contact force among the other joints is zero expect for the C5-C6 segment which indicates a contact happening between the facet joints and the reported contact force is about 45 N.

In extension rotation, as the spine moves backwards, the facet joints come in contact and start pushing onto each other. From the previous Figure 6.27, facet joints at all levels are in contact except for the C4-C5 segment. As the spine move in extension, the contact force at C0-C1 segment is higher than it is in flexion because in flexion, ligaments are more engaged in limiting the rotation while in extension, the spine mainly relies on the facet joints to limit the movement and to transfer the loads.

6.2.2 Axial Rotation

As the spine rotates to the left or right, one of the two pairs of the facet joint is being active. On each level, there is a pair of facet joint and when the spine goes through axial rotation, one joint is getting involved in limiting the movement while the other is having the facets moving apart from each other.

Positive Axial Rotation



Negative Axial Rotation

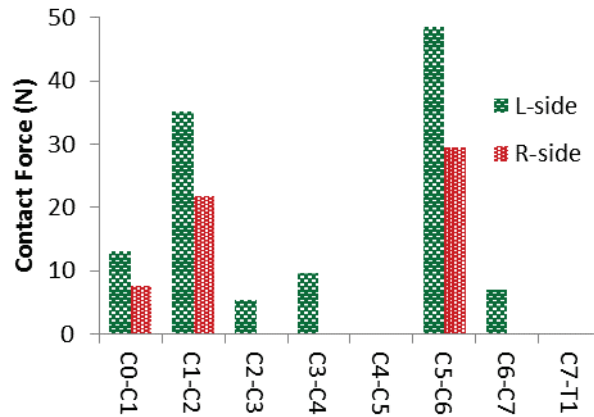


Figure 6.28. Contact force between facet joints at all levels of cervical spine in axial rotation with positive indicating rotation to the right while negative indicating rotation to the left.

As the spine rotates to the right, the facet joint on the left side move away from each other as it can be seen from Figure 6.28 in which the contact force between the facet joints is zero. At the same time, the facet joints on the right side come in contact and start pushing on each other making the spine rotates to the right. On the other hand, when the spine rotates to the left, the facet joints on the left side are active pushing the spine to rotate to the left while the facet joint on the right side are being inactive.

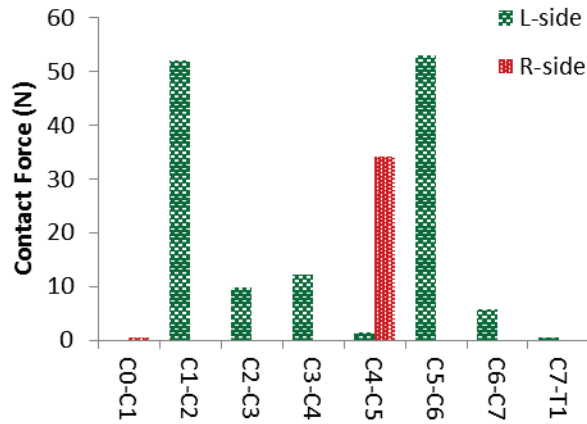
The highest force in the facet joint is detected at the C5-C6 segment in both rotations. In the right side rotation, the force is about 45 N while in the left side rotation is about 50 N. the difference in the contact force between the two sides is due to ligament involvement in resisting

the applied force as the ligaments are more involved in one side than the other side. Also, it can be noticed that the facet joint at the top two levels are always active whether the spine is rotating to the left or right. Also, segment C4-C5 detects no contact force at its facet joint. The imperfection of the model resulted in a no force facet joint at C4-C5 segment due to the gap between the facet surfaces.

6.2.3 Lateral Bending

Similar to the axial rotation when the spine sways to either direction, one side of the facet joints are active as the facet joints surfaces get closer and push on each other, while every facet joint couple on the other side is moving away from each other. When they come in contact, the facet joint exerts pressure on each other. The following Figure 6.29 shows the contact force among the facet joint in lateral bending.

Positive Lateral Bending



Negative Lateral Bending

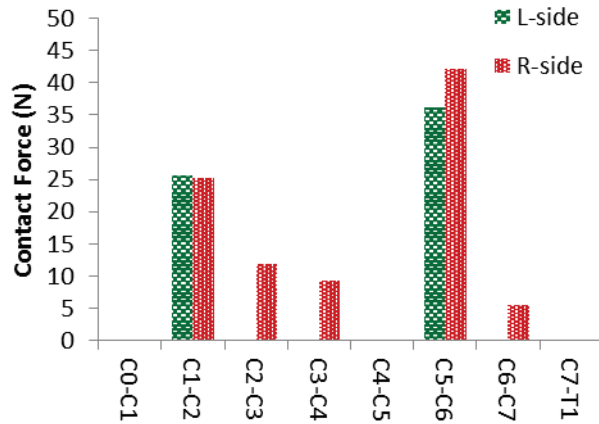


Figure 6.29. Contact force between facet joints at all levels of cervical spine in axial rotation. Positive rotation indicates spine rotation to the right while negative indicates the spine rotating to the left. L-side and R-side are set of facet joints on the left and right side of a single vertebra respectively from anterior view.

The most top (C0-C1) segment does not have any contact force as Atlanto-occipital joint acts as one unit in lateral bending rotation. When the head sways to the right (positive rotation), the left side facet joints are in contact and thus contact force can be detected in those facet joints. The highest force reported is at C1-C2 and C5-C6 segments where it reaches about 50 N. on the other hand, when the spine sways to the left (negative rotation), the highest force detected is at the C5-C6 joint. On the negative rotation, C4-C5 segment shows no contact between its right side facet joints.

6.3 Intervertebral Disc

Intervertebral disc is another component that helps in resisting and limiting spinal movement. It is located in-between two adjacent vertebral bodies. As the spine moves, the vertebrae exert pressure on the intervertebral discs via the vertebral body. Depending on the applied load, parts of the intervertebral disc go under pressure. The following contexts describes the applied load and the detected pressure on the intervertebral disc.

6.3.1 Flex-extension

When the spine move anteriorly (flexion rotation), the ligaments on the posterior side stretch holding vertebrae in place as well as limiting the spine movement. At the same time on the anterior part, vertebra presses on the intervertebral disc. The intervertebral disc acts as load transferring component as well as it helps in resisting the applied load. In flexion rotation case, most of the stresses are concentrated at the anterior part of the disc as the vertebral body leans forward and rotates which causes high compression on the anterior edge. At the same time, the compression force drives the nucleus pulposus onto the posterior wall of the disc causing a local high stress at the posterior edge. While in extension, the compressive force is acting on the posterior part of the disc, driving nucleus pulposus onto the anterior surface of the annulus. The following graph show the pressure generating in the nucleus as 1 N·m. is being applied in flexo-extension as well as the developed force into the annulus fibrosus as the end of applying the moment.

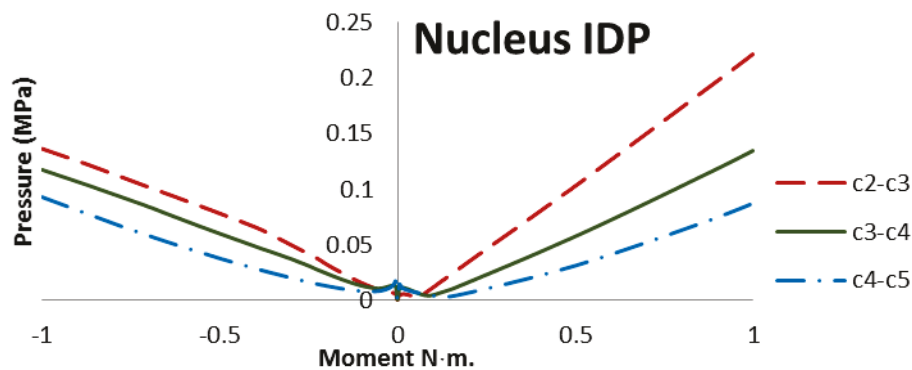


Figure 6.30. Stress distribution along nucleus pulposus in extension (negative moment) and flexion (positive moment).

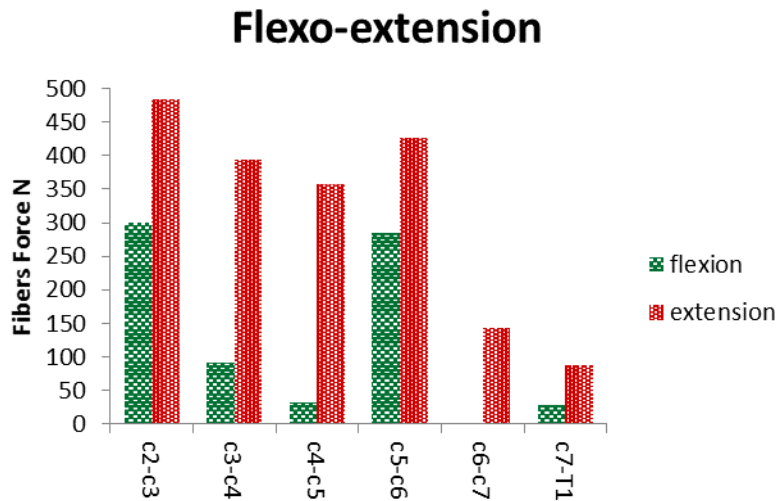


Figure 6.31. Total force in the annulus fibrosus at each levels.

Intervertebral disc has different response to the applied flexo-extension moment. From Figure 6.30, the pressure at C2-C3 nucleus in flexion is higher than it is in extension, indicating its contribution in resisting flexion is higher than resisting extension. C3-C4 and C4-C5 segments behave in the same manner. The tensile force in annulus fibrosus reflects the pressure in nucleus. The highest force is C2-C3 segment which is in agreement with the highest pressure which is also in the C2-C3 segment. C3-C4 segment has the highest force then C4-C5 segment. High stress on intervertebral disc generates high pressure on nucleus pushing it against the annulus pulposus and thus high force in annulus fibrosus.

6.3.2 Axial Rotation

As the spine goes in axial rotation, the rotational movement of the spine exerts stress on the intervertebral disc. As the spine rotates, nucleus goes under pressure and in turn, it pushes against the annulus. This process generates force in annulus fibrosus making it extend. The following Figure 6.32 shows the pressure in nucleus as well as force in the annulus fibrosus.

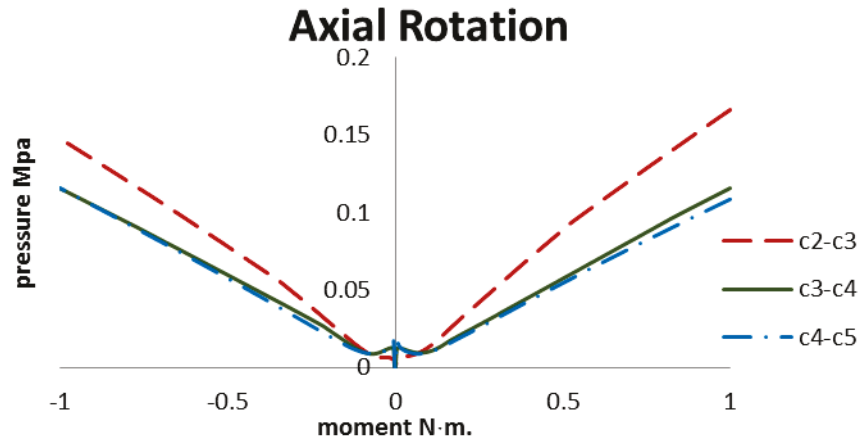


Figure 6.32. Stress distribution along nucleus pulposus in axial rotation, positive moment indicates spine turning to the right and negative moment indicates spine turning to the left.

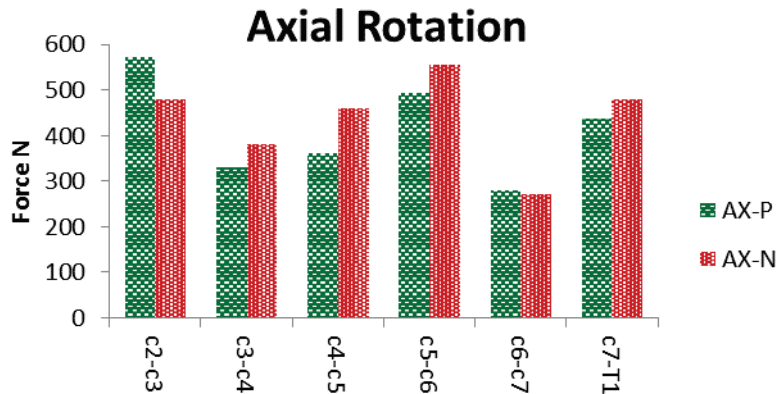


Figure 6.33. Total force in the annulus fibrosus at each level.

From the previous Figure 6.32, C2-C3 segment experiences the highest level of stress then C3-C4 and C4-C5 segments respectively. As the stress varies at each level, it also varies at each direction. C2-C3 and C3-C4 segments have higher stress in positive direction than in negative direction which reflects on the force in the fibers. In the positive direction rotation, high forces exerted on the fibers than in the negative direction rotation, indicating higher pressure on the nucleus and the intervertebral disc. However, for C3-C4 segment, it the opposite; although the pressure on the nucleus is higher in the positive direction, the force in the fibers is higher in the negative rotation. C4-C5 segment in similar to C2-C3 segment except the stress is higher in the negative rotation and thus the force in the fibers is higher in the negative rotation as well.

6.3.3 Lateral Bending

As the spine sways sideways, intervertebral disc is being compressed on its sides. As nucleus goes under pressure, it pushed against the annulus wall on the opposite side making it expand and thus the exert force on the fibers. Figure 6.34 shows the stress on the nucleus and Figure 6.35 presents the forces in the fibers.

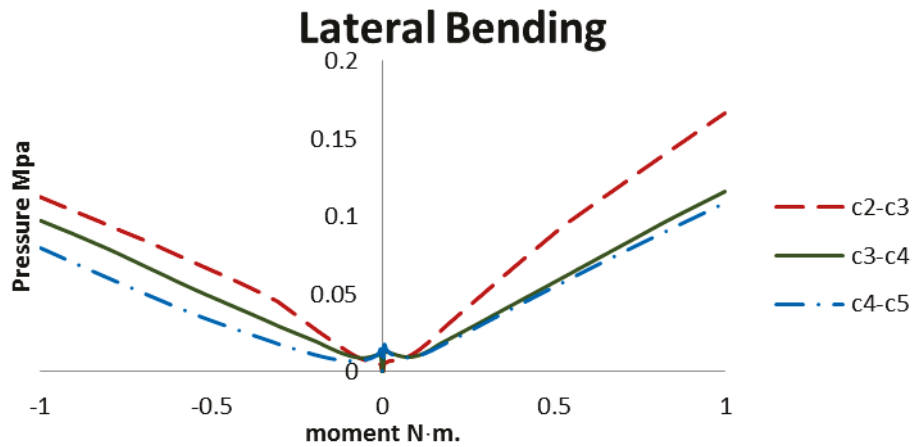


Figure 6.34. Stress distribution along nucleus pulposus in lateral bending, positive moment indicates spine rotating to the right and negative moment indicates spine turning to the left.

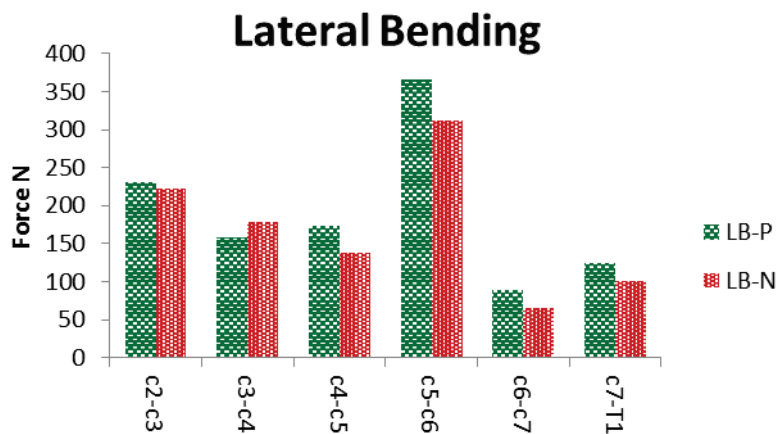


Figure 6.35. Total force in the annulus fibrosus at each levels.

Stress level at each segment is not similar indicating that the behaviour is not symmetrical. Right side rotation of segment C2-C3 exerts higher pressure on the nucleus than left side rotation. The reason behind the pressure difference comes from the difference in the contact force at the facet joints. In the left rotation, there is higher force on the contact force and thus less pressure on the intervertebral disc. However, the force in the fibers does not agree with that as the reported force

in the fibres indicate that higher force in the left side rotation. Pressure level and fibrosus force at C3-C4 segment in the fibers are in agreement as pressure on right side rotation is higher than the left side rotation and the force in the right side rotation is higher than the other side. C4-C5 segment is similar to C2-C3 segment in terms of the pressure level as well as the force in the fibers; pressure on nucleus is higher on the right side rotation but the force is higher on the left side rotation. Some imperfections come from the fixed surfaces of the vertebrae; the areas that had to be reconstructed due to surface interference.

7 Discussion and Recommendation

In the herein study, a three-dimensional complete ligamentous cervical spine had been used to assess and anticipate the stress distribution along the ligaments. The created numerical model consisted of skull, vertebrae (C1-T1), intervertebral disc, and bio-realistic geometry and refined mesh of ligament that would distinguish it from the previously published models Palomar et al. (2007); Moglo et al. (2012); N. Toosizadeh et al. (2011); and Zhang et al. (2006). The created ligaments would enable to simulate the contour plot of the stress on the ligaments as well as to anticipate the high stress initiation point and propagation path.

Using the current model, stress initiation and distribution was possible along the ligaments. In vitro studies, experiments presented the range of motion of the cervical spine under six rotational moments: flexion, extension, axial rotation in positive and negative directions as well as lateral bending in positive and negative direction. However, it failed to report the stress in the ligaments due to lacking the lab instruments that would measure the stress. For the numerical studies mentioned earlier, the used elements to represent ligaments would only output axial force and strain in the ligaments.

Validation of the range of motion of the current model was done by comparing with the in vitro experiments carried by Panjabi et al. (2001). The model was fixed at the bottom level (T1), while the spine was left unrestrained at the top. A moment of a value of 1 N·m. was applied on three different planes; two moments along sagittal plane, two along the transverse plane and the other two along the frontal plane. The load was applied on the most top component (C0). The obtained response from the current model was in agreement with the reported range of motion from the in-vitro experiment as well as the other finite element models. This indicates that the current model can provide relevant information regarding the cervical spine behaviour under any given static load.

The created model anticipated that the upper cervical spine (C0-C2) rotates more than the lower part of the spine. The rotation at this section is about half or higher of the total rotation of the cervical spine as shown in Figure 5.1 through Figure 5.3. This flexibility is a result of anatomic characteristics of the C0-C2 joints. In these segments, there is no intervertebral existing in

between the motion segments, but they are joined by ligaments only. A small load on the spine made the upper cervical spine go under large rotations due to the initial low stiffness of the ligaments. This makes ligaments in these regions vulnerable to high stresses comparing to the ligaments in the other segments.

In flexo-extension rotation, the highest stress in all ligaments was reported in the upper regions. In flexion, the applied moment was carried by intervertebral disc resulting in compression in the anterior part of the disc. With simultaneous contribution from the ligaments, flexion rotation resulted in tensile stress in the posterior ligaments of the spine.

As ligaments being stretched, tensile stress was initiated. Depending on the ligaments orientation with respect to the applied moment, high stress area concentrated on different areas on the ligament. In flexo-extension, stress was concentrated in the center region of the ligaments as shown in Figure 7.1. The stress initiated in the center region and propagated to the other regions on the ligament.

ISL was the only ligament that had stress being concentrated on different area on the ligament. As being on the posterior part of the spine, ISL was only stretched in flexion and the stress was on the inferior poster corner of the ligament. Figure 7.2 shows high stress area in ISL.

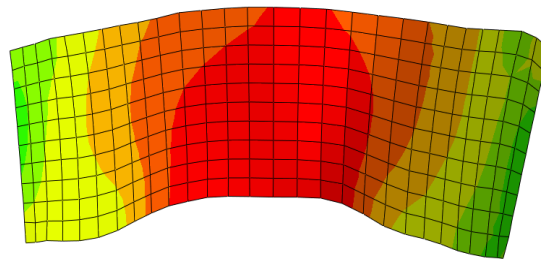


Figure 7.1. High stress region in ligamentum flavum in flexion rotation at 1 N·M

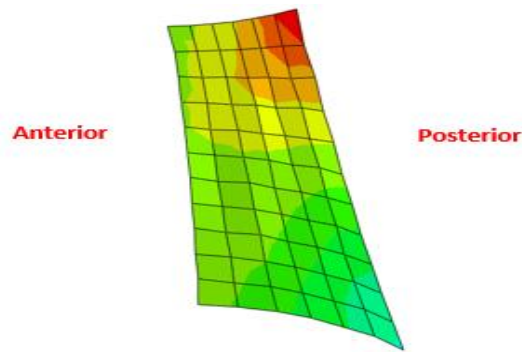


Figure 7.2. High stress region in supraspinous ligament in flexion rotation at 1 N·M

About 70 percent of the total load in flexion is carried by ligaments while 4 percent by the intervertebral disc and 26 percent by the facet joints. Out of that 70 percent, 40 percent is concentrated in the upper cervical spine with 17 percent in C0-C1 segment and 23 percent in C1-C2 segment. The stress in this region reflects the high rotation in the upper cervical spine. The remaining 60 percent of the stress in ligaments is distributed accordingly in each segment based on the rotation at each level. The range of motion was smaller as moving down the spine and so did the stress at each level. Minimal stress in the lower spinal section emphasise the significance of intervertebral disc's role in resisting external load.

In the upper cervical spine, the highest stress was in the posterior longitudinal ligament with 54 percent of the total stress in the C0-C1 segment. However, in C1-C2 segment, capsular ligament experienced the highest stress with 60 percent of the total stress in the segment. In the lower cervical spine, capsular ligament experienced the most of the tensile stress as the spine went in flexion.

The stress on the intervertebral disc correlated to the range of motion in the spine. C2-C3 has the highest rotation and thus stress in the disc was the highest comparing to the lower levels with 31 percent of the total stress in the disc. The stress on the disc drops in the lower with smaller rotation in the region. The 26 percent stress on facet joint was based mainly on the upper cervical spine due to anatomic geometry of the top two segments. 20 percent of the stress in facet joint was concentrated in C0-C1 segment while 48 percent in the C1-C2 segment. A minimal stress was detected in the lower regions except in C5-C6 segment with 32 percent of total stress in the facet joint.

In extension, unlike flexion, most of the load was carried by the facet joints, which was reflected on the stress level at the facet joint with 62 percent of the total stress. 36 percent of the total stress was in the ligaments and 2 percent in the intervertebral disc.

The highest stress on facet joints was reported at the C5-C6 segment with 33 percent indicating that it is a fluctuation point on the spine in extension. Segments below C5-C6 have small rotations while upper segments go through rotation. The stress in the facet joint in the upper cervical spine (C0-C2) makes 40 percent of the total stress on the facet joints with about 20 percent at each level. With high stress on facet joints, intervertebral discs experience a small pressure from vertebral bodies as small portion of the extension moment was transferred to the intervertebral discs.

The vast majority of the total stress was concentrated in anterior longitudinal ligament during extension, while the disc is being compressed on the posterior part and only anterior ligaments being engaged in limiting the rotation. 54 percent of the total stress in the ligaments was at the C0-C2 segments with about 28 percent at each level. Out of 28 percent of the stress in the ligaments, 58 percent was concentrated at ALL and 35 percent at the capsular ligament. This indicates that high rotation in the upper cervical spine comes with the cost of having high stress in the ligaments.

In axial rotation, the three components of the cervical spine collaborate together in resisting the load in both directions. As the loading starts on the spine, stress start developing in the ligaments immediately. In the ligaments, the stress was noticed to have a diagonal pattern with high stress levels at the corners of which the ligaments is being pulled by. While the low stress areas are at the other two corners. The following Figure 7.3 shows the high stress areas in ALL in axial rotation.

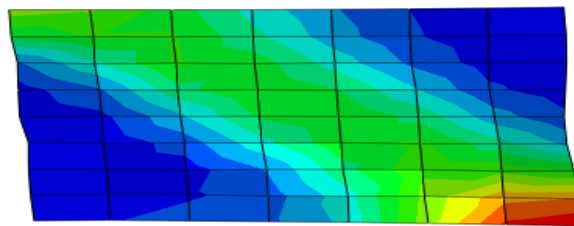


Figure 7.3. Front view of high stress region in ALL in positive axial rotation at 1 N·M

The facet joint and ligaments share the stress coming from the applied load with 45 percent in the ligaments and 48 percent in the facet joint while the intervertebral disc experiences 7 percent. The highest rotation angle was noticed at the C1-C2 segment, which was associated with highest stress in the ligaments with 22 percent of the total stress in the ligaments. The second highest stress in the ligaments was at C0-C1 segment, which also happened to be the second highest rotation detected in the spine. This indicated the association of the high stress with the high rotation in the spine.

Capsular ligament had the highest stress with an average of 75 percent at each segments. In the most top segment (C0-C1), it carried about 40 percent of the total stress in the section, while it reached 87 percent in the C1-C2 segment. The second most ligaments contributing in resisting the load were ALL and PLL with an average of 8 percent each. ALL and PLL had the highest stress in the C0-C1 segment with 32 and 23 percent respectively of the total stress in the section. Their role was minimal in the lower regions as most of the stress was concentrated at capsular ligaments. Other ligaments also had stress developed in them, however it was nominal comparing to capsular ligament. This observation indicates that in axial rotation, most of the stresses were carried by CL and it shows essentialness of CL in limiting axial rotation.

For facet joint, most of the stress was concentrated at the C5-C6 segment with about 50 percent of the total stresses in the facet joints. Here again, C5-C6 segment acting as fluctuation point between the upper part (C0-C5) and lower part (C6-T1). The upper segments are more mobile and thus they are more flexible and responsive to an applied load while lower segments are stiffer. The second highest stress was at the C1-C2 segment which also happens to have the highest rotation. The third highest stress was C0-C1 segment. This also proves that the upper cervical spine (C0-C2) is more flexible than the rest of the spine.

Just like facet joints, the highest compressive stress on the intervertebral disc was at the C5-C6 segment and that is due translation from flexible part of the spine (C0-C5) to the stiffer part (C6-T1). 42 percent of the total stress in disc was at this level. 36 percent was in the upper level and 20 in the C6-T1 sections.

In lateral bending, the spine rotates to the left and to the right accordingly. Two things were taken from this movement; one of them is that the ligaments on one side undergo tensile stress and thus stretches and the second thing is that ligaments in the middle of the spine are divided

into two halves, one half getting stretched while the other half being lax. For instance, anterior longitudinal ligament is located in the middle region of the spine, when lateral load was applied, it was half stretched as seen in the following Figure 7.4. Another noticeable takeout from this test was that C0-C1 segment was acting as one unit. From the previous cases, it was clear the influence of facet joint in transferring the load to the lower levels, but in lateral bending, there was merely any stress developed in the joint indicating that this segment was acting as one unit held together by ligaments.

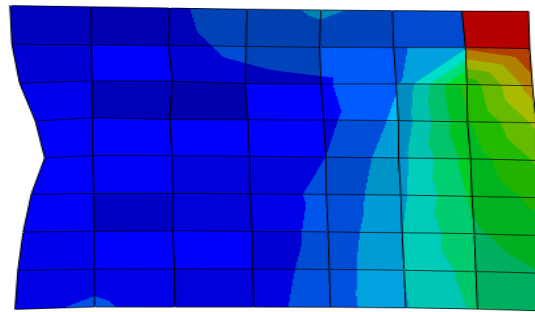


Figure 7.4. Front view of high stress region in ALL in positive lateral bending at 1 N·M

The stress distribution among ligaments and fact joints was equal with 48 percent each and 4 percent carried by the intervertebral disc. The highest stress value was at the C0-C1 segment and it was all concentrated in the ligaments as they held up C0 and C1 together. Most of the stress was shared between CL and ITL with 96 percent and 4 percent in each respectively. Ligaments in C1-C2 segment had 34 percent of the total stress in the segment with most of it being in CL as well.

C4-C5 segment has the second highest stress with 89 percent of the total stress in the segment. The rest of the stress was developed in the intervertebral disc and no stress was detected at the facet joints. CL along with ITL shared most of the stress with 60 percent in the Cl and 33 percent in ITL. The value of the stress fluctuates with the rotation angles in each segment as it varies moving down the spine.

The facet joint played a major role in stabilizing the supporting the spine in lateral bending. 46 percent of the total stress on the spine was shared by facet joint. Similar to the ligaments, the stress values ranged in each segment based on the rotation at each level. Analogous to the axial rotation and flexo-extension rotations, C5-C6 segment facet joint experienced the highest stress in the cervical spine. The stress in the discs was minimal as only 3 of the total stress was carried

by them. The stress in C2C3 was the highest with 23 percent of the total stress in all the intervertebral discs. The stress in discs was in agreement with the stress in ligaments as high stress was observed in the C4-C5 segment. This was due no contribution of the facet joints in limiting the rotation at this level.

From the 6 different rotation moments, it was noticeable that CL played a major role in resisting most of the moments in the spine with an average of 72 percent of the total bending moment. Any damage to this ligament would result in instability to the spine. The second most critical ligament was found to ALL with 17 percent. While PLL and ITL are equivalently important to the spine as both contributing in resisting about 8 percent of the total stress each. The other ligaments are also important however their role depends mainly on the applied load.

Using this model, it was able to predict the high stress areas in the ligaments as well as the initiation as well as path prediction. This model now can be used for future projects where given proper material properties, a damage prediction would be possible under any given load.

For obtaining better results using the created numerical mode, the material properties could be improvised. The current model was tested using only elastic material properties, to achieve better results, hyper-elastic material properties could be adjusted to the ligaments. Also, adding density characteristic of the bones and head weight would result in better approach to a realistic spinal behaviour. By adding hyper-elastic material properties, dynamic loadings could be applied on the model as the hyper-elastic material properties is time dependent. Furthermore, the weight of the skull and the vertebrae would add a compressive load on the spine especially the facet joints.

8 References

- A. Shirazi-ADL, Ahmed, A., & Shrivastava, S. (1987). Mechanical response of a lumbar motion segment in axial torque alone and combined with compression. *Clinical Biomechanics*, 2(3)
- Abaqus 6.14. (2015). Rigid body Simula.
- Adams, M. A., & Roughley, P. J. (2006). What is intervertebral disc degeneration, and what causes it?., 2013, from http://www.medscape.com/viewarticle/543611_2
- Areolar connective tissue., 2013, from http://medsci.indiana.edu/a215/virtualscope/docs/chap2_1.htm
- Bass, C., Lucas, S., Salzar, R., Oyen, M., Planchak, C., Shender, B., et al. (2007). Failure properties of cervical spinal ligaments under fast strain rate deformations. *Spine*, 32(1), E7.
- Berovic, M. (2015). Spinal facet joint The Sports Massage Blog.
- Bogduk, N., & Mercer, S. (2000). Biomechanics of the cervical spine I: Normal kinematics. *Biomechanics of the Cervical Spine I: Normal Kinematics*, 15(9), 633.
- Bridwell, K. (2016). Vertebral column Vertical Health.
- Bridwell, K. (2013). Ligaments., 2013, from <http://www.spineuniverse.com/anatomy/ligaments>
- Centeno, C. (2015). Alar ligament treatment for CCJ instability Regenexx.
- Cervical spine anatomy. (2011). , 2013, from <http://www.eorthopod.com/content/cervical-spine-anatomy>
- Crowell, R., Shea, M., Edwards, T., Clothiaux, L., White, A., & Hayes, C. (1993). Cervical injuries under flexion and compression loading. *Journal of Spinal Disorders*, 6(2), 181.
- Dariusz J. (2012). Balance in the control plane. part 2. Biokinetic Golf Swing Theory.
- DeWit, A., & Cronin, S. (2012). Cervical spine segment finite element model of traumatic injury prediction. *Journal of the Mechanical Behavior of Biomedical Materials*, 10, 138.
- Dugan, L. (2011). Atlanto occipital joint
- Dyke, J. (2014). Find your direction. Torrance, CA: CrossFit.

- EL-Rich, M., Arnoux, J., Wagnac, E., Brunet, C., & Aubin, E. (2009). Finite element investigation of the loading rate effect on the spinal load-sharing changes under impact conditions. *Journal of Biomechanics*, 42(9), 1252.
- Flanders, A. (2008). Spine - cervical injury., 2013, from <http://www.radiologyassistant.nl/en/p49021535146c5/spine-cervical-injury.html>
- Galileo Site Manager. (2016). The axis vertebra [] edoctronline.
- Haghpanahi, M., & Javadi, M. (2012). A three dimensional parametric model of whole lower cervical spine (C3-C7) under flexion, extension, torsion and laterla bending. *Scientia Iranica*, 19(1), 142.
- Han, I. S., Kim, Y., & Jung, S. (2012). Finite element modeling of the human cervical spine: Role of the uncovertebral joint. *Journal of Mechanical Science and Technology*, 26(6), 1857.
- Hata, T., & Todd, M. (2005). Cervical spine considerations when anesthetizing patients with down syndrome. *American Society of Anesthesiologists, Inc. Lippincott Williams & Wilkins, Inc.*, 102, 680.
- Ishii, T., Mukai, Y., Hosono, N., Sakaura, H., Fujii, R., & Nakajima, Y. (2006). Kinematics of the cervical spine in lateral bending. *Spine*, 31(2), 155.
- Ivancic, P. C. (2012). Neck injury response to direct head impact. *Accid Anal Prev*, 50, 323.
- Kallemeyan, N., Gandhi, A., Kode, S., Shivanna, K., Smucker, J., & Grosland, N. (2010). Validation of a C2-C7 cervical spine finite element model using speciment-specific flexibility data. *Medical Engineering & Physics*, 32(5), 482.
- KenHub. (2013). Transverse ligament of the atlas
- Know your back., 2013, from <http://www.knowyourback.org/Pages/Definitions/AnatomySpine/Bones/Vertebrae.aspx>
- Kopf-Maier, P. (2005). *Atlas of human anatomy (6th edotion ed.)*. Berlin: Wolf-Heidegger's.
- Kumaresan, S., Yoganandan, N., Pintar, A., & Maiman, J. (1999). Finite element modeling of the cervical spine: Role of intervertebral disc under axial and eccentric loads. *Medical Engineering & Physics*, 21(10), 689.
- Mattucci, F., Moulton, A., Chandrashekar, N., & Cronin, S. (2012). Strain rate dependent properties of younger human cervical spine ligaments
- . *Strain Rate Dependent Properties of Younger Human Cervical Spine Ligaments*, 10, 216.

- Maurel, N., Lavaste, F., & Skalli, W. (1997). A three-dimensional parameterized finite element model of the lower cervical spine. study of the influence of the posterior articular facets. *Journal of Biomechanics*, 30(9), 921.
- Mechanical properties of bone. (2013). , 2013, from http://www.doitpoms.ac.uk/tlplib/bones/bone_mechanical.php
- Medical MultiMedia Group. (2002). Cervical spine anatomy Orthopod.
- Megan, L. (2014). Roof of neck Study Blue.
- Mesfar, W., & Moglo, K. (2013). Effect of the transverse ligament rupture on the biomechanical of the cervical spine under a compressive load. *Clinical Biomechanics*, 28(8), 846.
- Mustafy, T., El-Rich, M., Mesfar, W., & Moglo, K. (2014). Investigation of impact loading rate effects on the ligamentous cervical spinal load-partitioning using finite element model of functional spinal unit C2–C3. *Journal of Biomechanics*, 47(12), 2891.
- Nikolai, B., & Mercer, S. (2000). Biomechanics of the cervical spine. I: Normal kinematics. *Clinical Biomechanics*, 15(9), 633-648.
- Okawara, S., & Nibbelink, D. (1974). Vertebral artery occlusion following hyperextension and rotation of the neck. *Stroke*, 5, 640.
- OpenStax College. (2013). Human axial skeleton (6th ed.)
- OpenStax College. (2013). Human axial skeleton (6th ed.) OpenStax College.
- Palomar, A., Calvo, B., & Doblaré, M. (2008). An accurate finite element model of the cervical spine under quasi-static loading. *Journal of Biomechanics*, 41(3), 523.
- Panjabi, M., Crisco, J., Lydon, C., & Dvorak, J. (1998). The mechanical properties of human alar and transverse ligaments at slow and fast extension rates. *Clinical Biomechanics*, 13(2), 112.
- Panjabi, M., Crisco, J., Vasavada, A., Oda, T., Cholewicki, J., Nibu, K., et al. (2001). Mechanical properties of the human cervical spine as shown by three-dimensional load-displacement curves. *Spine*, 26(24), 2692.
- Panjabi, M., White, A., Keller, D., Southwick, W., & Friedlaender, G. (1978). Stability of the cervical spine under tension. *Journal of Biomechanics*, 11(4), 191.
- Panjabi, M., White, A., Keller, D., Southwick, W., & Friedlaender, G. (1978). Stability of the cervical spine under tension. *Journal of Biomechanics*, 11(4), 189.
- Parker, L. Cervical spine fractures. Hattiesburg, Mississippi:

- Physical therapy in corpus christi for lower back., 2013, from <http://www.humpalphysicaltherapy.com/article.php?aid=320>
- Physiotherapy in banff for lower back. (2009). , 2013, from <http://www.activemotionphysio.ca/article.php?aid=48>
- Pooni, S., Hukins, W., Harris, F., Hilton, C., & Davies, E. (1986). Comparison of the structure of human intervertebral discs in the cervical, thoracic and lumbar regions of the spine. *Surg Radiol Anat.*, 8(3), 175.
- Przybyla, S., Skrzypiec, D., Pollintine, P., Dolan, P., & Adams, M. (2007). Strength of the cervical spine in compression and bending. *Spine*, 32(15), 1612.
- Pujari, S. (2015). The cervical vertebrae; innter-vertebral and cranio-vertebral joints
- R. C. Schafer. The cervical spine ., 2013, from http://www.chiro.org/ACAPress/Biomechanics_of_Cervical_Spine.html
- Sareen, A. (2014). Supraspinous ligament Physiopedia.
- Clark, C., & Benzel, E. (2005). *The cervical spine* (4th ed.) Philadelphia: Lippincott Williams & Wilkins.
- Kim, D., Vaccaro, A., Dickman, C., Cho, D., Lee, S., & Kim, I. (2013). Surgical anatomy and techniques to the spine
- Shapiro, I., & Risbud, M. (2014). *The intervertebral disc: Molecular and structural studies of the disc in health and disease*
- Schmidt, H., Kettler, A., Heuer, F., Simon, U., Claes, L., & Wilke, J. (2007). Intradiscal pressure, shear strain, and Fiber strain in the intervertebral disc under COmbined loading . *Spine*, 32(7), 748.
- Shae, A., Edwards, W., White, A., & Hayes, W. (1991). Variations of stiffness and strength along the human cervical spine. *J biochem. Journal of Biomechanics*, 24(2)
- Spine glossary-odontoid process (dens). (2013). , 2013, from <http://www.grhealth.org/neuroscience-center/spine/spine-glossary/ContentPage.aspx?nd=3353>
- sussman. (2013). Superficial back., 2013, from <http://www.studyblue.com/notes/n/superficial-back-/deck/1825926>
- The art of medicine. (2015). Atlas-C1 vertebra C1 Vertebra – Atlas and Accompanying Structures.

The Chiropractic Resource Organization. Atlas Chiro org resources.

Toosizadeh, N., & Haghpanahi, M. (2011). Generating a finite element model of the cervical spine: Estimating muscle forces and internal loads. *Scientia Iranica*, 18(6), 1237.

Understanding spinal anatomy: Ligaments, tendons and muscles., 2013, from <http://www.coloradospineinstitute.com/subject.php?pn=anatomy-ligaments-17>

The vertebral column or spinal column(2016). NCS Pearson.

Vertical health. (2014). Cervical spine anatomy animation Spine Universe.

Warrior, W. (2015). Cervical spine

Watkins, J. (2009). Structure and function of the musculoskeletal system (second ed., pp. 131-141-21-58). united kingdom: Human Kinetics Publishers.

Which X-ray views should be obtained?(2016). ED Medicine.

Williamson, . (2011). ANTPHy 1 study guide Georgia Southern University.

Yoganandan, N., Kumaresana, K., & Pintar, F. (2001). Biomechanics of the cervical spine part2. cervical psine soft tissues responses and biomechanical modeling. *Clinical Biomechanics*, 16(1), 1.

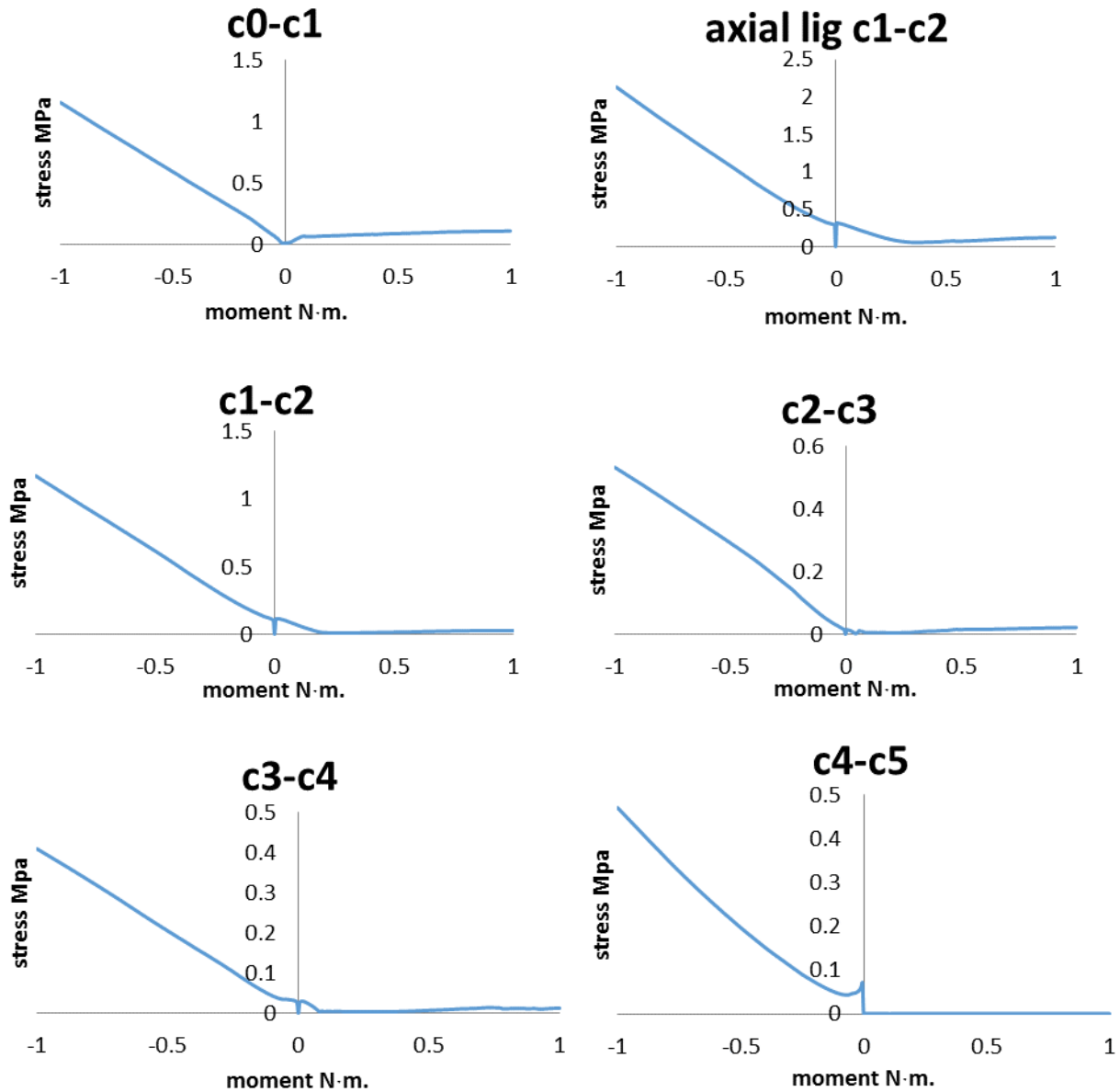
Zhang, Q., Teo, C., Ng, W., & Lee, S. (2006). Finite element analysis of moment-rotation relationships for human cervical spine. *Journal of Biomechanics*, 39(1), 189.

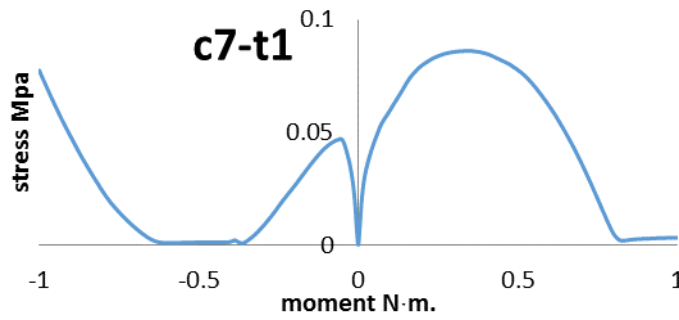
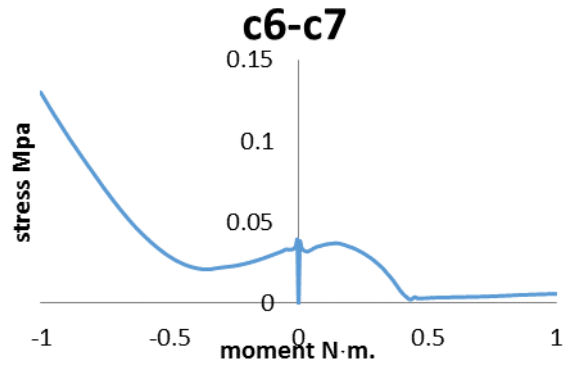
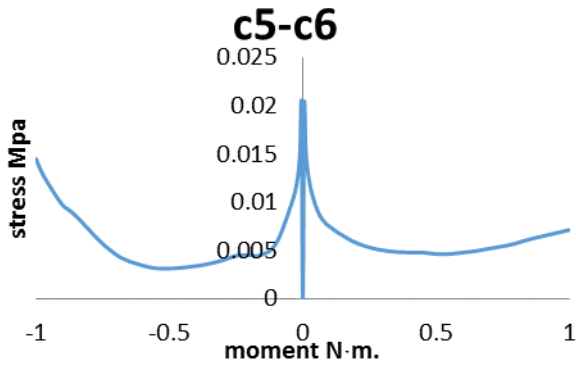
Appendix

The data presented herein is continuation for chapter 6. The graphs represent the stress in each ligament of the cervical spine under the six different moments.

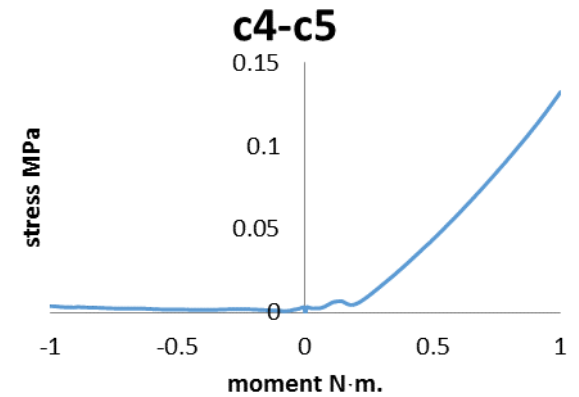
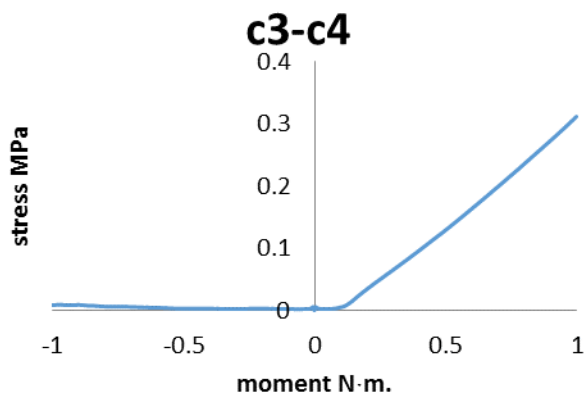
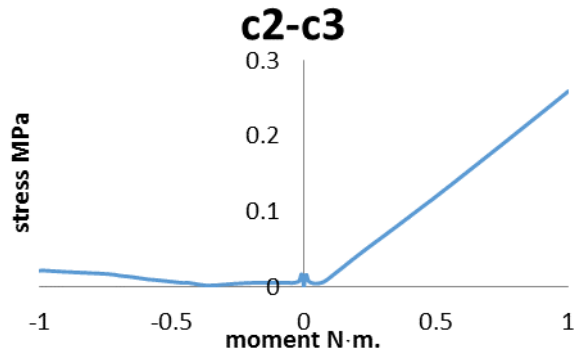
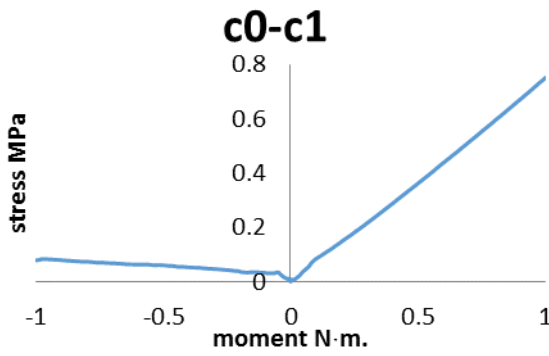
Flexo-extension:

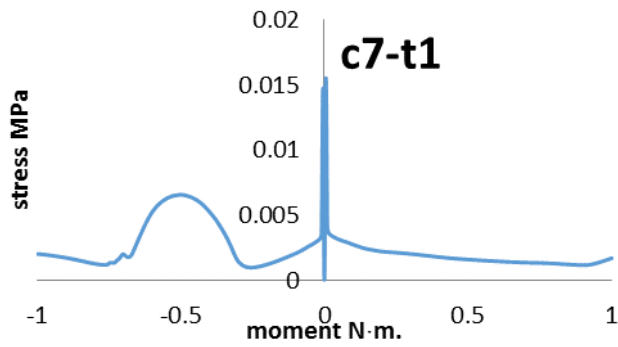
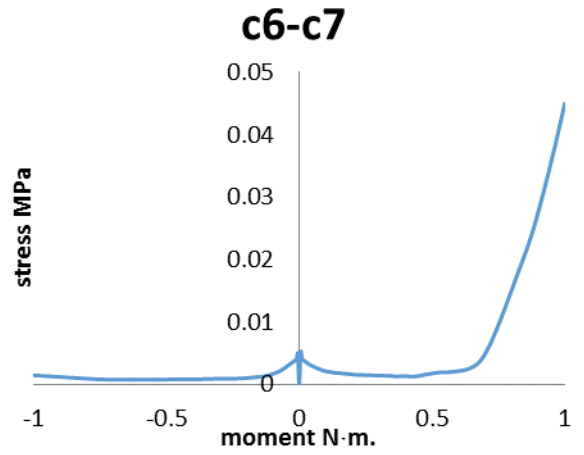
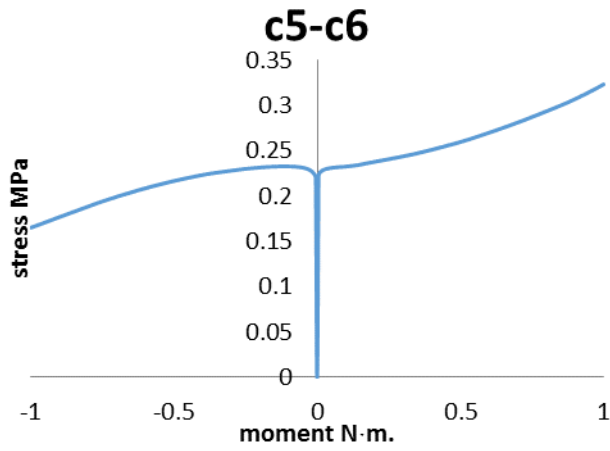
Anterior longitudinal ligament:



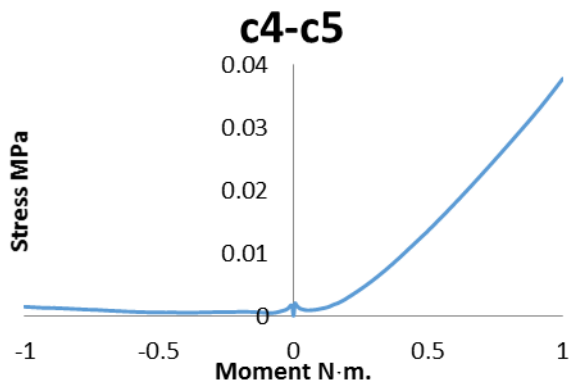
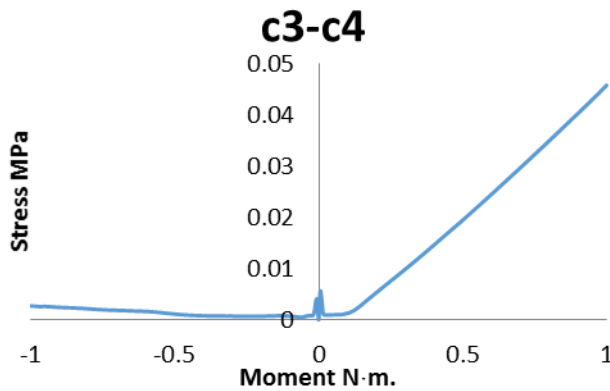
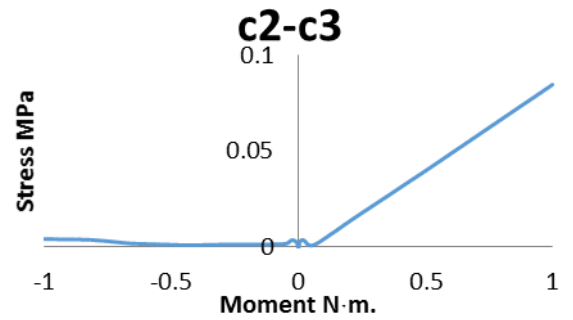
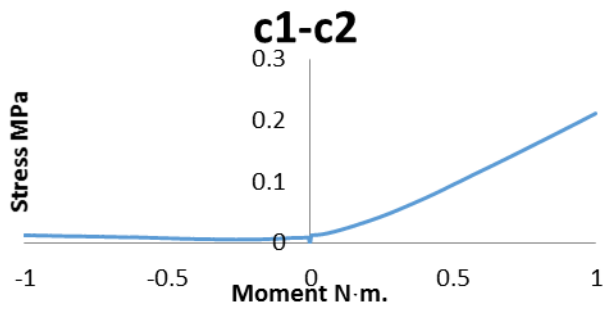


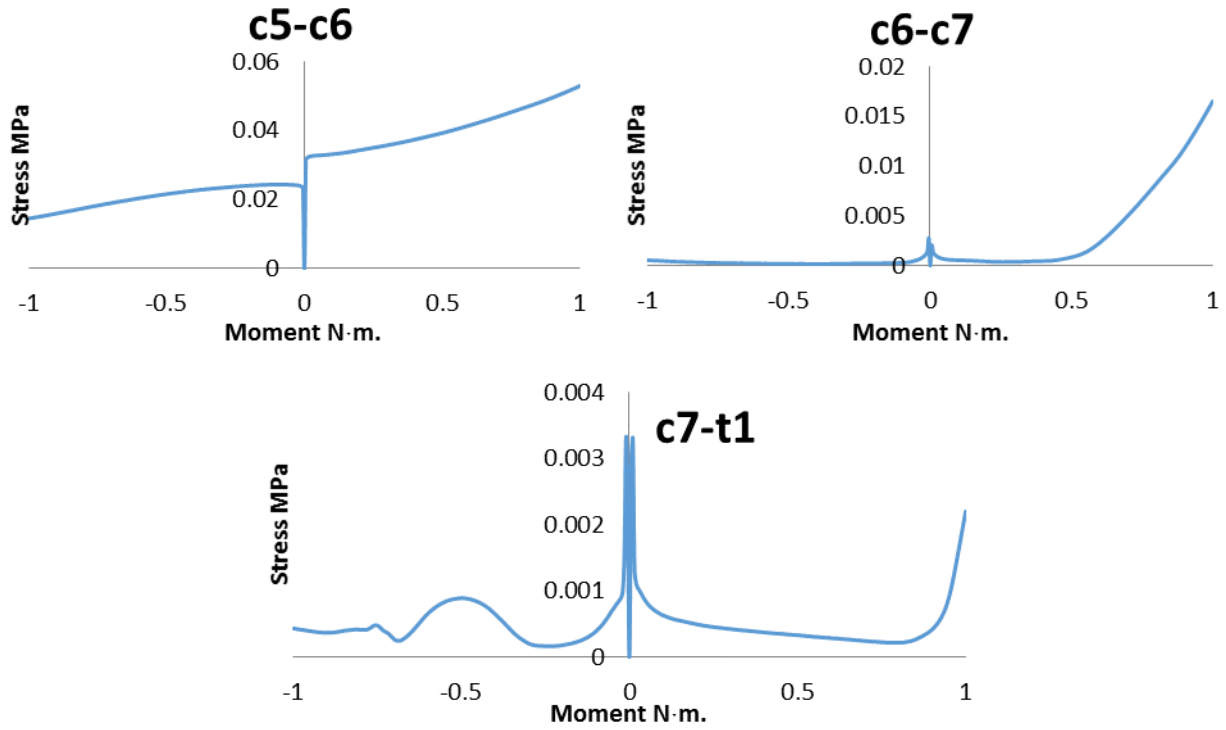
Posterior longitudinal ligament:



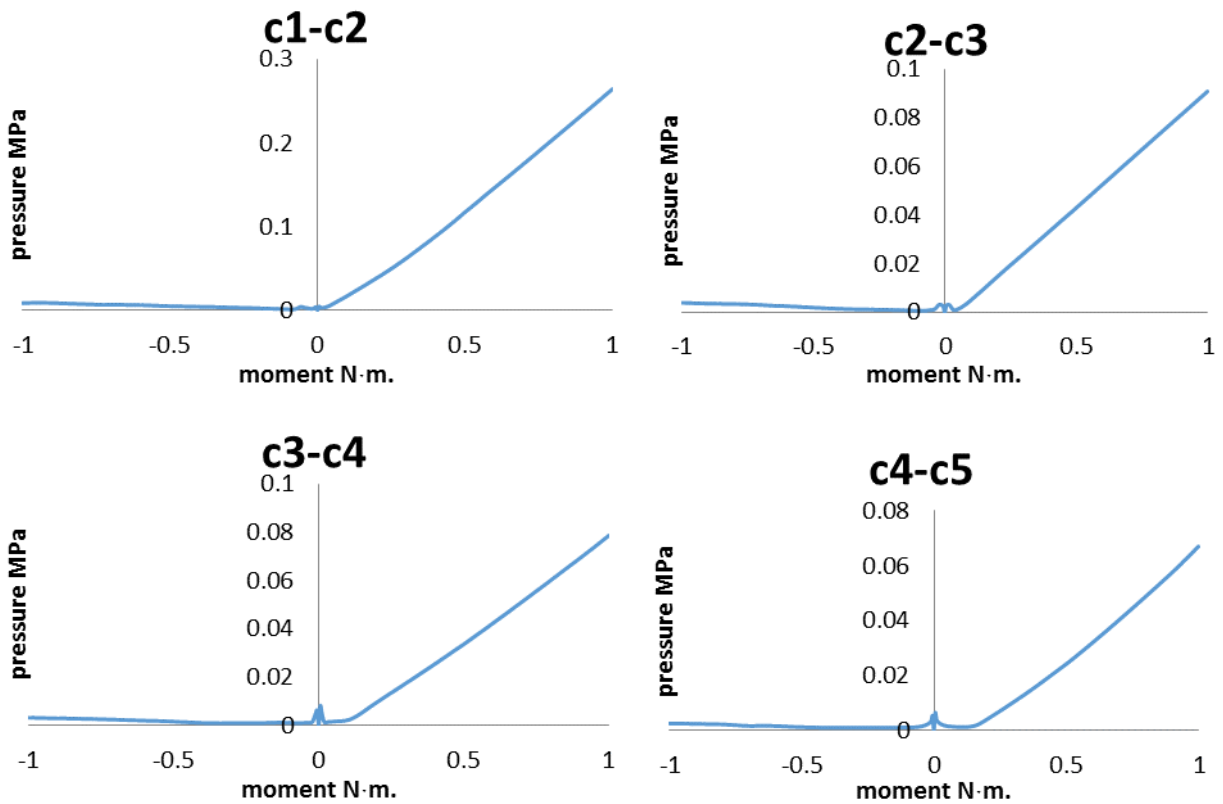


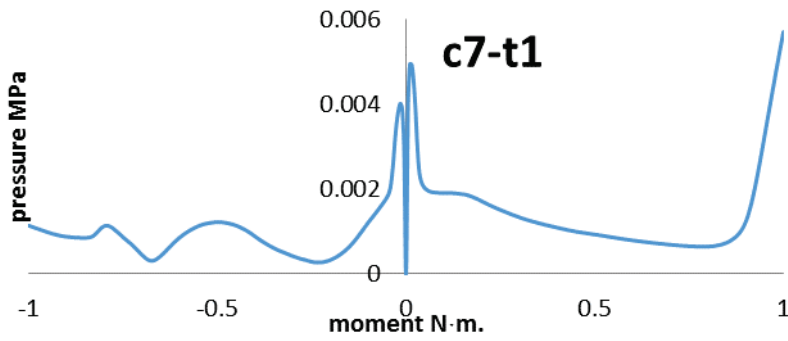
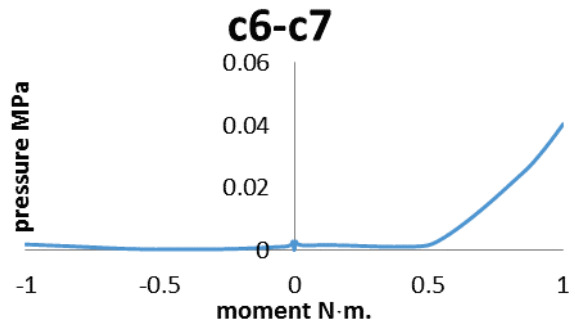
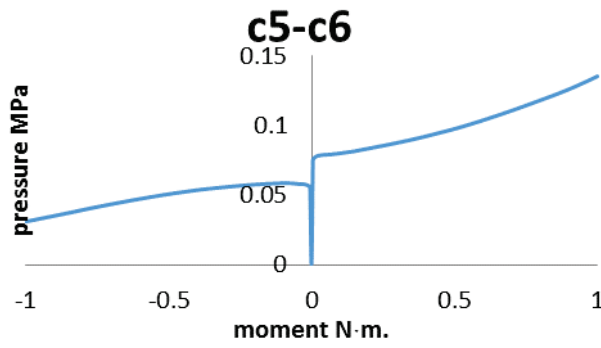
Ligamentum flavum:



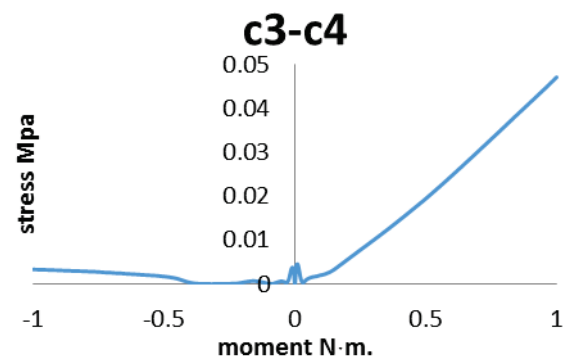
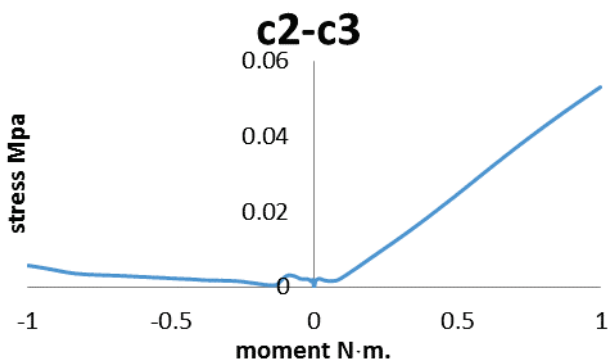
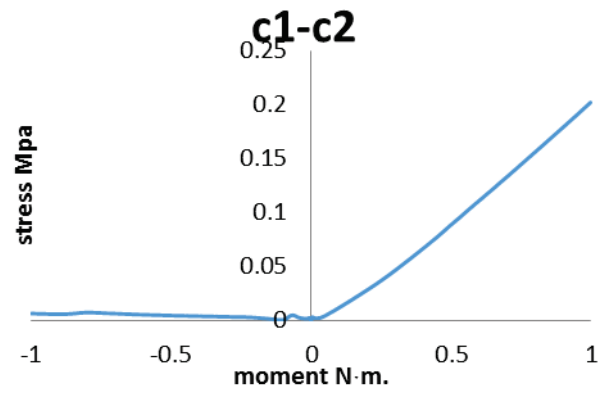
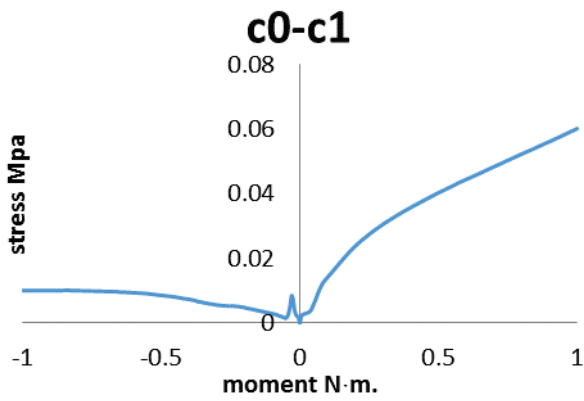


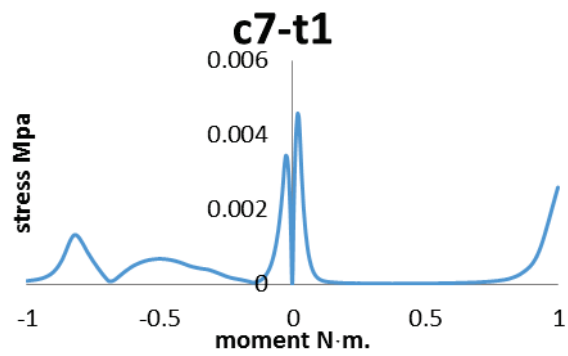
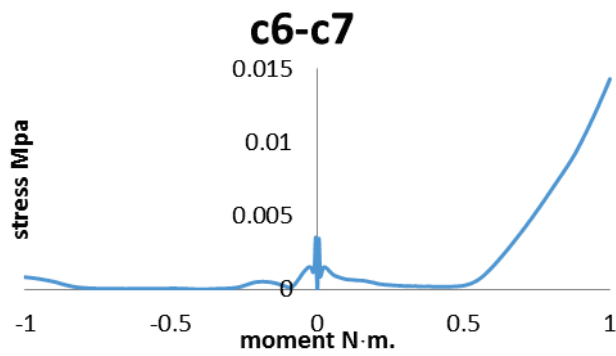
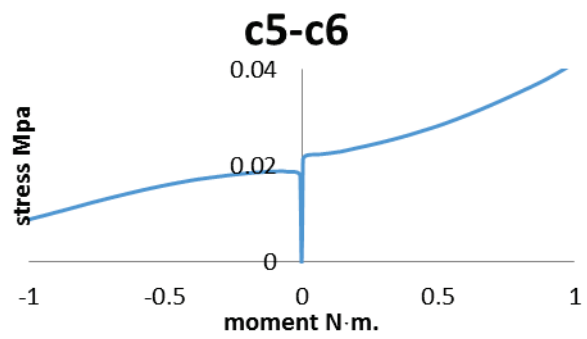
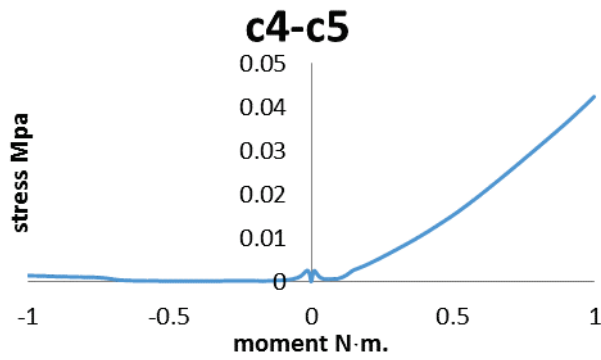
Intertransverse ligament:



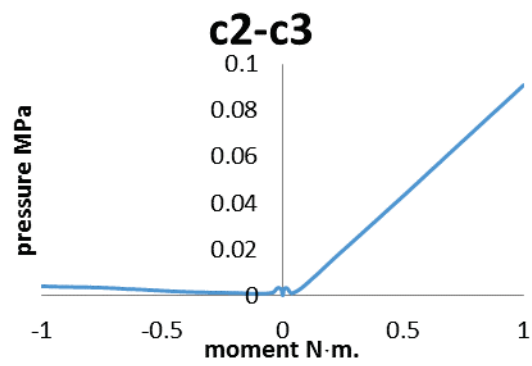
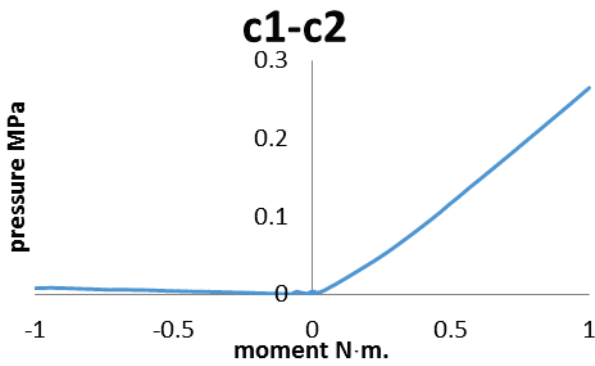


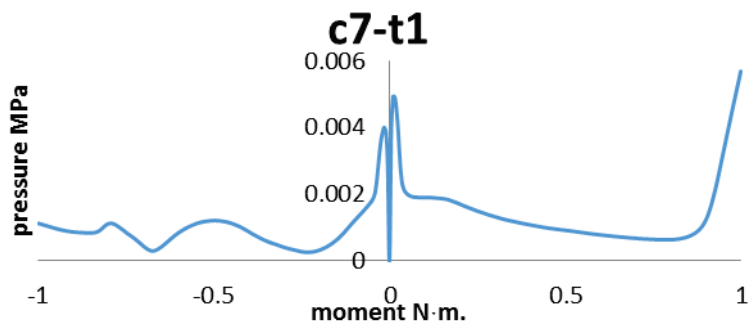
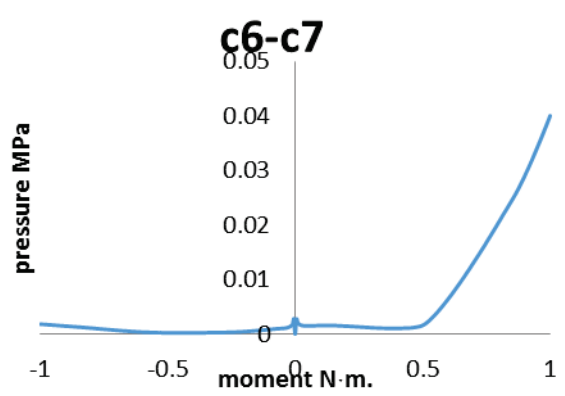
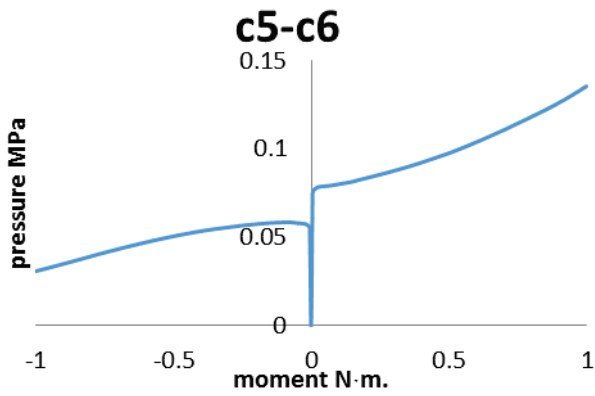
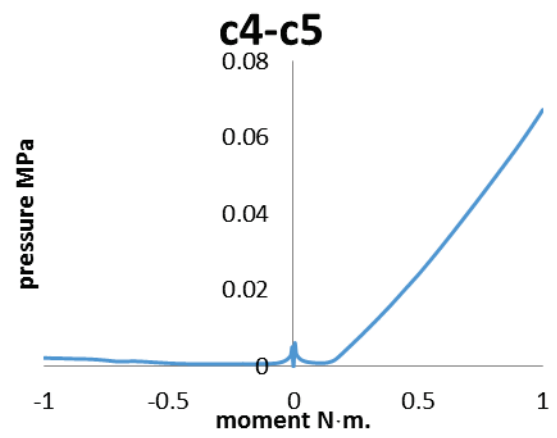
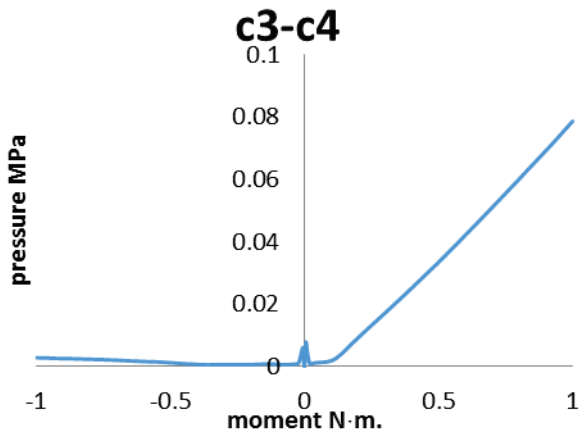
Supraspinouse ligament:



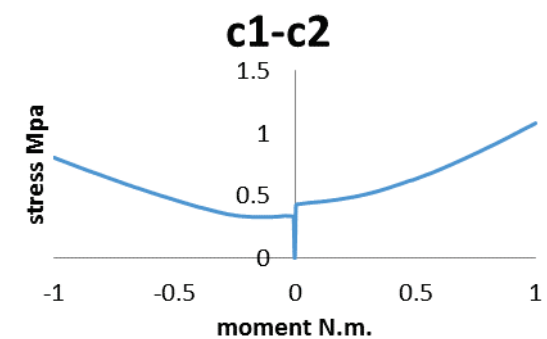
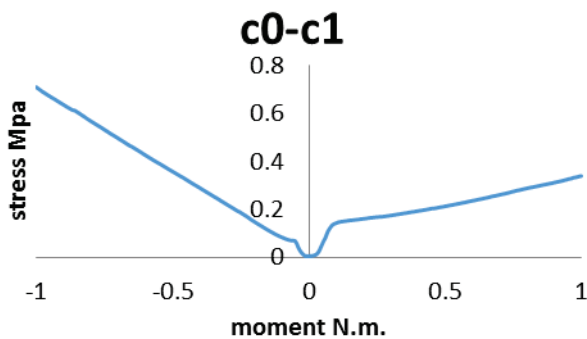


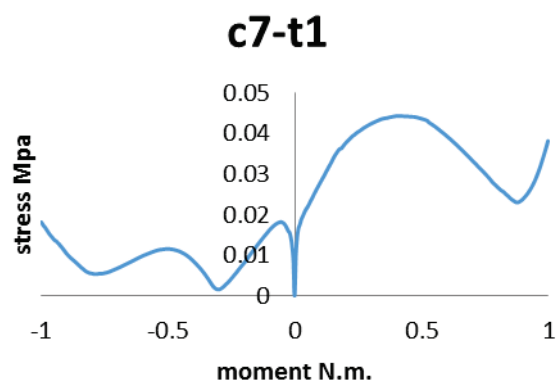
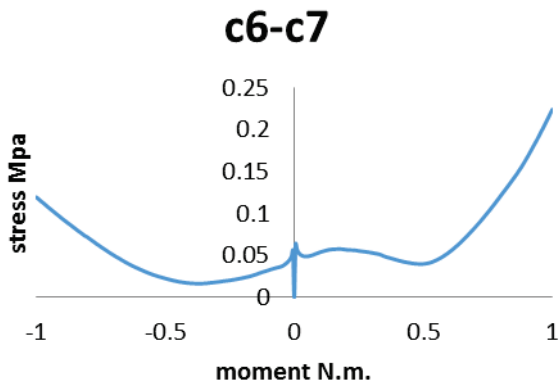
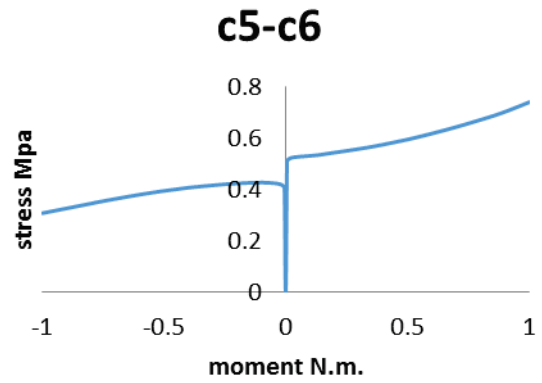
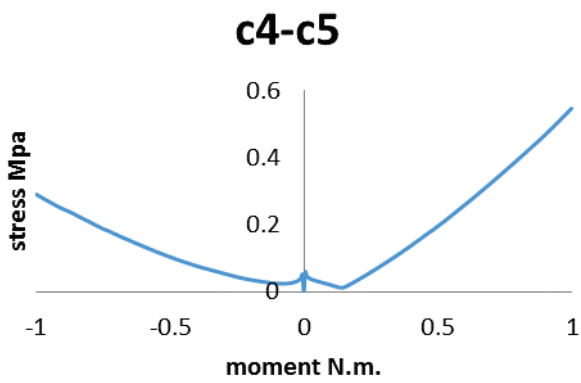
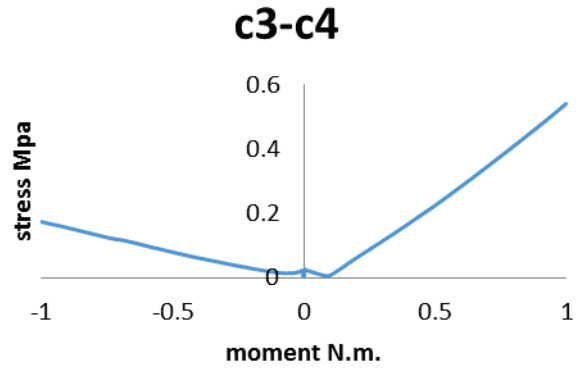
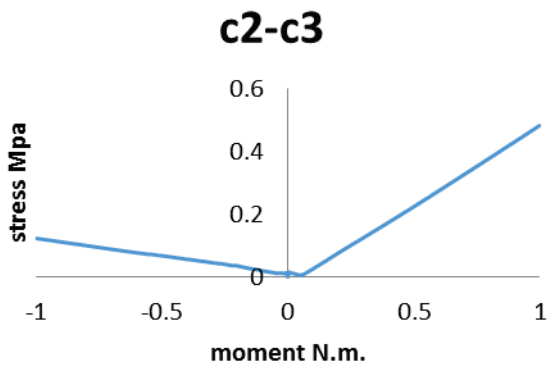
Interspinous ligament:





Capsular ligament:

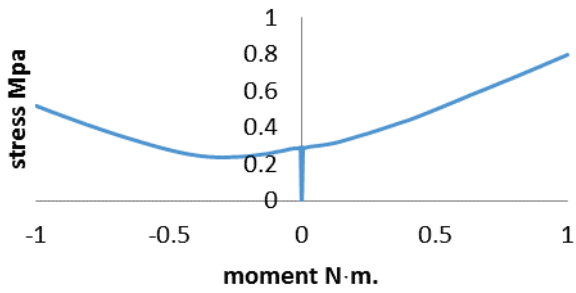




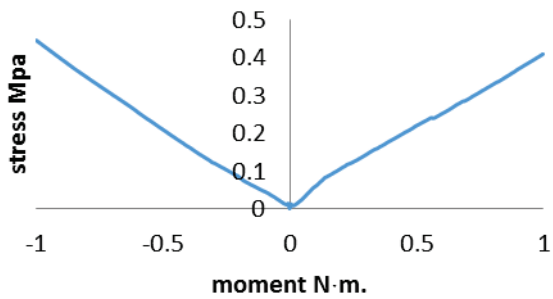
Axial rotation:

Anterior longitudinal ligament:

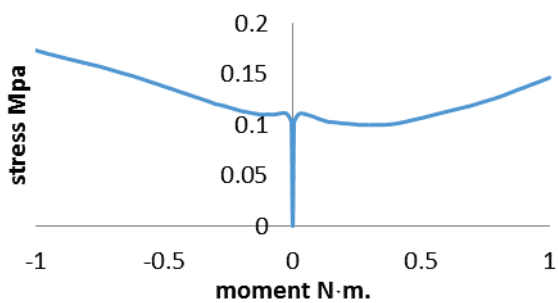
axial lig c1-c2



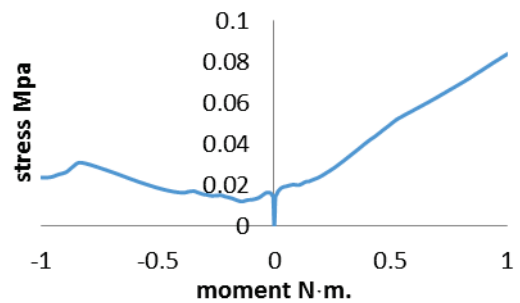
c0-c1

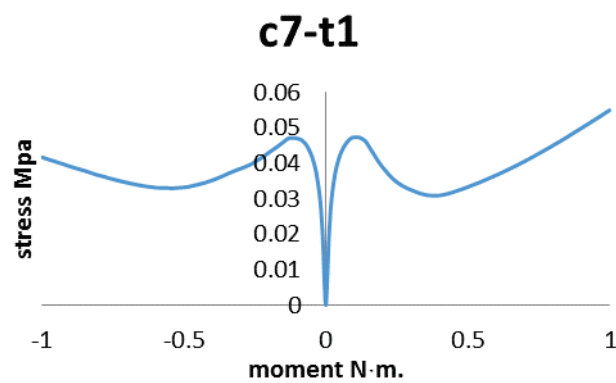
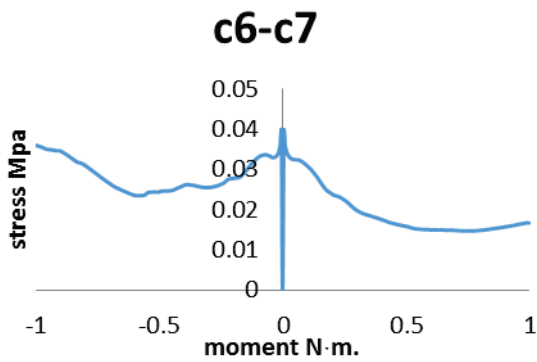
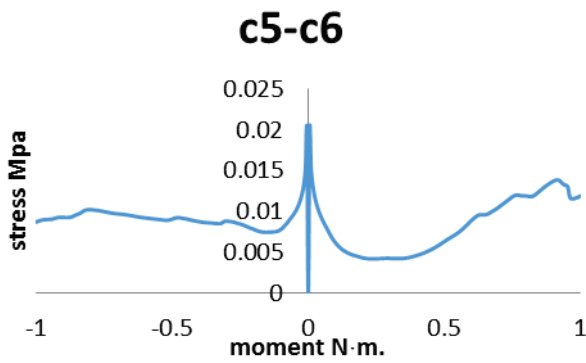
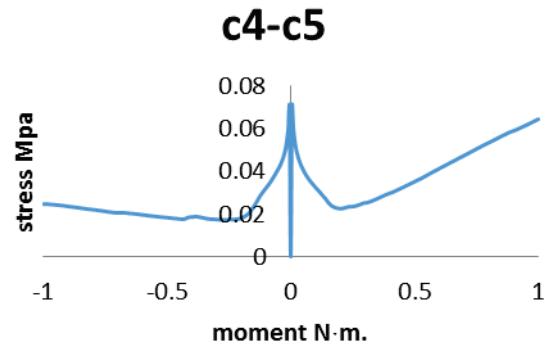
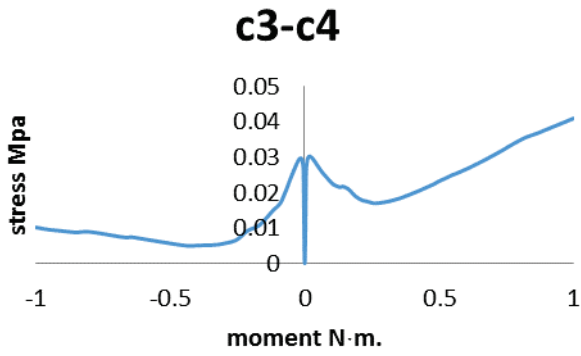


c1-c2

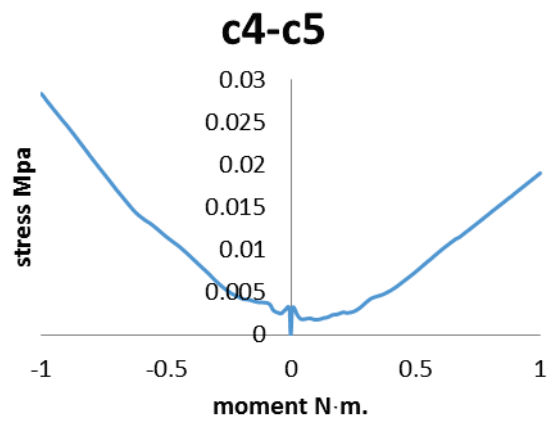
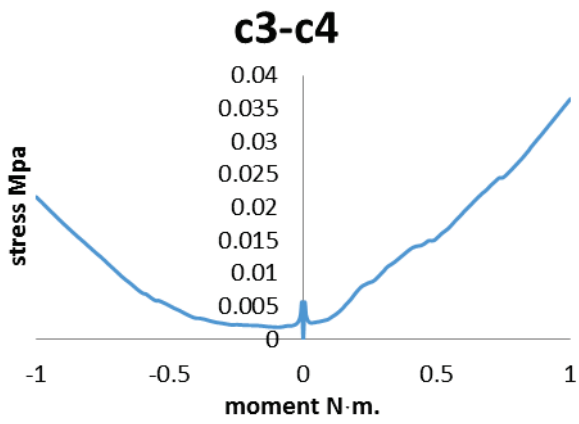
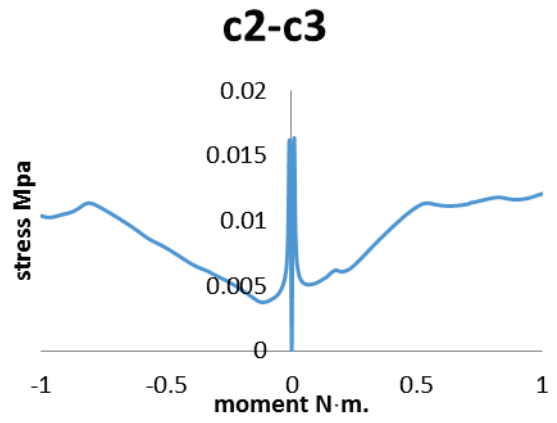
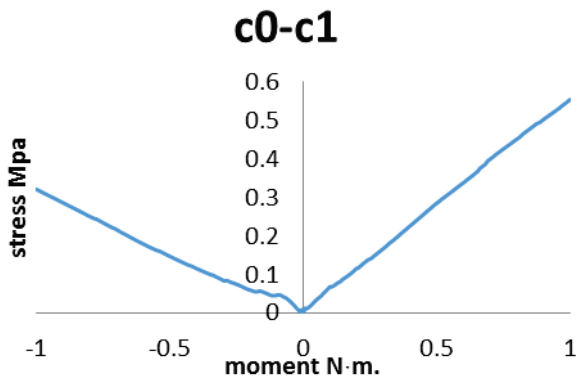


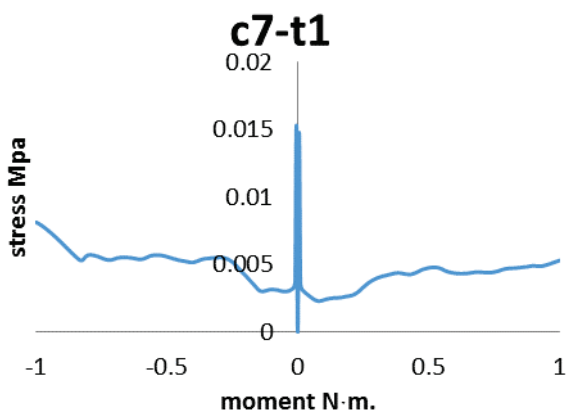
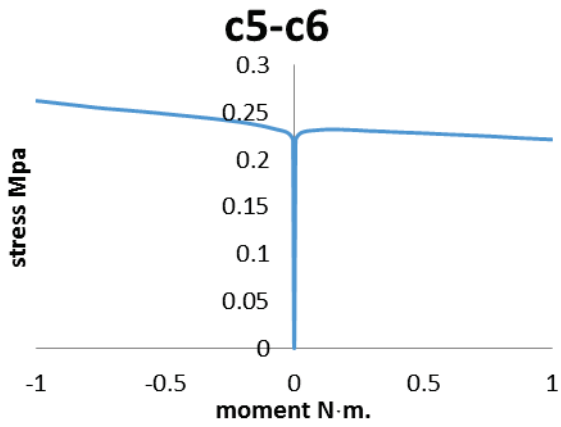
c2-c3



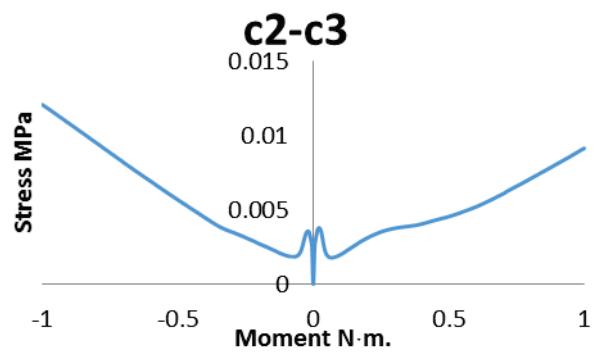
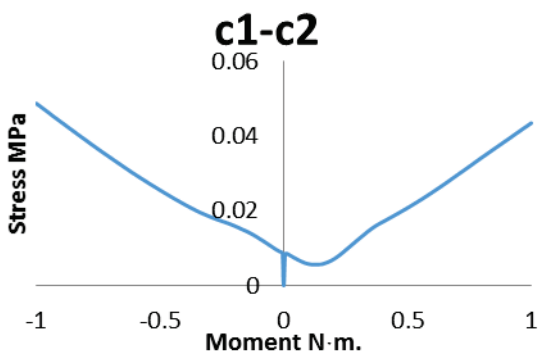


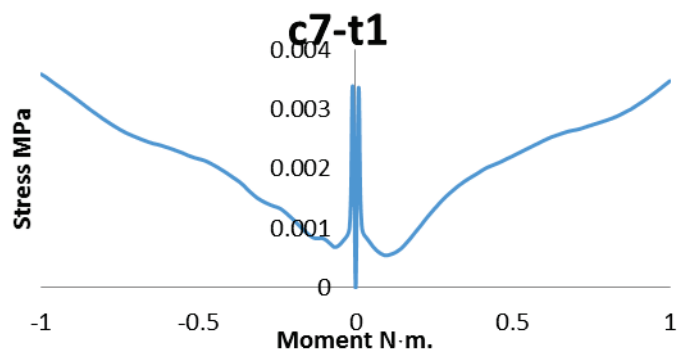
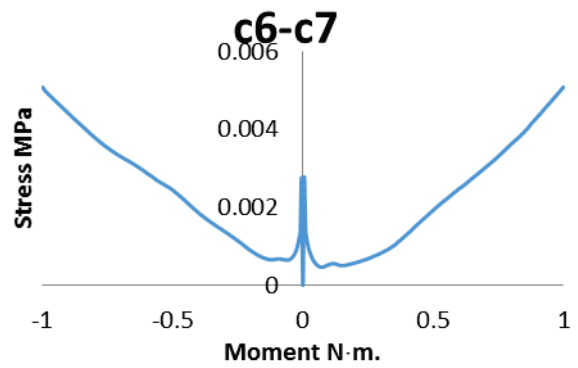
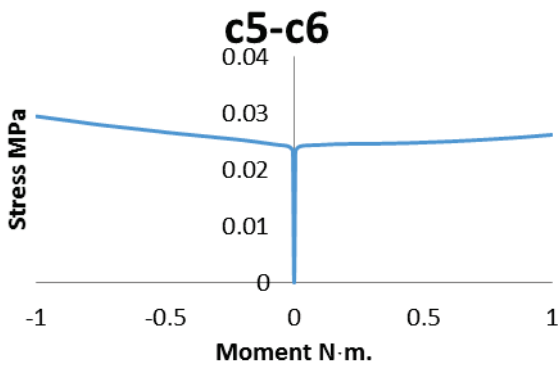
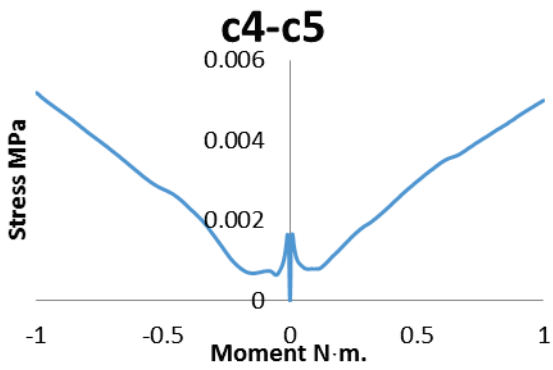
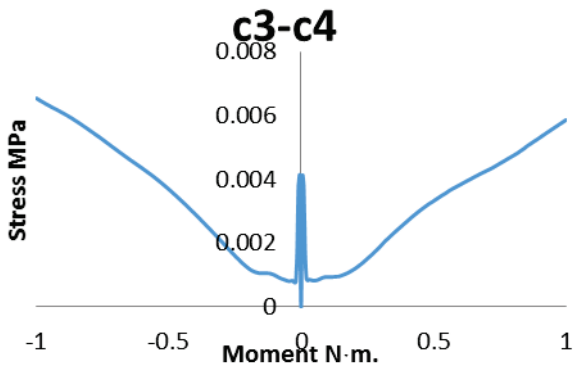
Posterior longitudinal ligament:



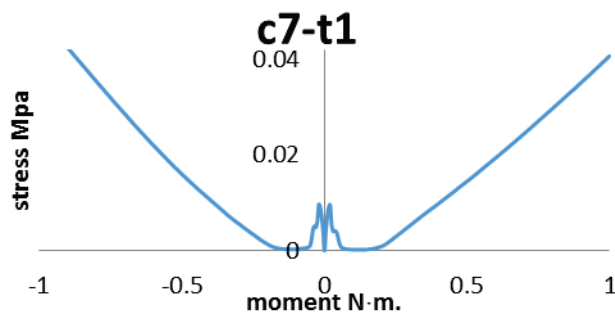
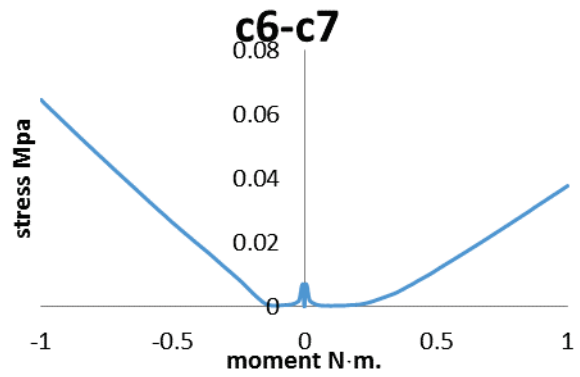
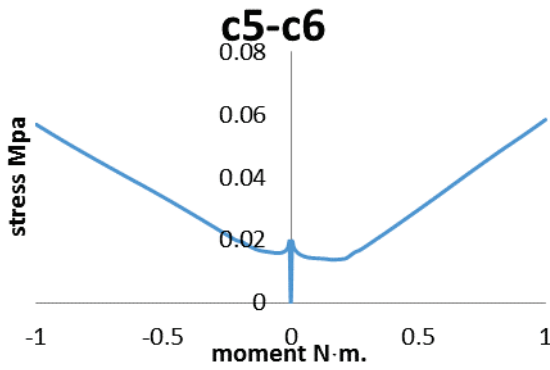
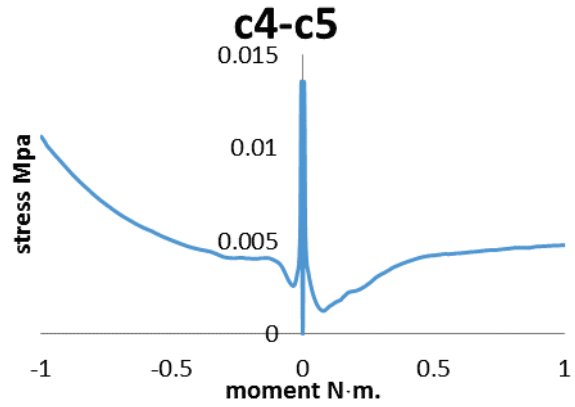
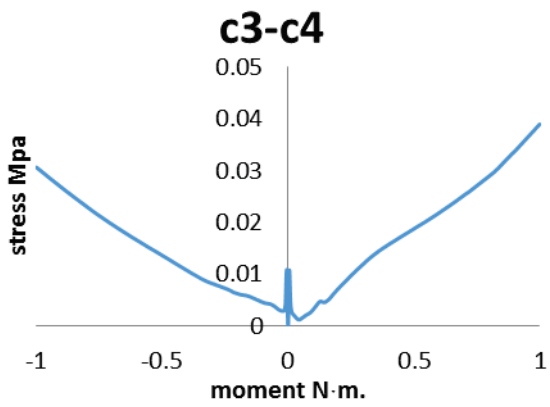
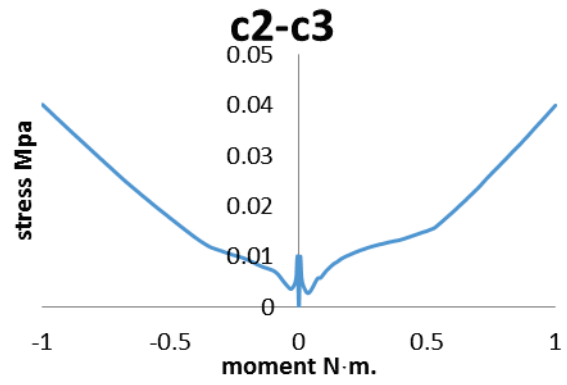
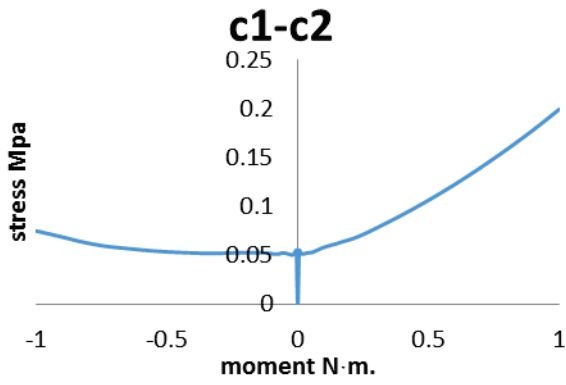


Ligamentum flavum:

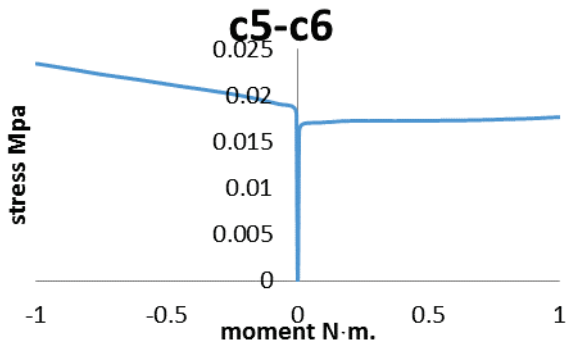
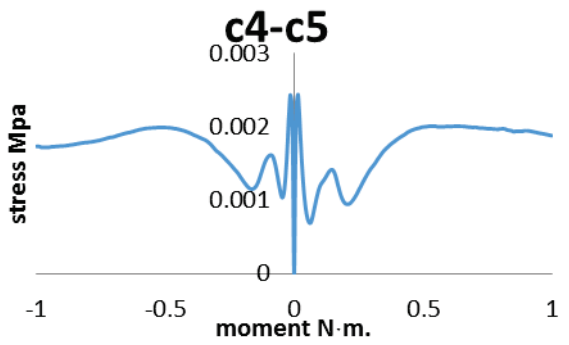
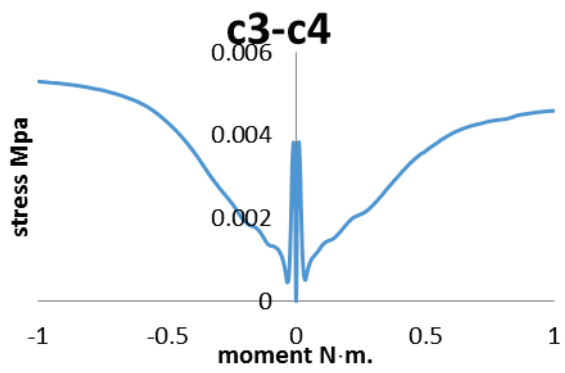
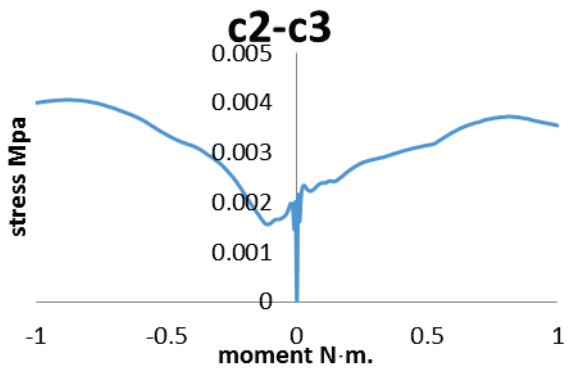
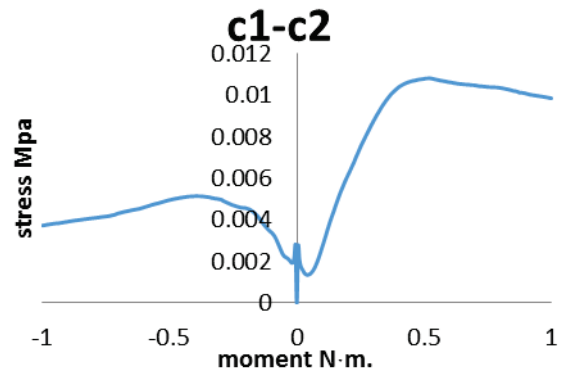
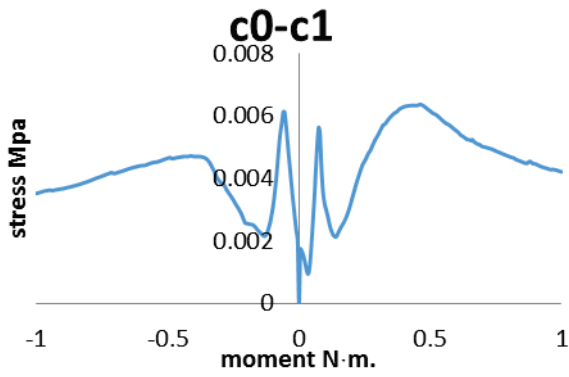


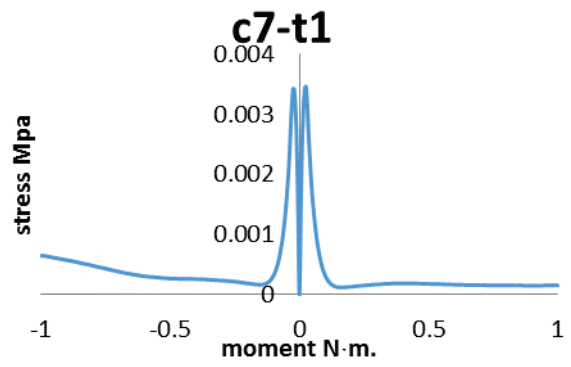
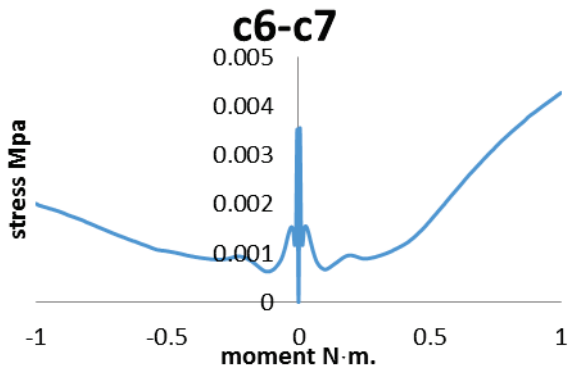


Interspinous ligament:

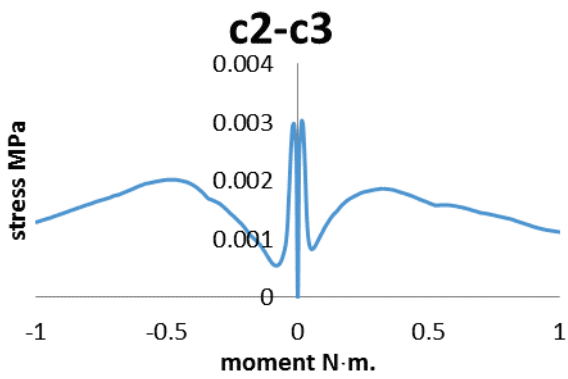
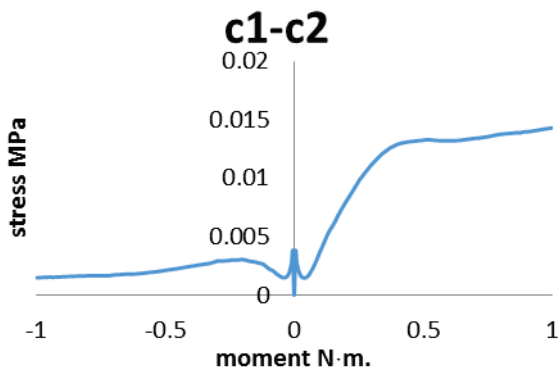


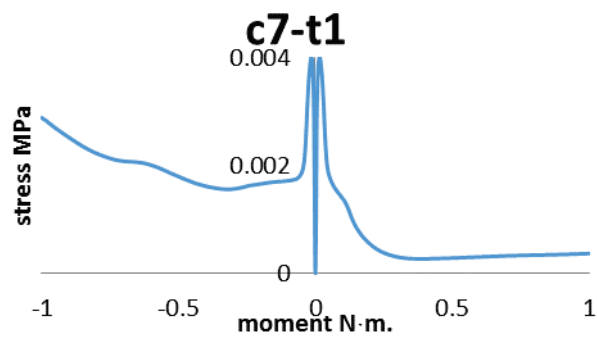
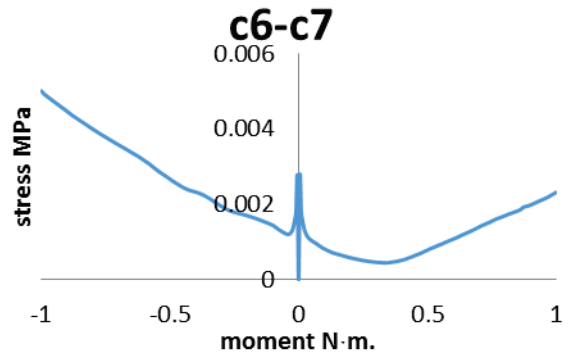
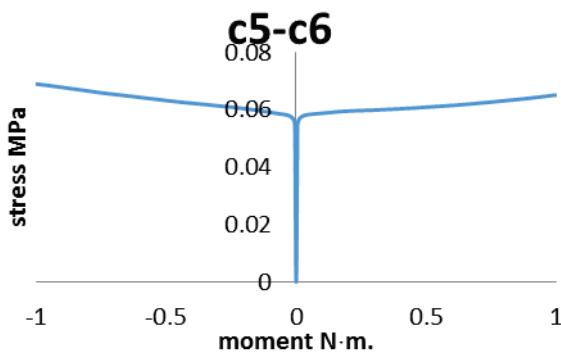
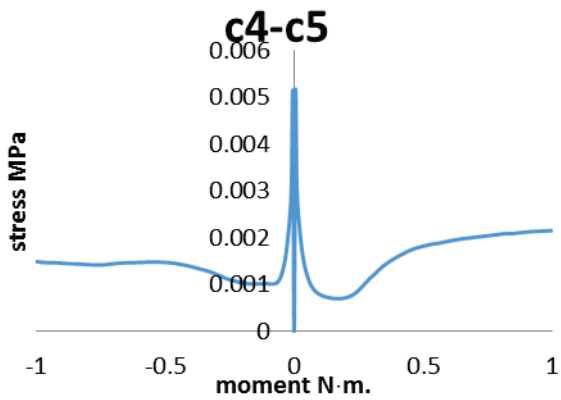
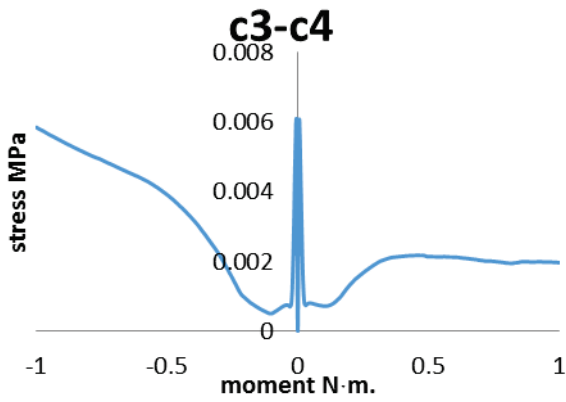
Supraspinous ligament:



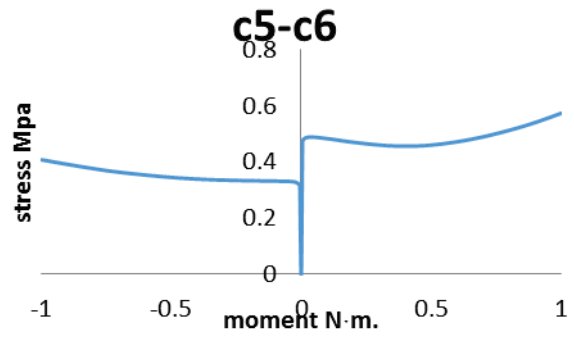
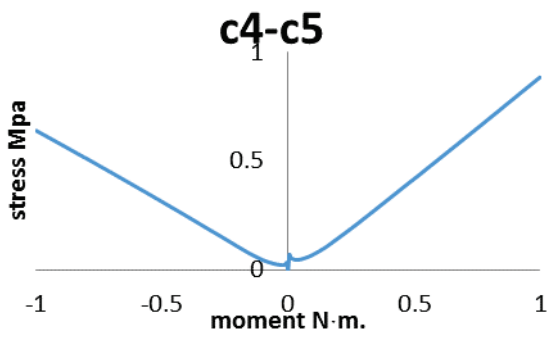
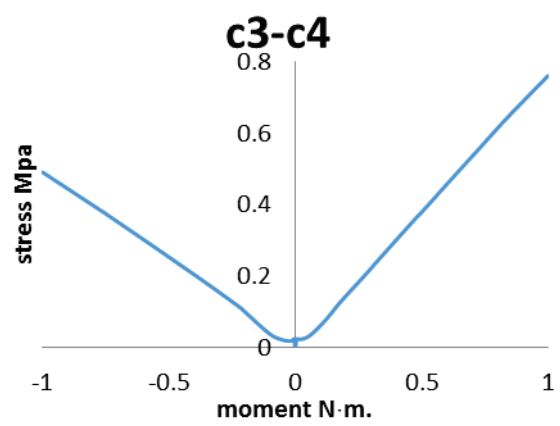
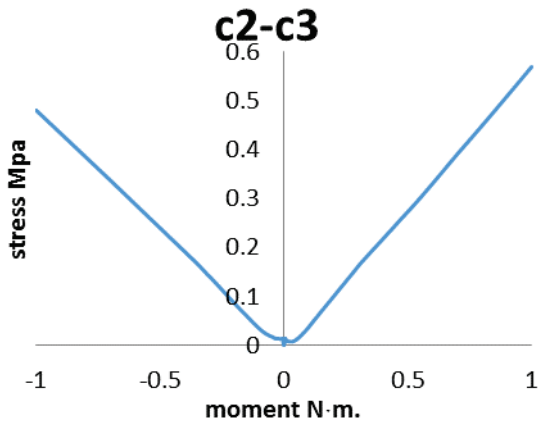
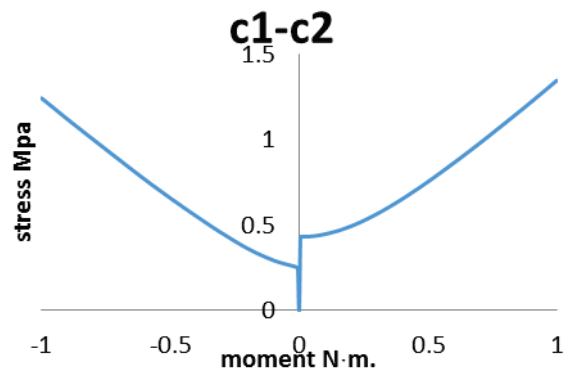
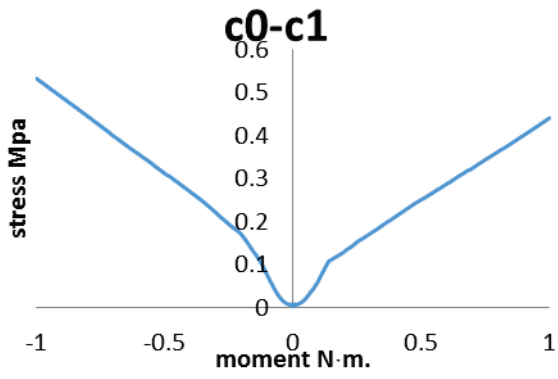


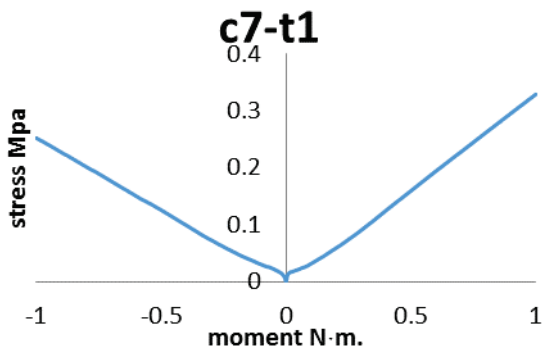
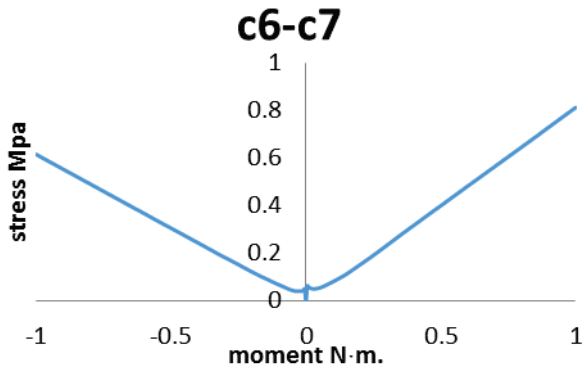
Interspinous ligament:





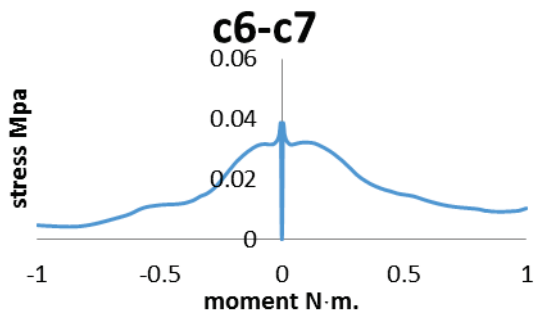
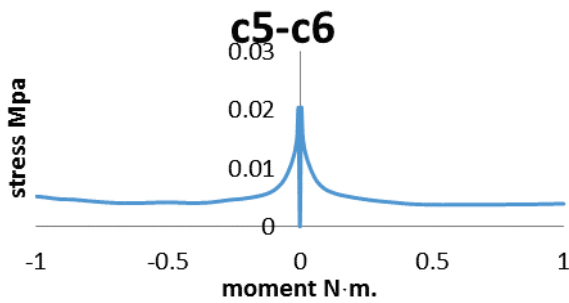
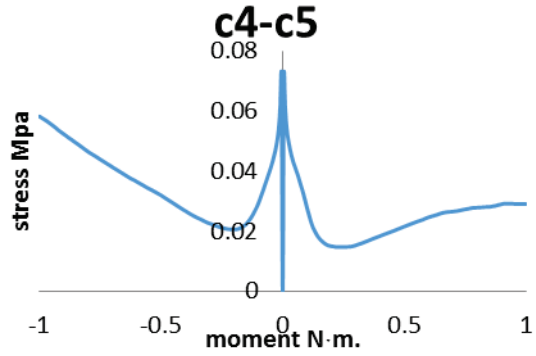
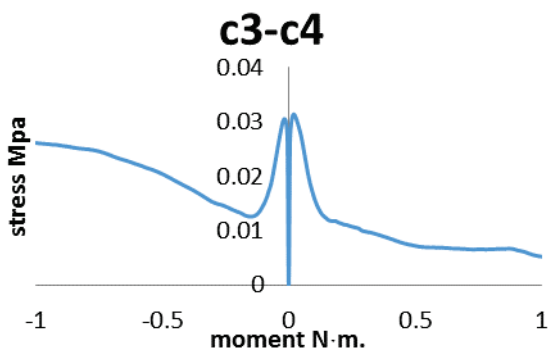
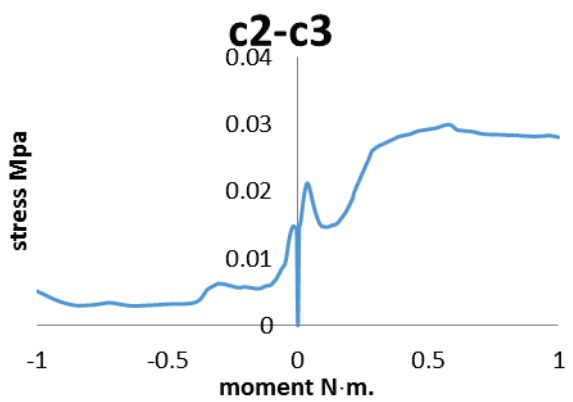
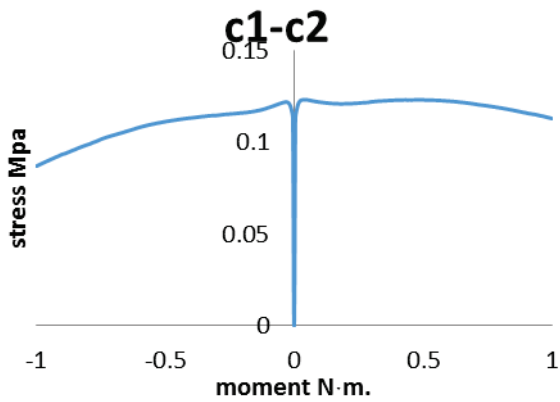
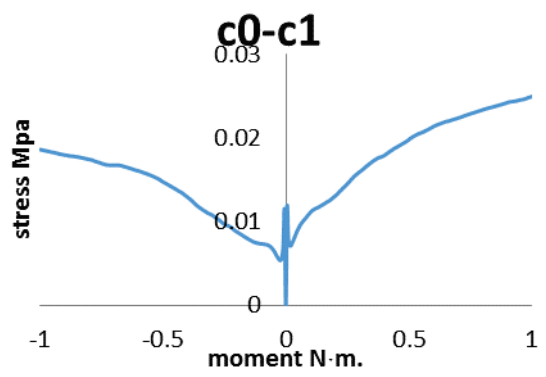
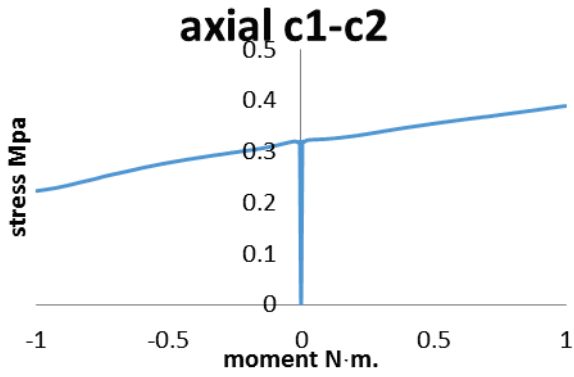
Capsular ligament:

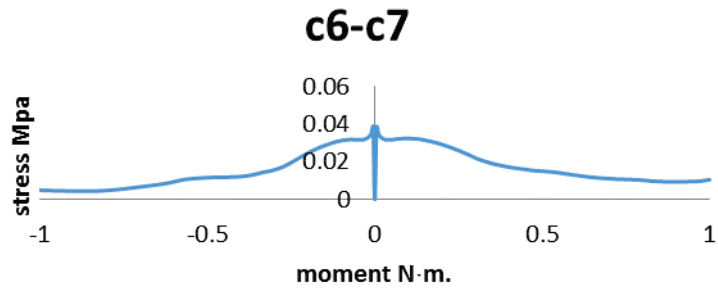




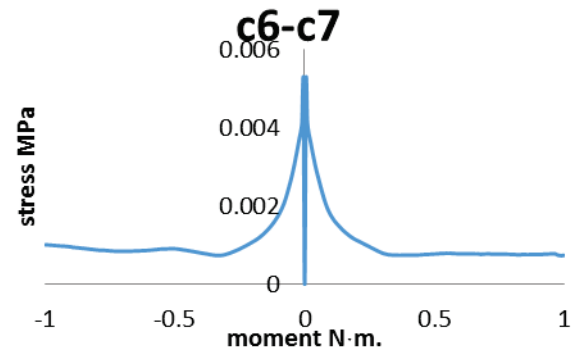
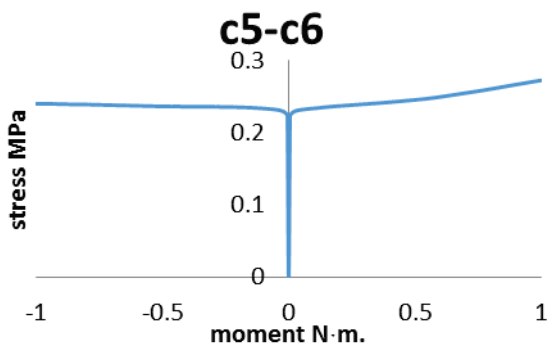
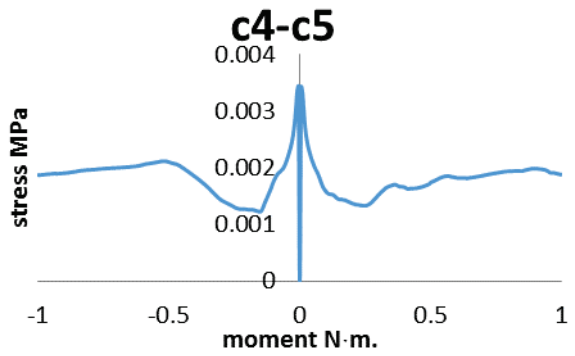
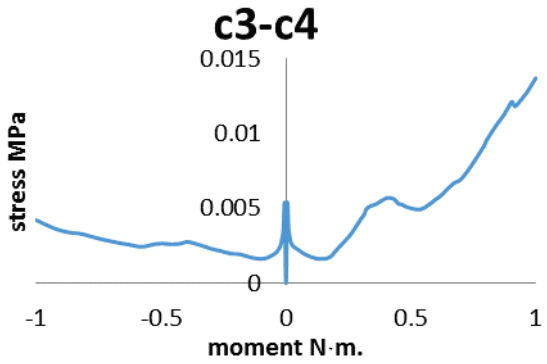
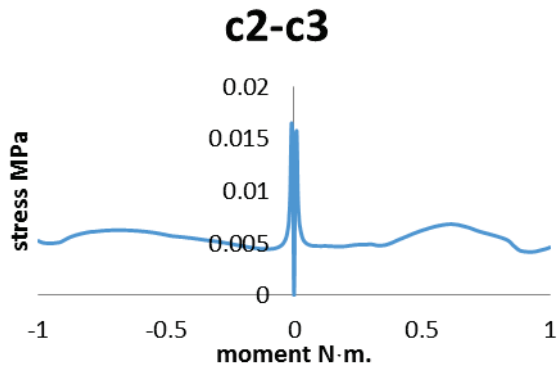
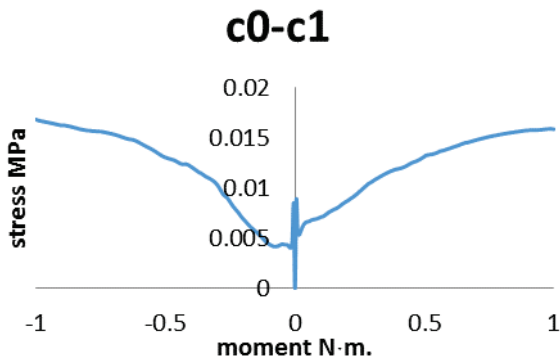
Lateral Bending:

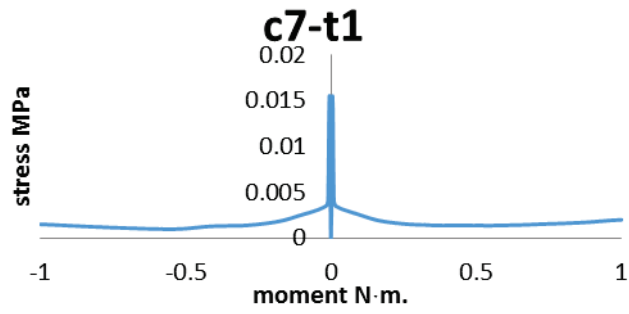
Anterior longitudinal ligament:



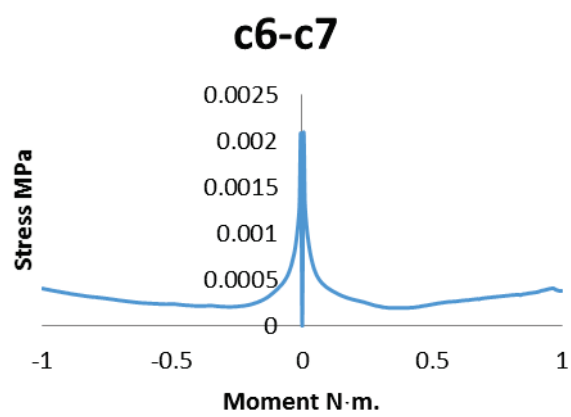
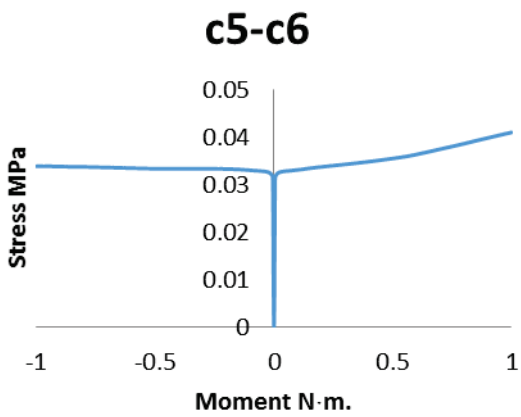
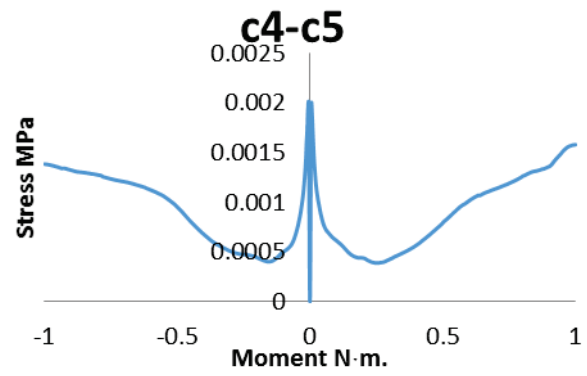
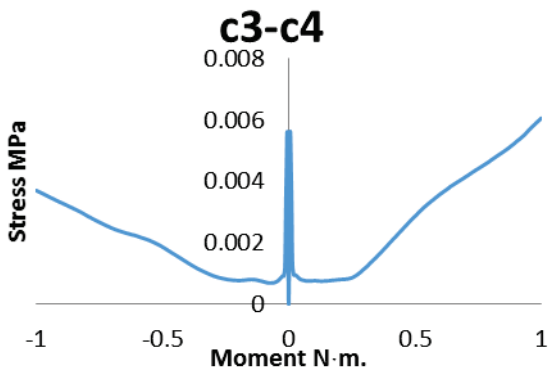
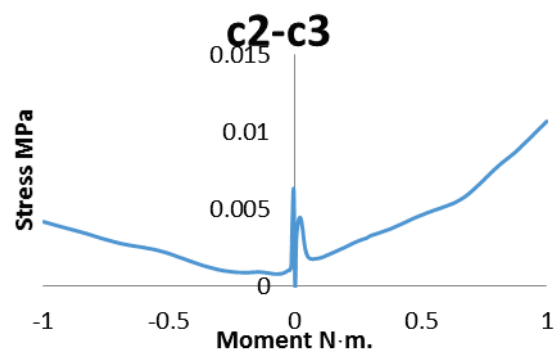
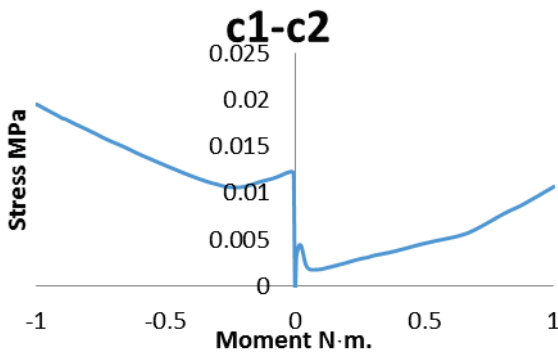


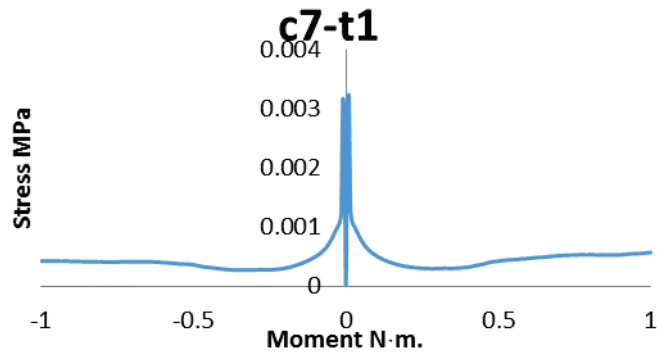
Posterior longitudinal ligament:



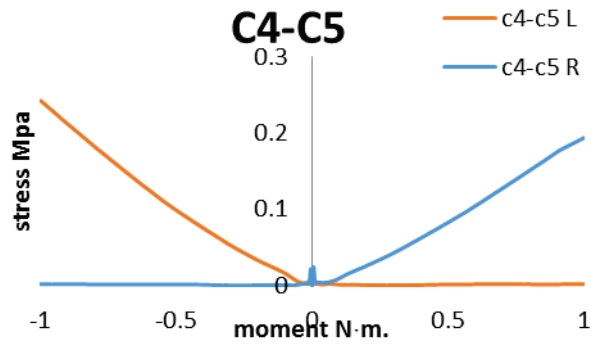
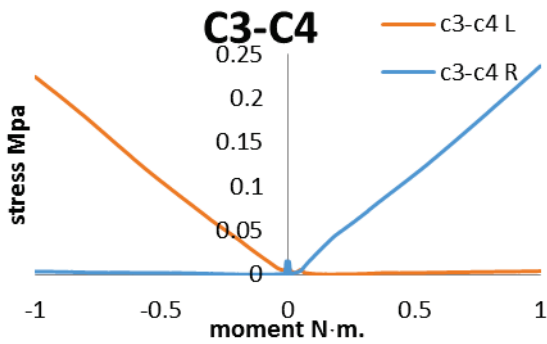
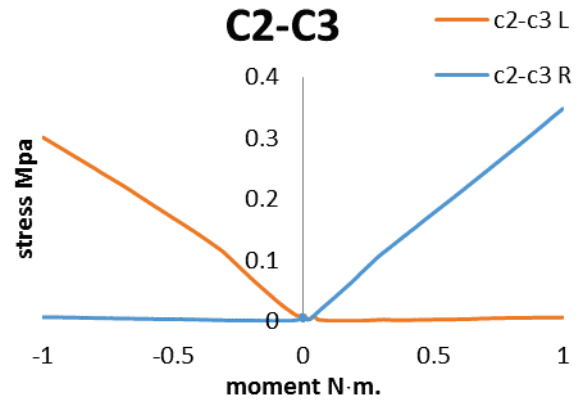
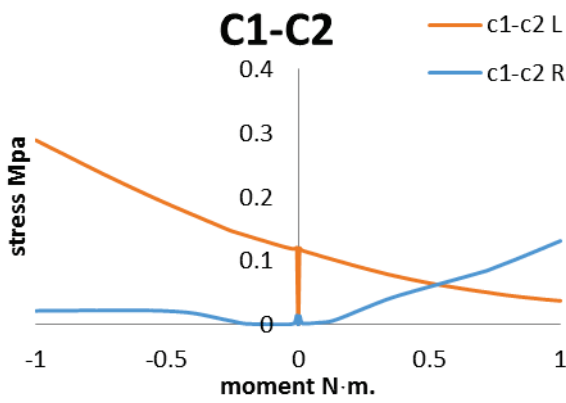


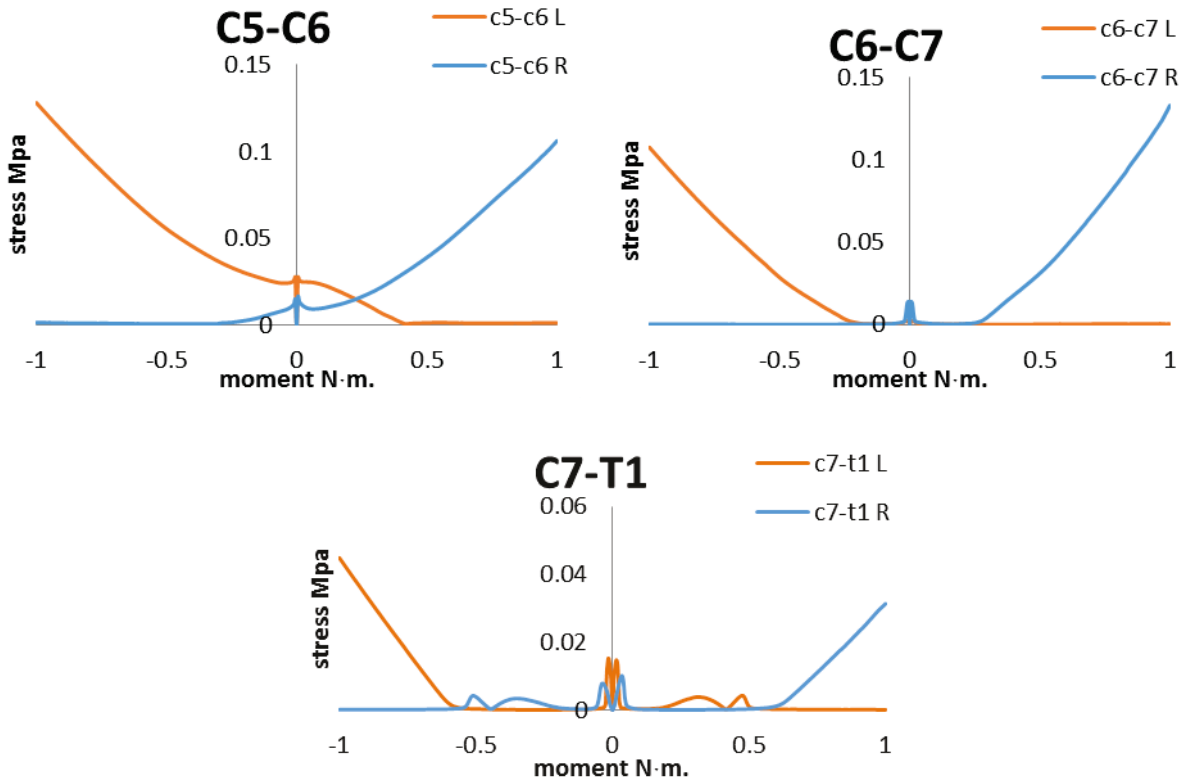
Ligamentum flavum:



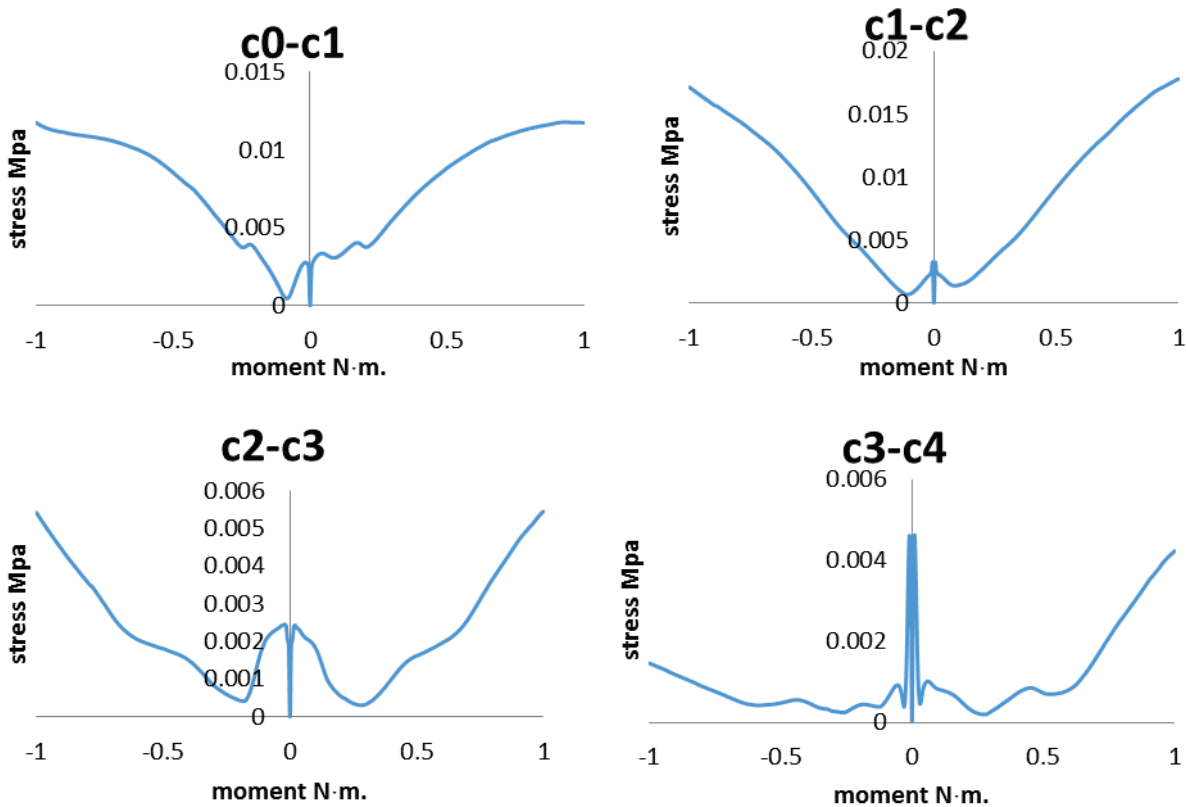


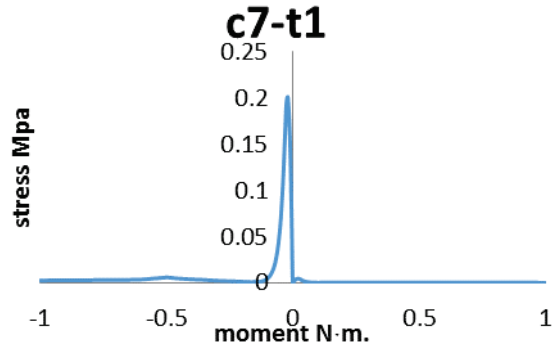
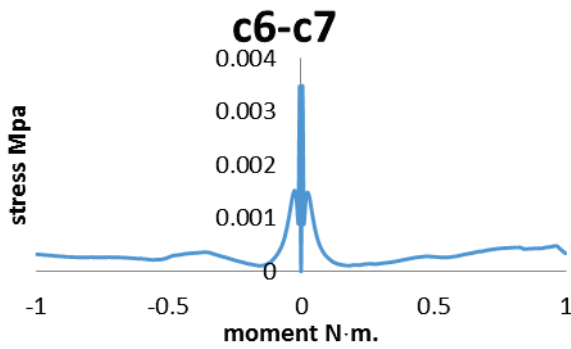
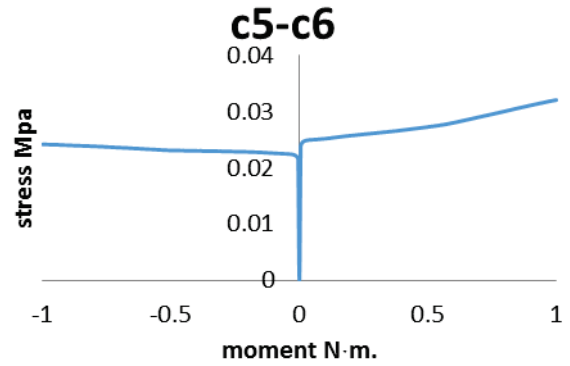
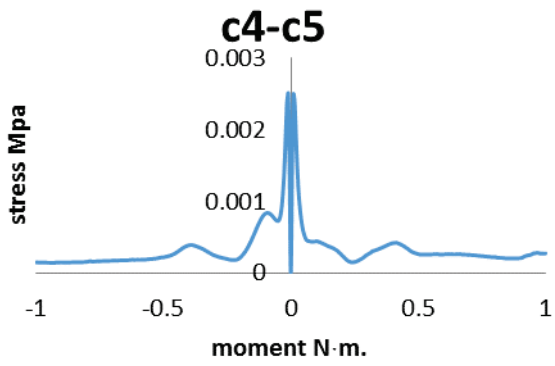
Interspinous ligament:



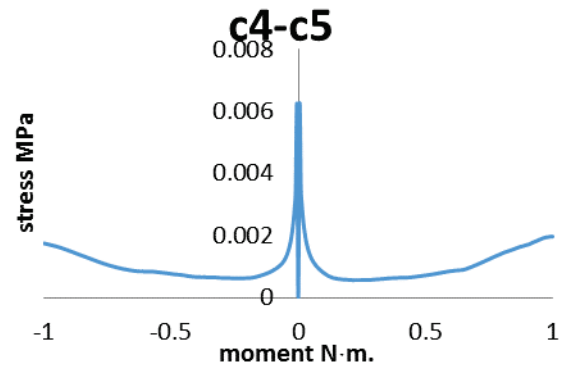
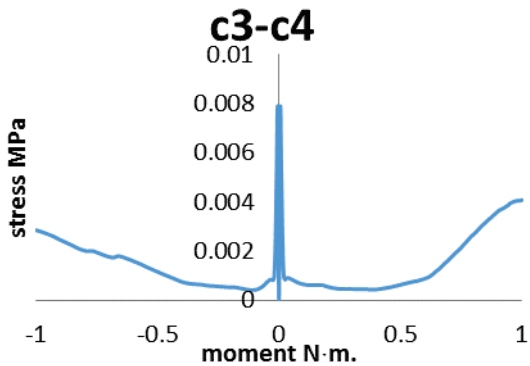
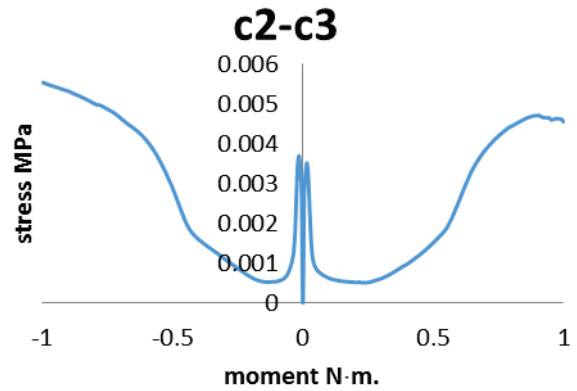
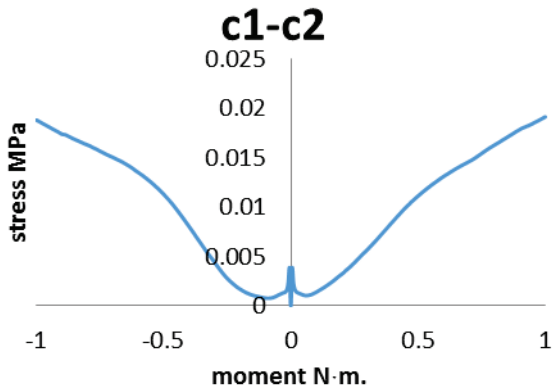


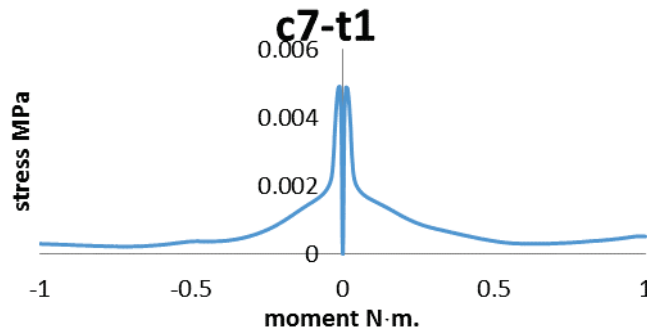
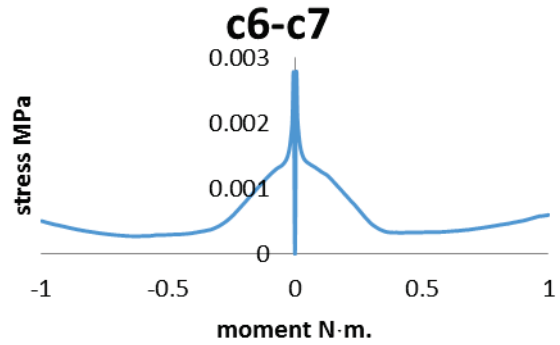
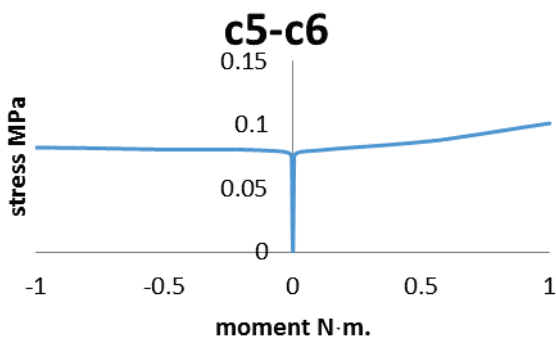
Supraspinous ligament:





interspinous ligament:





Capsular ligament:

